Determination of Optimum Moisture Content and degradation of shear strength over time for Hamilton Ash materials

A thesis
submitted in partial fulfilment
of the requirements for the degree
of
Master of Science in Earth Sciences
at
The University of Waikato
by
Doney Kuman

THE UNIVERSITY OF
WAIKATO
Te Whare Wānanga o Waikato

2019

Abstract

Hamilton Ash is one of the widely used materials in earthwork projects throughout the Waikato region. Regardless of its frequent and widespread usage, limited research has been undertaken regarding its geotechnical properties. It has been observed that after the completion of fill construction, Hamilton Ash unit tends to saturate overtime thus leading to a gradual loss of shear strength and ultimately resulting in ground instability. Common instabilities associated with soil fills are settlement and subsidence which in excess can result in distortion and damage to structures, services and infrastructures that are founded on the material subjected to the movement. The compaction stage, wherein the problem originates, can be optimized if better understanding of the geotechnical properties of Hamilton Ash is attained.

My project focused on determining the key compaction parameters of Hamilton Ash which are the optimum moisture content and maximum dry density. Further investigation into the degrading influence of prolonged exposure to moisture on the shear strength is also undertaken. The use of laboratory compaction tests have been recognized as mandatory procedures in determining the crucial parameters for field-based applications. The Standard Proctor test is implemented in this research will help determine the key compaction parameters; Optimum Moisture Content and Maximum Dry Density of Hamilton Ash. Prior to the compaction tests, the important index properties of the soil that influence compaction will be identified via several soil characterization tests, namely Atterberg Limits, grainsize and mineralogical analyses. Laboratory vane shear testing was also employed in this research to determine the strength of the compacted soil before and after wetting periods.

Acknowledgements

I would like to take this opportunity to acknowledge the contributions of the following people towards the completion of this thesis:

Firstly, I would like to offer special thanks to my Heavenly Father, through whom all things are possible.

A massive thank you to my supervisor Dr. Vicki Moon who recommended me to HD Geotech to allow me to work on this project. Your unwavering support and guidance every step of the way, even at times when I thought I wouldn't finish due to unforeseen circumstances, are greatly appreciated. Thank you very much!

A thank you to MFAT New Zealand Aid Scholarship for the financial support for the past 18 months of my life as a student at the University of Waikato. I would not be here writing up a thesis if a scholarship was not awarded to me.

To Annette Rodgers, Noel Bates, Renat Radosinsky and Kirsty Vincent; thank you for showing me how to operate the particle sizer, driving me out to the field to collect my samples, for promptly organizing my field gears and lab equipment when needed and helping me with my XRD tests and data analysis. A big thank you to Tom Robertson for proof-reading, editing and giving me really good feedbacks.

To my family back home, your constant prayers, unconditional love and unwavering support have encouraged, motivated and strengthened me to push through and better myself throughout the course of this study. Thank you, I love and miss you guys and cannot wait to reunite with you lot.

To my "OBT" (Operation Burukim Tulait) crew, Mose, Miriam and Rovina, thank you for spending countless nights with me in the computer lab, office and library from 9 pm till the crack of dawn just so I can work on my thesis.

And finally to my sis Rovina for offering to print, bind and submit my thesis on my behalf, you are an absolute gem!

Table of Contents

List of Figures

List of Tables

Chapter 1

Introduction

1.1 Background

Urban development within the city of Hamilton and its outskirts has been on a rise since the financial crisis in 2008. Prior to any design or development of an area, it is standard practice that preliminary site investigations are carried out by a geotechnical engineer or the developer. The purpose of these site investigations is to evaluate the general nature and character of the site in order to determine the parameters for earthworks or, if need be, to prompt further investigations into the feasibility of the founding conditions and the stability of the natural ground.

Hamilton Ash, a soil unit that comprises of fine-grained silt and clay minerals of volcanic origin is a widely used material in earthwork projects around Hamilton. Compacted clay fills of this material have been observed to lose strength over time due to prolonged saturation from the environment, which in the long term can be deemed as undesirable for the stability of any building, infrastructure or services. In order to prevent future instability issues associated with weakened clay fills, an extensive and thorough investigation was conducted Hamilton Ash samples to determine its key index and mechanical properties, especially the attributes that play predominant roles during compaction. By doing so, the compaction parameters necessary to achieve the highest degree of compaction can be specified.

The occurrence of Hamilton Ash units are widespread in the Waikato region (Pullar, 1967) but no specific location was selected to study in this research. Instead, the Hamilton Ash samples tested were extracted from a stockpile of a residential development area that was under construction at that time.

1.2 Aims and Objective

The aim of this research is to explore the relationship in the use of Hamilton Ash as fill materials between air voids or dry density at time of compaction and long term strength. The following objectives were proposed to achieve this aim:

1. To conduct a comprehensive review of existing literature on the index and mechanical properties of Hamilton Ash and the effects of moisture on it shear strength after compaction.
2. Investigate the index properties Hamilton Ash that influence its strength via a series of laboratory tests including grain-size distribution, Atterberg Limits and mineralogical analysis.
3. Determine the optimum moisture content and maximum dry density through standard compaction methods according to New Zealand Standards of soil testing for civil engineering purposes (NZS 4402:1986). The determination of these two compaction parameters will define the optimal shear strength of Hamilton Ash.
4. Subject compacted samples to various soaking periods to determine the effect of elevated soil moisture content on the long term shear strength

1.3 Thesis Structure

This thesis is divided into 6 different chapters with chapter 1 comprising of a brief background information on the soil under study, the motivation behind this research, the aims and objectives of this study and a general outline of the overall structure of the this thesis. Chapter 2 constitutes a comprehensive review of previous work conducted on volcanic soils of New Zealand and the world, especially pertaining to their index and geotechnical characteristics. Other studies relating to widely used methods used for soil strength and stability improvement besides standard compaction were also reviewed. The purpose of these reviews was to identify the knowledge gap whereby the findings from the present study can bridge. The methods used in this study to collect data for analysis are presented in Chapter 3. These include of series of laboratory tests for soil characterisation which involved laser diffraction, Atterberg Limits and X-ray diffraction; and geotechnical properties determination which included standard compaction, soaking and vane shear tests.

Chapter 4 consists of all the results that were either generated or derived from individual tests. The results are presented in an orderly fashion starting with soil characterisation tests followed by compaction and strength tests results. In chapter 5, detailed interpretations and discussions of the results are attempted following the

same order of presentation established in chapter 4. In this chapter, the results are interpreted and speculated based on earlier work and further evaluated through comparisons with published literature for the purpose of identifying differences and similarities between the current study and previous studies. Chapter 6 summarises the key findings of this research, identifies the limitations encountered throughout this study and propose recommendations for future research involving the use of Hamilton Ash in geotechnical engineering in New Zealand.

Chapter 2

Literature Review

2.1 Introduction

Soil compaction is a viable and economical measure of soil improvement that's applicable to shallow and deep foundation alike (Massarsch & Fellenius, 2002). It is understood that the process of compaction densifies the soil in order to increase its strength and durability (Craig, 1997). On the basis of attaining maximum compaction of any given soil, two controlling factors come into play; optimum moisture content and maximum dry density (Rahmat & Ismail, 2018). The optimum moisture content (w_{opt}) of a soil is the water content wherein the maximum dry density ($\rho(_d)_{max}$) is obtained under a given compactive effort (Craig, 1997). During the process of compacting, moisture is gradually added to the soil to increase the moisture content. This in turn lubricates the soil skeleton and nudges it towards a more compact state until the maximum dry density is reached (Gue & Liew, 2001; Rahmat & Ismail, 2018). However, water in excess can fill up the voids of the soil which can in turn, act absorb and dissipate compaction energy, thus resulting in lower compactness (Gue & Liew, 2001).

2.1.1 Geology of Hamilton Ash Formation

The deposition of a series of airfall tephras occurred during the Quaternary period of Hamilton Basin infilling and subsequent erosion that formed the characteristic landscapes (Selby & Lowe, 1992). Pullar (1967) asserted that the exact source of Hamilton ash could not be ascertained but Selby and Lowe (1992) postulated that the Hamilton Ash beds may have originated from the Taupo Volcanic Zone (TVZ). Despite its uncertain origin, Hamilton Ash is widely distributed within the Waikato Region (Pullar, 1967) and evidently extends further into Henderson, Wellington, Gisborne and Raglan (Selby & Lowe, 1992). According to Selby and Lowe (1992) the patchy distribution of Hamilton Ash within Hamilton is attributed to erosion and depositional proximity to volcanic source.

In a brief account of the overall stratigraphy of the Hamilton Basin, Lowe (2010a) described the typical landforms that are associated with, and somewhat indicative,

of the underlying geological units. The soil of interest for the proposed project, Hamilton Ash is included in the four main characteristic landscapes that Lowe (2010a) identified, typically represented by low rolling hills as illustrated in Figure 2.1.

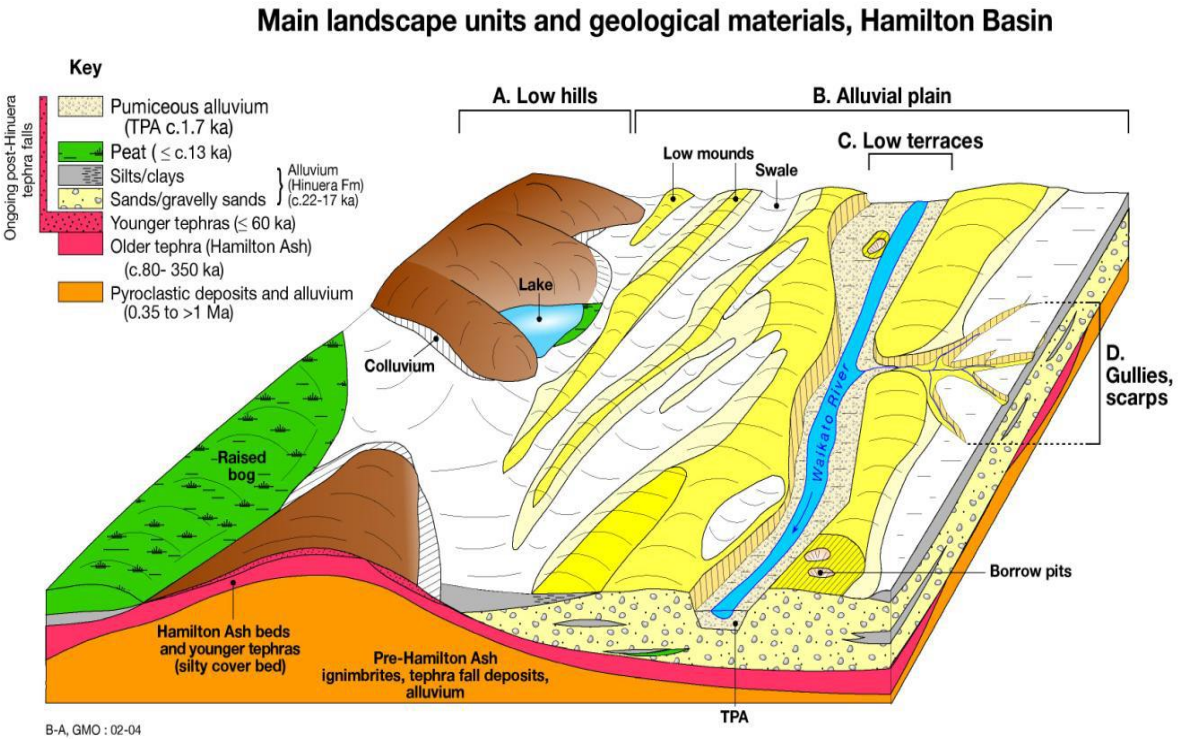

Figure 2.1.Hamilton Basin stratigraphic units and associating landscapes (After Lowe, 2010).

The first layer in the Hamilton Basin sequence is approximately 0.5m in thickness and blankets the low rolling hills (Lowe, 2010a; Selby & Lowe, 1992). It comprises of silty post-Hamilton-Ash tephra deposits that are ≤ 60,000 years old. Immediately beneath this formation is Hamilton Ash, subsequently followed by the gravelly alluvial clay formation; pumiceous alluvium and older Kidnapper's Ignimbrite formations (Lowe, 2010a). Hamilton Ash formation is the primary study material in this research. Lowe (2010) broadly identified two distinct clayey, weathered tephra beds within the Hamilton Ash formation; the top bed which is 80, 000 to 125, 000 years old and basal bed which is 250,000 years of age. However, Selby and Lowe (1992) recognized at least eight distinct beds, labelled H1 to H8 (from bottom to top) within the Hamilton Ash formation that differed in colour, texture and mineral content.

In a comprehensive study by Ward (1967), all eight (8) beds constituting the Hamilton Ash formation were described. The oldest bed H1 belongs to the Huntly Variant from the Ohinewai Ash Member and is estimated to be 350,000 years old. H1 is identified as a firm, pinkish grey, blocky ash that's dominated by white veins and stains of yellowish red (Selby & Lowe, 1992; Ward, 1967). Overlying the oldest bed in the sequence, H2 is derived from the Te Uku Variant of the Ohinewai Ash Member. In addition to advanced weathering, this layer is characterized by friable brown to yellowish red ash rich in rootlet pseudomorphs and large halloysite nodules close to the basal area. H3 and H4 beds have been further separated into subgroups because of slight variations in their appearance. H3 ash bed has two subgroups, H3a and H3b, which differ from each other in a number of ways. H3a has a blocky structure, dull yellowish brown and is very rich in greyish white halloysite that's scattered throughout the bed. In contrast, H3b bed is friable, brown in colour and contains predominantly allophane. In bed H4; beds H4a, H4c and H4e bear similar resemblance in their physical attributes, therein they are pale brown and blocky. According to Ward (1967) these three beds rather indistinguishable in the field unless they contain the fossil soils H4b and H4d. Deposited immediately above H4 is H5 which was described by Ward (1967) as having a yellowish brown colour and earthy ash texture. It contains numerous halloysite nodules that tends to become friable when exposed on surface. The earthy ash bed H6 is distinguished by a greyish brown colour and is developed above the fossil soil H7. H7 bed is characterised as a compact, brown ash with blocky structure of the Tikotiko Ash Member. The youngest bed H8, is a compact, still brown clay with rich contents of halloysite. It also contains reddish stains and prominent clay veins in the lower parts of the bed (Ward, 1967).

Ward's (1967) detailed description of ash beds of Hamilton Ash formation suggests that the soils within the Hamilton Ash formation are clay-rich with minor silt components. In addition, a comprehensive liquefaction assessment report by Beca Limited (2018) classified Hamilton Ash as stiff to very high plasticity clayey SILT and silty CLAY. Another study that agreed with Beca Limited (2018) and Ward (1965) on the mineral composition of Hamilton Ash is Pullar's (1967) documentation of Hamilton Ash from a 40 inch (1m) deep excavation site. He recorded that kaolin made up 30% of the clay fraction whereas halloysite accounted for only 40% but increased dramatically to 100% in the 33-40 in. horizons. The

granular components consisted of quartz in the majority, followed by acid feldspar, volcanic glass, and then muscovite (Pullar, 1967).

According to New Zealand Soil Classification (NZSC), the tephra-derived soils of New Zealand were categorized into 5 orders; Tephric recent soils, Pumice Soils, Allophanic Soils, Granular Soils and Ultic soils (Lowe, 2010). This suggests that because of its rhyolitic origin and above classifications, Hamilton Ash unit should encompass both Allophanic and Granular soil which implies that the presence of allophane and halloysite (Lowe, 2010) will respectively exert dominance in the soil's chemical and physical properties. The percentage of both clay minerals in Hamilton ash will vary depending on depositional area and other key factors.

2.1.2 Significance of compacting fine-grained soils

Soil compaction is very important in the construction of earth structures such as embankments, fill, earth dams and other engineering structures because it is through this process that loose soils are compacted to improve their strength by increasing their unit weight. Numerous studies have addressed the importance of compaction, especially on fine grained soils, and considered this process to be a significant factor that dictates the behaviour of earthwork projects (Blotz *et al.*, 1998; Jesmani *et al.*, 2008; Rahmat & Ismail, 2018; Rollins *et al.*, 1998; Sivrikaya & Soycan, 2010; Yokohama *et al.*, 2014). Compaction, as defined by Craig (1997), is the process by which the soil density is increased through close packing and air void reduction.

There are several important soil characteristics that are drastically altered to ensure stability of earth structures after compaction. According to Rahmat and Ismail (2018), soil strength, volume, durability and permeability are some of the main properties of a soil that must undergo modification in order to achieve stabilization. Horn *et al.* (1995) reported that during compaction the soil structure and any physical or chemical processes that occur within the soil is radically altered. Major geotechnical problems can be avoided if the process of soil compaction is methodically achieved (Çokça & Tilgen, 2010). Soil strength is a good indicator of the degree of compaction (Gue & Liew, 2001) and essentially for ground stability. After compaction, changes in soil strength can give rise to geotechnical problems, hence the significance in maintaining an elevated soil strength after compaction.

However, there are several other elements that can affect the soil strength after compaction.

Soil suction as reported by Çokça & Tilgen (2010) is one of these elements and by definition, soil suction is a combination of forces that enables an unsaturated layer to attract water from the water table below (Ridley, 2015). Çokça & Tilgen (2010) investigated the relationship between soil shear strength and soil suction of Ankara clay using direct shear testing where samples were tested at three different water contents and densities; dry of w_{opt}, w_{opt} and wet of w_{opt}. Lambe and Whitman (1979 as cited in Çokça & Tilgen, 2010) stated that soils that are compacted in dry of optimum moisture content tends to be more flocculated whereas soils become more dispersive when compacted in wet of w_{opt}. This led to the generalization that flocculated soils have higher strength compared to soils in dispersive states (Çokça & Tilgen, 2010). The results revealed a close relationship between soil suction, moisture content and shear strength which led Çokça & Tilgen (2010) to conclude that an increase in soil suction increases the shear strength of the soil. Furthermore, the study showed that upon soaking the compacted sample, the initial moisture content of the sample is no longer considered in the shear strength and suction relation. According to Çokça & Tilgen (2010), it is highly unlikely for the shear strength to increase after soaking or when the soil is compacted wet of w_{opt} due to loss of soil suction because of the change in nature of soil particles from flocculated to dispersive. Finally, Çokça & Tilgen (2010) recommended that if the possibility of saturation after compaction is to be considered, tests should be conducted on soils in their compacted states and after soaking.

2.1.3 Key compaction parameters influencing stability of earth structures

In a study of subjecting clayey gravels to various compaction energies in order to determine the optimum moisture content (w_{opt}) and maximum dry density ($\rho(_d)_{max}$), Jesmani et al. (2008) concluded that a linear relationship exists between compaction effort and maximum dry density whereas an increase in clay content results in an inverse correlation between the compaction energy and optimum moisture content. This supports the general notion that higher compaction degrees lead to higher shear strengths and reduced soil compressibility (Craig, 1997; Gue & Liew, 2001).

The w_{opt} and $\rho_{(d)max}$ is recognized by Rahmat and Ismail (2018) as key players in compaction along with soil strength and durability. The understanding that moisture content largely influences the degree of compaction and ultimately its stability is emphasized greatly by Rahmat and Ismail (2018). The focus of their study was to stabilize clayey soil by obtaining the optimum clay moisture content using combined mechanical and chemical effort. Despite the main focus of the study was to chemically stabilize clay, Rahmat and Ismail (2018) were able to clearly define the relationship between soil shear strength, w_{opt} and $\rho_{(d)max}$ during compaction, that is; shear strength of an uncompacted soil is augmented considerably under a given compactive effort, at the w_{opt} and corresponding $\rho_{(d)max}$. Rahmat and Ismail (2018) further emphasized that the degree of compaction depends on the friction between the granular components or strength of the clay nodules which are largely influenced by moisture content during compaction.

After running a series of tests, Lambe and Whitman (1969) summed up the effects of varying compactive effort on a given cohesive soil as follows; the higher the compactive effort, the lower the w_{opt} and higher the $\rho_{(d)max}$. Their results suggested that the degree of compaction directly impacts the soil void ratio, i.e. voids volume decreases with respect to increasing water content under a given compactive effort (Lambe & Whitman, 1969). Lambe and Whitman (1969), was simply describing the mechanisms of compaction whereby air voids are expelled by the rearrangements of soil particles with the aid of moisture. This reaffirms that voids or pore spaces are key factors in compaction.

When examining the mechanical properties of soil that influences its stability, inherent anisotropy should be considered also, as suggested by Yokohama *et al.* (2014), because of its effect on shear strength. The findings of Yokohama *et al's*. (2014) concluded that the soil's anisotropy influences the mechanical properties, such as those mentioned by Wesley (2009), under saturated conditions during compaction. Furthermore, Toll (2000, as cited by Çokça & Tilgen, 2010) added that soil fabric plays an important role in the engineering behaviour of compacted soils because during compaction they can undertake various forms to the dry of w_{opt}; aggregated or "packet" fabric being the prominent one. This change in microstructure was described by Lambe (1985b, as cited in Fener & Yesiller, 2013)

as the flocculated arrangement that is commonly associated with compaction of clay to dry of w_{opt}.

2.1.4 Shear strength of compacted volcanic ash fills

The shear strength of compacted fills also play a key role in ensuring its stabilization. After compaction, compacted fills can become saturated which can have direct implications on the soil shear strength and thus its overall stability (Çokça & Tilgen, 2010). Studies have shown that high compactness have direct correlations to high soil strength, lower permeability and compressibility, and lower susceptibility of other engineering properties of soil to alter when subjected to changes water contents (Gue & Liew, 2001; Wesley, 2010). Çokça & Tilgen (2010) cited two primary sources of fill saturation after compaction as rainfall and or rising groundwater. Even though the idea of completely dismissing rainfall and groundwater rise is unrealistic, these natural elements can be controlled to a certain extent. The solution lies in higher compactness as mentioned earlier. A study by Gregory *et al.*, (2006) showed that compaction, whether inadvertent or intentional, significantly reduces (70 -90 %) infiltration rates in the soil structure. Since compaction automatically changes the soil's structure, the manner in which air and water move throughout the soil mass is also affected. This implies that if higher compactness is achieved, the potential for oversaturation will be minimized because infiltration rates will consequently be reduced also.

Many studies have reported on how influential soil water content is, i.e. the degree of saturation before, during and most importantly, after compaction and its effects on soil strength. Samim and Sugiyama (2016) conducted a study on the strength and deformation characteristics of unsaturated volcanic soils where tri-axial and elasto-plastic finite element analysis methods were employed on statically compacted soils. Even though the compaction method employed in their study differs markedly to the impact method proposed for implementation in this research, they were able to prove degree of saturation and matrix suction to be the two key components affecting the shear strength and deformation characteristics of the unsaturated soils.

Another major factor that controls the shear strength, water retention capacity, and volume change behaviour and soil hydraulic conductivity is pore size distribution (Otalvaro *et al.*, 2016). The "combined use of mercury intrusion porosimetry (MIP) and determination of the water retention curve (WRC) along a drying path" was reviewed in Otalvaro *et al.* (2016) to analyse the structural behaviour and water retention characteristics of compacted residual soils. Fener and Yesiller (2013) cited numerous previous studies that used MIP along with scanning electron microscopy (SEM) to gather information regarding the arrangement of particles, pores, pore sizes and distribution, particle assemblages.

Another comprehensive study was undertaken by Fener and Yesiller (2013) on pore structures in compacted clay to demonstrate the relationship between pore size distribution and compaction using Pore Area Ratio (*PAR*) parameter to quantify the pore structures. The *PAR* results showed that the trends were stronger in the dry of w_{opt} and near w_{opt} compared to wet of w_{opt} where it is less pronounced. The results from the compacted specimens revealed that the presence of pore spaces increased succinctly from top to bottom within the specimens. Fener and Yesiller (2013) attributed this to the fact that layers near the bottom of the specimen are more compacted then the layers on top because of the higher cumulative compaction energy that's received by the bottom layers during compaction.

2.2 Alternative methods to determine the Optimum Moisture Content and Maximum Dry Density of volcanic soils

Over the years, numerous attempts were made to determine the $\rho(_d)_{max}$ and w_{opt} of fine-grained compacted soils. Blotz *et al.* (1998) developed an empirical method to estimate the maximum dry density and optimum moisture content for clayey soils. Their method encompassed two variations where one variation used liquid limit (LL) and a compaction curve while the other used only the LL. The results concluded that the variation involving the LL and compaction curve generated more precise results than the LL variation (Blotz *et al.*, 1998). All the soil specimen used in their research was compacted using four different compactive efforts including standard Proctor, modified Proctor, "reduced" Proctor and "super" modified Proctor. Overall, a slightly different approach to the proposed methods to be

implemented in this study, i.e. only standard and modified Proctor tests will be conducted.

In another study, Jesmani *et al.* (2008) expounded on the compaction of clayey gravels and the implementation of mathematical models to determine the $\rho(_d)_{max}$ and w_{opt} parameters under various compactive energies, clay percentage and the spatial surface. A comparison of the results between the empirical methods and the predicted $\rho(_d)_{max}$ and w_{opt} values revealed high accuracy, thus validating the empirical methods (Jesmani *et al.*, 2008). The method applied in their study is different from the conventional methods of standard compaction tests proposed to be applied in this research where $\rho(_d)_{max}$ and w_{opt} are calculated and graphically derived after Standard Proctor Tests. Despite performing the tests on clayey soils with granular components, Jesmani *et al.* (2008) reported that $\rho(_d)_{max}$ and w_{opt} are functions of the fines content only, hence their method was applicable to the clay content of the compacted soil. Matsumura and Tatsuoka (2018) supported this concept by stating that fines content of a compacted soil largely influences the water content and dry density when determining the cyclic undrained strength in a stability analysis of compacted soil structures.

Another method of estimating the $\rho(_d)_{max}$ and w_{opt} was proposed by Sivrikaya and Soycan (2010) called artificial neural network (ANN) modelling. According to Sivrikaya and Soycan (2010), this method has gained recognition and popularity in geotechnical engineering applications in the recent years. In their research, Sivrikaya & Soycan (2010) used data collected from previous Standard Proctor and Modified Proctor tests to develop ANN models using what is known as a "feed-forward back-propagation algorithm" which they claimed generated reliable estimations of the compaction parameters, $\rho(_d)_{max}$ and w_{opt}.

2.3 Knowledge Gap

Regardless of the numerous studies conducted on the compaction of volcanic soils (Orense *et al.*, 2006; Rahmat & Ismail, 2018; Samim & Sugiyama, 2016; Wesley, 2009), none directly addresses the Hamilton Ash unit of North Island, New Zealand. The methodology implemented in previous studies to determine the optimum moisture content and maximum dry densities differ from one study to another but

all emphasized the importance of degree of compaction and the importance of a soil's mechanical properties with correlation to achieving the two primary compaction factors. In this research, the geotechnical characteristics of Hamilton Ash such as the index properties, permeability, compaction characteristics and strength and deformation behaviour in undrained conditions will be investigated. Previous studies have indicated these characteristics to be exerting dominant influences in the compaction of clay fills and will therefore be assessed to determine optimum moisture content under which maximum dry density and corresponding maximum compaction are achieved. The possibility of shear strength degradation due to soil saturation after compaction and corresponding degradation rate will also be explored. The outcome of this study will provide the engineers with the necessary design parameters and guidelines regarding the use of Hamilton materials for geotechnical purposes.

Chapter 3

Research Methodology

3.1 Introduction

This chapter outlines the field and lab methods used to obtain data for this research. During field work, 13 sample bags of reworked soil were sampled from an existing stockpile and transported to the laboratory, transferred onto trays and then fragmented into workable sizes. Laboratory tests were carried out in accordance with New Zealand (NZS) and ISO standards. Lab analyses used included grainsize analysis using Laser Diffraction, X-Ray Powder Diffraction (XRD), Atterberg (Consistency) Limits, Standard Compaction Test, and Vane Shear tests to determine the geo-mechanical characteristics and mineralogical composition of the soil used in this study.

3.2 Field Methods

3.2.1 Site Selection

The area of sampling used for this study was a new residential block in the Rotokauri area in Hamilton, New Zealand that was under construction at the time of sampling (Figure 3.1).

Figure 3.1 Location of the residential construction site in the Rotokauri area of Hamilton, New Zealand where Hamilton Ash materials were sampled (sourced from Google Maps, 2019).

The materials were sourced from an existing stockpile of disturbed Hamilton Ash that had undergone extensive reworking, with the soil having little preserved structure. The stockpile was situated towards the entrance of the site's active construction area, sitting adjacent to a series of catchment ponds (Figure 3.2).

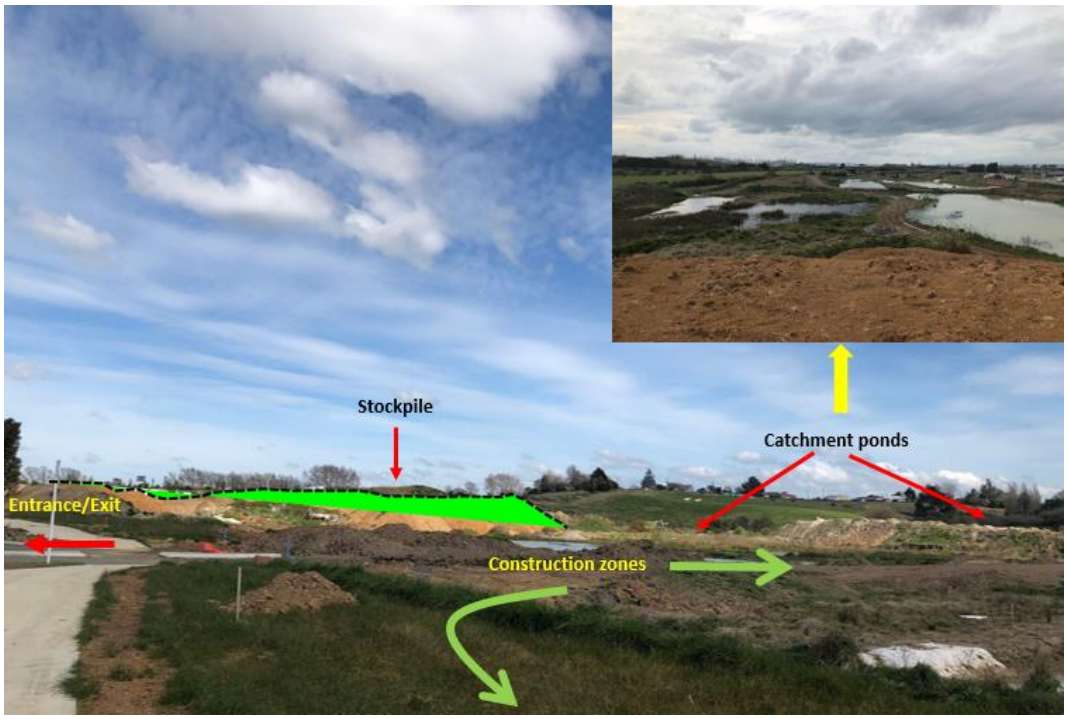

Figure 3.2 Location of stockpile and catchment ponds where the samples were sourced.

3.2.2 Sampling Methods

No existing standards were used to guide the sampling process. Samples were excavated using metal spades and roughly 1-1.5 kg of soil was loosely packed into each high grade plastic bag for transportation (Figure 3.3). In total, 13 bags of Hamilton Ash samples were collected for testing (Figure 3.4).

Figure 3.3 Samples excavated from the stockpile.

Figure 3.4 Thirteen (13) bags of sample collected and transported to the laboratory for processing.

3.3 Laboratory Methods

3.3.1 Sample Preparation

3.3.1.1 Preliminary Sample preparation

All 13 bags of samples were transferred onto medium-sized, plastic (30 x50 x 10cm) and aluminium trays of 9 cm diameter by 3 cm height. Samples exceeding 100 mm were fragmented by hand into smaller portions to accelerate the air-drying process (Figure 3.5). Samples were allowed to air-dry at room temperature of ~24°C with 70% humidity, for a maximum of 7 days during which daily tending and reworking was performed to ensure thorough drying of the soil. Upon completion of the drying period, the soils were packed away in air-tight plastic bags to prevent further loss of moisture and stored away.

Figure 3.5 Samples were air-dried for 7 days.

3.3.1.2 Standard Compaction Test Sample Preparation

This section describes the procedure engaged for sample preparation prior to standard compaction tests that were performed to determine the soil's optimum moisture content at which the maximum dry density was achieved. The samples were prepared in accordance with New Zealand Standards NZS 4420:1986 Test 4.1.1 (Standards Association of New Zealand, 1986).

Apparatus

a) 19.00 mm sieve and receiver
b) 1 Medium plastic tray
c) A 700 mL beaker
d) Spray bottle containing tap water
e) 5 high grade plastic bags with seals
f) A hand trowel
g) Two triangular spatulas for mixing
h) A balance scale measuring to 0.001 grams

Procedure

1. Moisture content determination placed the natural moisture content of the soil at 50.7 % but since the soils were intended to be tested in an air-dried state, the samples were dried back to 26 % moisture content for a period of 7 days. Basing off the air-dried moisture content, an assessment for the added water content range for all 5 tests was estimated. In all 5 tests, moisture was added to the soil by increments of 2 percent from the initial test, i.e. Test 1 = 9 % (225 g), Test 2 = 10 % (275 g), Test 3 = 13 % (325 g), Test 4 = 15 % (375 g) and Test 5 = 17 % (425 g). The 2 % increments were aimed at acquiring 2 samples dry of optimum and 3 samples wet of optimum moisture content.
2. 2.5kg of air-dried soil passing through the 19.0 mm sieve were received and emptied into a tray for mixing.
3. 225 g of tap water was weighed in a beaker and added to the tray of soil (Figure 3.6).
4. The soil was mixed until an even consistency was attained.
5. The wet soils were transferred into a labelled, high grade, plastic bag and sealed tightly while making sure to not trap any air in the bag.

6. The tray was cleaned out and dried for the next test.
7. Steps 2 – 6 were repeated for the remainder of the tests with variations in Step 3 according to Step 1.
8. All the samples were placed in a dry area to cure at room temperature for 16 hours.

Figure 3.6. (i) The designated water content for the test was weighed, added to the dry soil and (ii) mixed till even consistency was achieved.

3.4 Soil Characterisation Tests

3.4.1 Grain Size Analysis

Aim

Laser diffraction was used to accurately measure the particle size distribution of Hamilton Ash in this study. By determining the distribution of this particular property, an understanding of the packing density and porosity within the soil matrix can be gained. A total of 5 different runs were performed for repeatability purposes.

A Malvern Mastersizer3000 laser diffractometer capable of measuring precisely particles in the size range of 10 nm to 10 mm was used to determine the particle size distribution instead of implementing the more traditional techniques like sieving and procedures based on sedimentation, such as pipette and hydrometer methods. LD employed the Mie theory of light scattering to measure and analyse the distribution of particles within the test sample. The dispersed particles that passed through the optical bench that housed the angle detectors, sample measurement cell and laser compartment, were illuminated by a laser beam. With great precision, a series of detectors then measured the light that was scattered by

the different sized particles from a wide range of angles. The angle at which the laser beam was diffracted was inversely proportional to the particle size, and the number of particles in the cross-sectional area of the beam's path was calculated by a measure of the intensity of the diffracted beam.

Apparatus

1) Malvern Mastersizer 3000
2) Five 250 mL beakers
3) One teaspoon
4) One disposable pipette
5) At least 200 mL of Calgon
6) Spray bottle containing distilled water

Procedure

1) A teaspoon of dry soil was placed in each of the 5 beakers
2) Distilled water was added in each beaker until the soil was fully submerged and the water level was about 2-3mm above the surface of the soil.
3) Approximately 2-3 mL (a splash) of Calgon was added into each beaker.
4) Using the teaspoon, the soil was mixed thoroughly and left to soak overnight to allow the particles to deflocculate (Figure 3.7).
5) The Mastersizer 3000 software was launched on the computer and a previously created folder was opened from FILE.
6) The option SOIL was selected in RUN SOP to open the main working space where all the commands and graphs are displayed.
7) Clicked START to commence.
8) The tank was automatically filled. Using the disposable pipette (Figure 3.8), the sample was extracted from the beaker and added slowly into the mixer (tank), making sure not to add past the set obscure limit of 20 %.
9) The sample was automatically mixed for a few minutes before passing through the tubes into the laser compartment where the particles were measured using laser projections.
10) The results and graphs for the test were displayed on the monitor where they were exported as a PDF file.

11) Tank draining commenced automatically and the command for refilling for cleaning was activated at least 4 times to thoroughly clean out the tank.
12) Steps 7-11 were repeated 4 more times for the remainder of the samples.

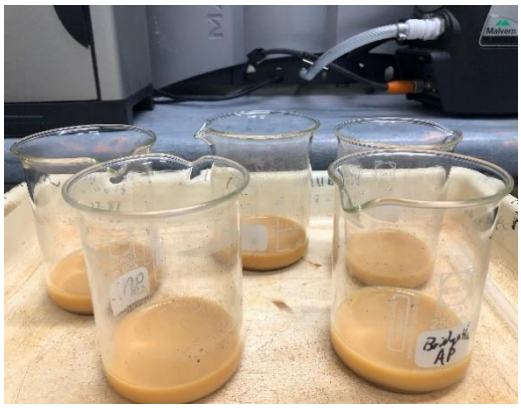

Figure 3.7 All five samples after soaking overnight in calgon and distilled water.

Figure 3.8 Using a disposable pipette to extract the sample and adding it into the mixer.

3.4.2 Mineralogical Analysis

Aim

The mineralogical analysis of a sample of Hamilton Ash was assessed through X-Ray Powder Diffraction (XRD). The machine used was a Panalytical Empyrean XRD in the Faculty of Science and Engineering, University of Waikato. The standard operating procedure (SOP) used was the University of Waikato SOP for XRD, modelled after Cunningham (2012), Whitton & Churchman (1987) and Lowe & Nelson (1983). Mineralogical analysis was undertaken to determine the mineral composition of soil in order to identify the different mineral species present and gain a better understanding of their characteristics and properties. The XRD method is a powerful analytical technique that is used primarily for phase identification of crystalline materials and quantification of unit cell dimensions. The entire test procedure which included sample preparation and XRD was carried out for a period of 5 days.

Apparatus

a. Panalytical Empyrean X-Ray Diffractometer
b. Two 15 mL centrifuge tubes and a rack for holding
c. A small spatula

d. Sieves – 200 μm and 500 μm
e. Sodium hexametaphosphate solution (8mL/sample)
f. Automatic pipette – 1 and 8 mL and pipette tips (3 for each sample)
g. Disposable pipettes (2/sample)
h. Saturated magnesium chloride ($MgCl_2$) – 2mL/sample
i. Two 50 mL beakers (1/sample)
j. 1:1 Hydrochloric acid (HCL) – 1 drop/sample
k. pH test paper
l. Distilled water
m. Two ceramic tiles that are cut to size with relative thickness to fit holder (1/sample).
n. Quartz standard, blank ceramic tile.
o. Formamide (1 drop/sample)
p. Ultrasonic bath
q. Centrifuge
r. Desiccator with distilled water
s. Desiccator with 10% ethylene glycol
t. Oven and furnace
u. Large dry desiccator for cooling

Procedure

1. Day 1 – Sieving
    i. Prior to sieving, both sieves (200 μm and 500 μm) were rinsed for 5 minutes in the ultrasonic bath and dried overnight.
    ii. The clay fraction sample was sieved firstly through a 200 μm sieve and then through a 500 μm sieve. Approximately 2 mL of soil that passed through the individual sieves were placed in two separate centrifuge tubes using a spatula and labelled accordingly as seen in Figure 3.9. It was later decided that only one of the clay samples was to be used in the analysis; clay sample 2 (200 μm) was used and sample 1 was discarded.
    iii. Samples for bulk analysis did not require sieving, therefore 2 mL of the air-dried sample was placed directly into a different centrifuge tube and labelled accordingly.

Figure 3.9 Centrifuge tubes containing 2 mL of the bulk and sieved clay fraction samples.

2. Day 2 – Separation of clay fraction
    i. 8mL of sodium hexametaphosphate solution was added separately into the centrifuge tubes containing the clay fraction and bulk samples using a 10 mL automatic pipette and shaken well.
    ii. Making sure that the heat function was turned off, both centrifuge tubes were placed in the ultrasonic bath for 5 minutes, ensuring that the tubes were completely submerged.
    iii. The clay sample was shaken well and placed in the centrifuge for 3 minutes at 800 rpm. All 4 carriages were occupied with blanks and sample having equal weights of 15 g (blanks were used to maintain proper balance throughout).
    iv. The suspended clay particles were sectioned into 3 distinct layers after being rotated in the centrifuge (Figure 3.10). The clay portion (upper layer) of the sample was drawn out using a disposable pipette and placed in a beaker for $MgCl_2$ treatment (Figure 3.11). The silt and sand fraction of the sample was retained.

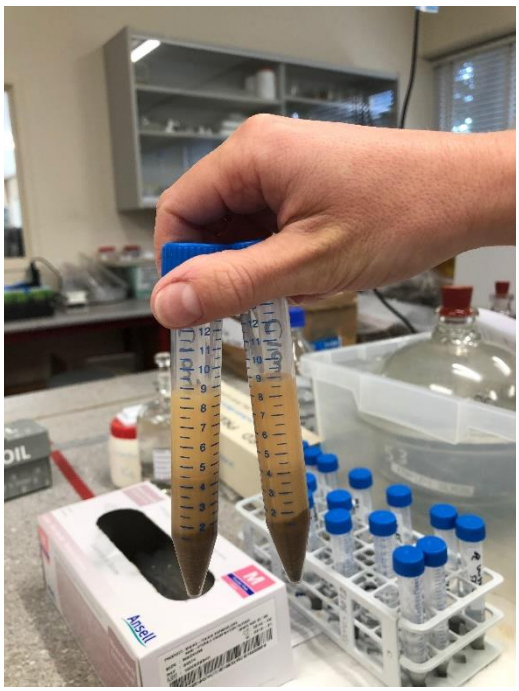

Figure 3.10 Clay fraction samples after 3 minutes run in the centrifuge – clay particles occupied the topmost layer and the silt/sand portions settled beneath it.

Figure 3.11 Extracting the suspended clay fraction from topmost layer of the sample.

3. Mg^{2+} saturation

    i. 2mL of saturated $MgCl_2$ was added to the beaker containing the suspended clay fraction using a 1 mL automatic pipette. Immediately after this, a disposable pipette was used to add barely a drop of 1:1 HCL to the beaker until the pH was about 3.5 (Figure 3.12).

    ii. Distilled water was added to the suspended clay fraction bringing the total volume to 50 ml and was set aside to flocculate/settle overnight.

Figure 3.12 $MgCl_2$ was added to the suspended clay sample and allowed to settle overnight.

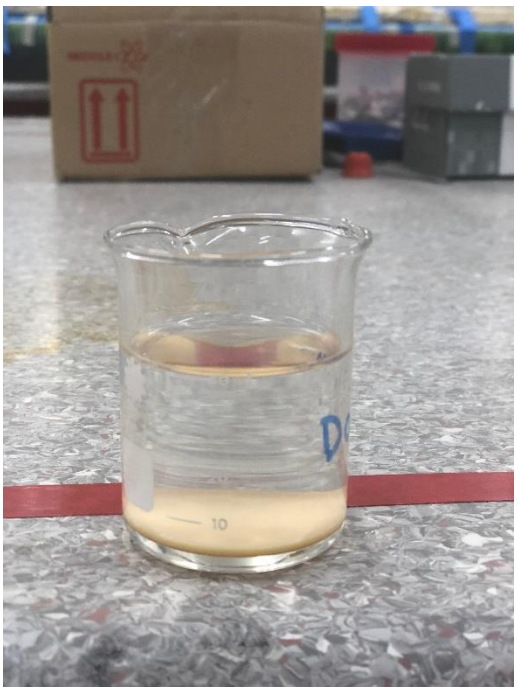

Figure 3.13 After 24hrs – clay particles have settled to the bottom for the beaker.

4. Day 3
    i. The clear supernatant liquid layer above the settled clay particles was carefully removed from the beaker using the 10 mL automatic pipette followed by the smaller 1 mL pipette (Figure 3.13). Care was taken not to disturb or remove the clay particles at the bottom of the beaker. The beaker was then topped up with distilled water up to 50 mL and allowed to settle overnight.
5. Day 4
    i. The clear supernatant liquid was again removed and discarded, leaving only the saturated clay behind. The Mg^{2+} saturated clay was then ready for slide preparation.

6. XRD slide preparation
    i. A desiccator containing about a 1 cm deep layer of distilled water at the base was set up at a suitable location on the bench so as to limit any movement once the samples were placed in.
    ii. About 0.5 mL of clay was transferred onto two clean ceramic tiles using a disposable pipette, making sure to even out the surface of the

clay and avoid clustering in one area. The samples were then left to dry in the desiccator for 72 hrs (Figure 3.14 and Figure 3.15).

Figure 3.14 Preparing the slides to add the saturated clay on to them.

Figure 3.15 Slides placed in the desiccator for drying for 72 hours.

XRD Runs

This section of the procedure includes 4 XRD runs: (1) Dry (untreated), (2) after glycolation, (3) heated to 110°C, (4) heated to 550°C.

7. Day 1 of XRD

   i. XRD (1) was performed once the sample was dry enough. The two clay XRD slides, quartz standard and blank ceramic tiles were placed in the x-ray diffractometer and run according to the following specifics: 2- 45 ° 2θ at 120 seconds per step.

   ii. Immediately after XRD (1), one clay sample (slide) was placed inside a desiccator that contained 10 % ethylene glycol at its base for 36 hours. This was to allow the absorption of ethylene glycol.

   iii. Formamide test – one drop of formamide was added to the other clay sample (slide) and analysis was conducted within 1 hour of adding formamide using the same settings in XRD (1).

8. Day 2 of XRD

   i. XRD(2) - After 36 hours of glycolation, the clay sample (slide) including the quartz standard and blank ceramic tiles were placed in the x-ray diffractometer and run according to the same settings in

XRD(1). Meanwhile, the oven temperature was set to 110°C and heating commenced.

ii. The clay sample was placed in a clean pie tray and heated for an hour at 110°C. While the sample was heated at 110°C, the temperature was raised to 550°C because the oven normally takes about 40 minutes to reach 550°C. After heating at 110°C for an hour, XRD (3) which included the clay sample, quartz standard and blank ceramic tiles was run under the same settings as XRD (1) and (2).

iii. The clay sample was placed on a larger tile in a pie tray and heated in the furnace at 550°C for 1 hour. The sample tray was removed after an hour and placed in a large desiccator to cool down. After 15-20 minutes of cooling period, XRD (4) which included the clay sample, quartz standard and blank ceramic tiles was executed under the same settings as XRD (1).

9. The sample for bulk analysis was not treated with any of the treatments applied to the clay sample (ethylene glycol, heated at 110°C and 550°C). The sample was crushed to fine powder with a porcelain mortar and pestle, a small portion was carefully placed on a ceramic tile and was run in the diffractometer under 5-80 ° 2θ, at 50 seconds per step.

3.4.3 Soil Consistency - Atterberg Limits

Aim

Atterberg Limits tests were carried out to determine the consistency of Hamilton Ash. The limits tested for included liquid (LL) and plastic (PL) limits from which the plasticity (PI), liquidity (LI), activity (AI) and consistency (CI) indices were derived. In addition, the water contents of the soil under different states were determined; natural moisture content (NMC), moisture content after 7 days of air-drying (NMC_i) and moisture content of the soil paste at which 15 mm of cone penetration was achieved (w_i). All tests were carried out using ISO/TS 17892-12:2004(E) (International Standards Organization, 2004) where the liquid limit was determined using the Cone Penetration method and plastic limit by thread-rolling.

Apparatus

The following apparatus were used in determining the Atterberg Limits:

a. Automated Cone Penetrometer (Figure 3.16)
b. Two flat glass plates
c. Two triangular spatulas
d. A palette knife
e. An evaporating dish
f. Balance with accuracy of 0.03 g and readable to 0.01 g
g. At least 10 small aluminium dishes for water content determination
h. A wash bottle containing distilled water
i. A 0.4 mm test sieve and receiver
j. Air-tight plastic bags, at least 2 of them

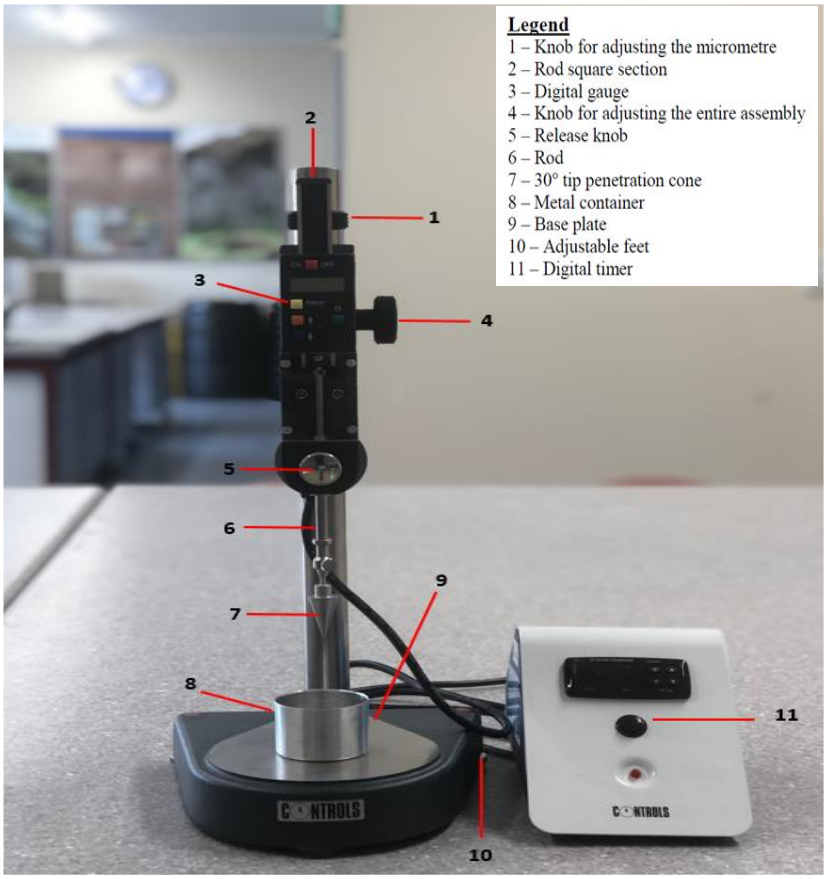

Figure 3.16 Drop Cone Penetrometer

Procedures

Liquid Limit

1. Sample preparation included passing 200 g of air-dried soils through a 0.4 mm sieve.
2. Distilled water was added to the dry soil and continuously mixed using the two triangular spatulas to form a structureless paste.
3. Roughly 20 g of the paste was placed aside in the evaporating dish and covered for the plastic limit determination.
4. Using a palette knife, a portion of the paste was placed in the metal cup making sure not to entrap air. Excess soil on the top was scraped off using the palette knife.
5. The metal cup was placed on the base, directly under the drop cone.
6. Ensuring that the penetration cone was secured and facing the downward position, the supporting assembly was lowered carefully and slowly until the tip of the cone slightly touched the surface of the soil.
7. The rod square section was pushed down until it was in contact with the top of the rod attached to the cone (Figure 3.16 - 2).
8. The initial reading on the automatic gauge was recorded.
9. The release knob was pressed to release the cone for 5 seconds.
10. The penetration of the cone was then recorded as the difference between the final and the initial reading.
11. The cone was lifted out of the metal cup and wiped clean.
12. A small portion of the paste was added onto the area of penetration and levelled out before further testing was conducted.
13. Steps 11 and 12 were repeated 4 more times to obtain a good average reading.
14. About 10 g of the penetration area was sampled at the end of the final test and placed in a small aluminium tray for water content determination.
15. The remaining paste in the metal cup was scraped out and added onto the rest of the sample paste on the mixing glass.
16. Steps 4 to 15 were repeated 4 more times using the same soil paste but different water contents. The amount of water added to the paste was done

so as to ensure that the penetration values increase with each tests and are evenly distributed.

Plastic Limit

1. Using the 20 g of paste that was set aside earlier, the specimen was placed on the glass plate and allowed to partially dry until it was able to be shaped into a ball.
2. The specimen was moulded between the palms until small cracks appeared on the surface of the specimen.
3. The specimen was then divided into two sub-specimens weighing about 10 g each for separate water content determination.
4. The first sub-specimen was further divided into four equal parts and steps 5 – 7 were repeated on each part.
5. Each sample was rolled between two fingers and the palm to form a thread.
6. The thread was placed on the mixing glass plate and rolled out using the tips of two fingers. Care was taken not to press hard and pressure was applied uniformly throughout the thread during rolling.
7. The thread was rolled out until the diameter was reduced to 3mm or until it cracked both longitudinally and transversely, an indication of the point of plastic limit.
8. The crumpled thread was placed in a small aluminium tray, labelled, covered.
9. The moisture content was immediately determined by placing the aluminium trays in the oven for 24 hrs.
10. Steps 4 to 9 were repeated for the second sub-specimen, placing the crumbled threads into a separate aluminium tray.

3.5 Standard Compaction Test

Aim

The primary objective of a standard proctor (compaction) test in this study is to determine the relationship between dry density and water content of Hamilton Ash using standard compactive effort in order to identify the point during soil compaction where optimum moisture content yields maximum dry density. All compactions tests were carried out according to New Zealand Standards NZS

4420:1986 Test 4.1.1. In every test, 5 samples with varying water contents were compacted with the aim of compacting 2 samples dry of optimum and 3 samples wet of optimum moisture content.

Apparatus

Listed below are the equipment used to conduct the standard proctor test.

a. A cylindrical metal compaction mould with internal diameter of 105 mm, 117 mm for internal height and a volume of 1013.1 ml (Figure 3.17)
b. A 2.5 kg standard compaction rammer comprising of 50 mm diameter of the flat surface and a free fall of 300 mm (Figure 3.17)
c. A palette knife
d. One balance scale measuring to 0.001 grams
e. A 19.0 mm test sieve and receiver
f. Two medium size trays
g. Five small aluminium sample trays for water content determination
h. Ten high grade plastic bags
i. Two triangular spatulas for mixing and extruding soil from mould
j. At least 2 wash bottles
k. A hand trowel
l. An oven

Figure 3.17 Standard Compaction mould (a) and rammer (b).

Procedure

1. Prior to every compaction test, the sample preparation procedure outlined in section 3.3.1.2 is carried out.
2. The mould and attached baseplate were weighed together and recorded. The extension collar was attached thereafter and placed on a smooth, solid floor to begin the test.
3. The cured sample was lightly shifted inside the plastic bag to release trapped air and moisture.
4. The first layer of soil weighing ~560 g was added into the mould followed by 27 consecutive vertical blows distributed evenly across the surface using the rammer. Layers 2 and 3 were added subsequently, each accompanied by 27 blows. Each layer of soil was measured prior to compaction to ensure that there was at least 3-5 mm of excess soil above the rim of the mould once compaction was completed. When the extension collar was removed, excess soil was gently scraped off using the palette knife. Each layer of soil weighed approximately 560 g. This number was increased by 10 g for the

remainder of the tests, i.e. the last test included layers that weighed 610 g each. The mass for each layer of soil was increased for each test to account for the elevated water contents. Figure 3.18 illustrates the samples compacted under increasing water contents.

5. The compacted soil, mould and attached baseplate were weighed together and recorded.
6. For water content determination, a portion of the compacted soil weighing roughly 20 g was extracted from the middle of the compacted soil after much digging using a spatula, placed in a small aluminium tray and oven-dried for 24 hours.
7. Steps 1 to 6 were repeated for the 4 remaining samples.

Figure 3.18 Compacted samples at increasing water contents: (i) 9 %, (ii) 11 %, (iii) 13 % (iv) 15 % and (v) 17 %.

3.6 Soaking Test

Aim

Eight samples were mixed and compacted to the optimum moisture content, which was established in Round 5 of Standard Compaction Testing as 13 % added w_{opt} (refer to section 3.3.1.2). The primary aim of these soaking tests was to investigate

the possibility of saturation and rate of seepage of moisture through the compacted soil over certain periods of time. The findings from these tests will enable further analysis on the influence of moisture from the environment on the soil shear strength. The NZS 4420:1986 Test 4.1.1 was used to compact the samples but regarding the soaking components of these tests, no standard procedure was engaged.

Apparatus

a) Standard Compaction rammer and moulds (x 5)
b) Six 18 L buckets with lids (Figure 3.19)
c) Distilled water – at least 5 L
d) Metal ruler
e) One balance scale measuring to 0.001 grams
f) A palette knife
g) 8 high grade plastic bags
h) A 600 mL beaker
i) A 400 mL spray bottle
j) Two triangular spatulas
k) A permanent marker
l) A 19.0 mm test sieve and receiver

Figure 3.19 Buckets used to carry out the soaking tests.

Procedure

1. Five separate samples were prepared and compacted according to section 3.3.1.2 and 3.5 of this chapter. Once compacted, the excess soil compacted past the rim of the mould was scraped off using the palette knife and a combined mass of the mould and compacted soil is obtained to the nearest 0.001 g using the balance scale.
2. Based on the combined height of the mould and base (117 mm) and an agreed excess water depth of at least 40 mm past the surface of the compacted sample, 160 mm was decided as the designated water limit to ensure full submersion. Using the metal ruler, the 160 mm limit was measured on the interior of the bucket.
3. After marking out the water limit, the bucket was filled up with distilled water to that set limit.
4. The compacted sample was carefully placed inside the bucket as depicted in Figure 3.20 and the soaking commencement time was recorded.

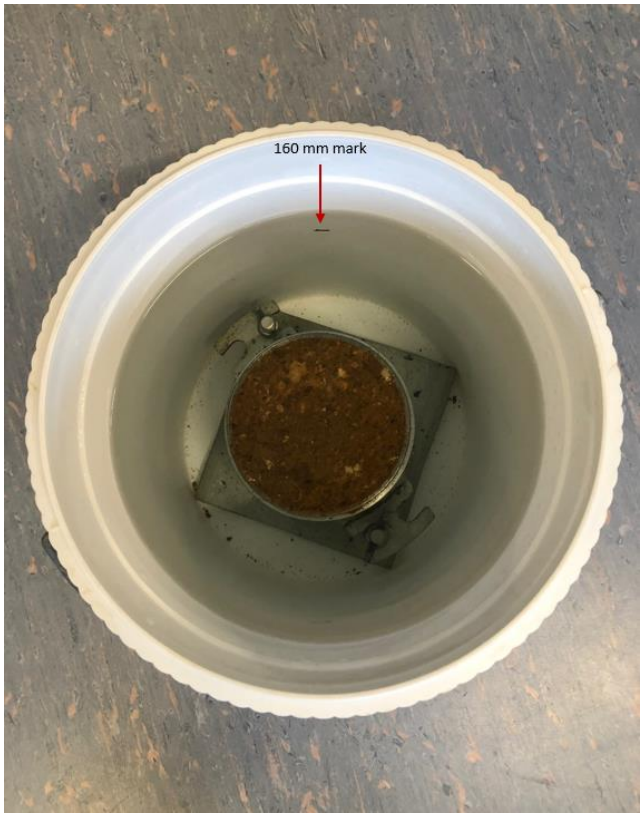

Figure 3.20 Compacted sample fully submerged in distilled water.

5. The depth of water above the surface of the compacted soil was measured and recorded.
6. In order to minimize loss of moisture to the environment, the mouth of the bucket was tightly secured with its lid.
7. Steps 2 to 6 were repeated 4 more times for the remainder of the samples.
8. At the end of the allocated soaking periods for each sample, a measurement of the water depth above the sample was obtained and the compacted sample and mould were carefully removed from the bucket and placed on a bench. Excess water on the base of the mould was wiped off.
9. The soaked sample was immediately weighed to attain its saturated mass and the surface of the sample was examined for any signs of swelling (Figure 3.21) and recorded accordingly.

Figure 3.21 Compacted samples after being soaked for a period of (i) 1 hour and (ii) 2 months.

3.7 Soil Strength Test

Initially, intended tests were the California Bearing Ratio (CBR), triaxial and vane shear tests. However, early compaction tests performed proved it impossible to extrude coherent, undisturbed triaxial samples from the compacted mass for testing in accordance with NZ standards. It became evident from the compacted mass that the degree of compaction subsequently decreased from the bottom of the mould up,

i.e. soil at the top of the mould was less compacted than soil at the bottom of the mould. For this reason, a sample of uniform coherence and consistency for triaxial testing could not be extruded, hence no triaxial test was performed. In addition, the tests planned for CBR were not conducted due to late arrival of equipment. As a result of this, laboratory vane shear was the only form of testing possible.

3.7.1 Vane Shear Test

Aim

The purpose of this test was to determine the undrained shear strength of the soil after undergoing compaction and being exposed to saturation. One dry (unsoaked) compacted specimen (sample 0) and 6 compacted, soaked specimens (samples 1-6) were subjected to vane shearing after being soaked for various time periods ranging from 1 hour to roughly 2 months (1248 hours). The findings will aid in determining the implications of prolonged exposure to saturation on the soil shear strength. The test was carried out in accordance with BS 1377 standard for Laboratory Vane Shear Testing for soils (British Standard, 1990).

Apparatus

a) A VJT5300 Motorised Vane Shear apparatus (Figure 3.22) which comprises of the following:
    i. Steel rod that has four steel blades (12.7mm wide x 12.7mm long) attached to the bottom of the rod at right angles
    ii. A circular graduated scale marked in degrees
    iii. Frame and stand
    iv. Vane mounting assembly
    v. Handle for rotating the vane head
    vi. Handle for raising and lowering the vane assembly
    vii. Base plate
    viii. Rotation pointer
    ix. Four distinct calibrated torsion springs to be used on the samples of different stiffness. In all 6 tests, torsion spring No.3 which was recommended for firm soils was utilized.
    x. Stationary graduated scale marked also in degrees
b) Compacted, soaked sample

c) Palette knife

d) Paper towels

e) Metal ruler

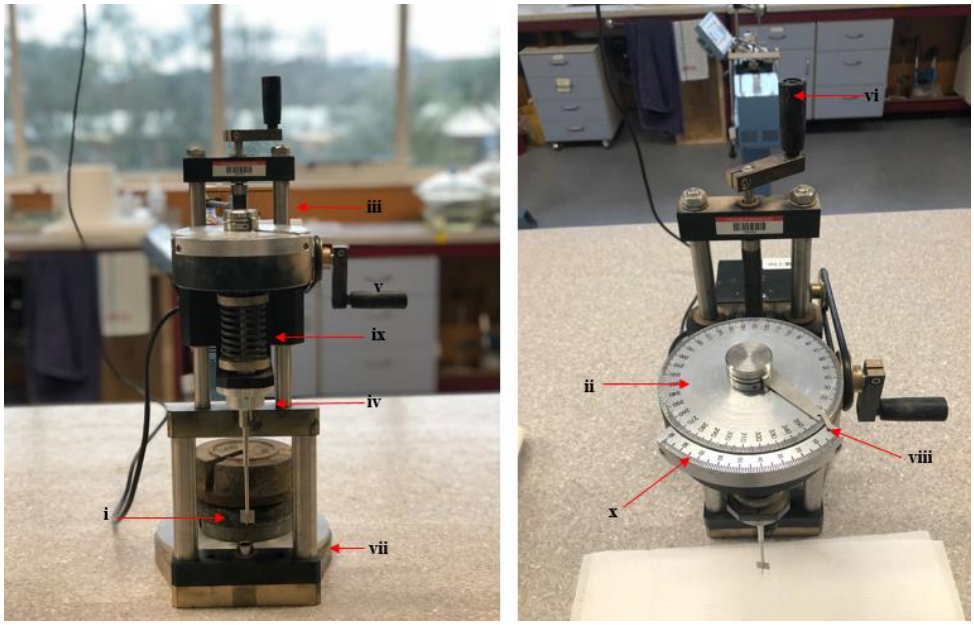

Figure 3.22 Motorised Laboratory Vane shear test apparatus.

Procedure

1. The motorised vane shear apparatus was assembled on a bench, the No.3 torsion spring was inserted, a clean vane was attached to the main frame, and the elastic band that connects both rotating wheels on the side of the main frame was fitted into place.
2. After the compacted soaked sample was dried of excess water and weighed, the sample was trimmed and levelled out evenly using the palette knife.
3. For sample 1, the test was to be conducted every hour for 3 hours, therefore 9 different spots on the surface of the sample were marked out evenly using the metal ruler and for every hour of soaking, the sample was subjected to vane shearing on 3 spots until all 9 spots were successfully penetrated (Figure 3.23). However, for samples 2-6 only 4 spots were marked out for vane penetration (Figure 3.24). Notice that sample 1 was repeatedly soaked and vane sheared 3 times whereas samples 2-6 were soaked once and then sheared. The reason being, early soaking tests conducted on the extensively air-dried soil from the first group of samples displayed almost instantaneous swelling upon interaction with distilled water so the sample 1 was soaked

for a short period (1 hour) and sheared repeatedly to determine if a similar pattern can be identified in the second group of samples.

Figure 3.23 Sample 1 – 9 different spots marked out on the specimen, 3 of which were tested after every hour of soaking for 3 hours.

Figure 3.24 Sample 2 presents how Samples 2-5 were marked out and tested.

4. Sample was mounted onto the base of the vane shear test apparatus.
5. The pointer on the graduated scale was set to zero (Figure 3.22- right).
6. The vane was gradually lowered into the marked out spot on the sample until the top of the vane was at a depth of 10-20mm below the surface of the sample.
7. The vane shear test apparatus was switched on by engaging the ON button which prompted the initiation of the application of torque to shear the sample. The vane was automatically rotated at approximately 12 degrees per minute.
8. Failure of the specimen was indicated by the snap backward movement of the strain indicator pointer on the circular graduated scale. The motor was switched off once the specimen failed. The final readings for the maximum angular deflection of the torsion spring and angle of rotation were recorded. The difference between the final and initial reading on the circular graduated scale is the angle of torque while the difference between the initial and final reading of the stationary scale is the angular deflection.

9. A remoulded test was initiated immediately after the vane was rotated rapidly through two revolutions in the sheared zone. Steps 7-8 were repeated for the remoulded sample.
10. The vane was gently removed from the sample to avoid tearing of the surface and rinsed out.
11. For Sample 1, steps 4-10 were repeated two more times on 2 different spots, soaked for the second hour, tested again on 3 different spots following steps 4-10 and then soaked again for the third hour and tested once again on the three last remaining spots. However, concerning samples 2-6, steps 4-10 were repeated subsequently without additional soaking until all 4 marked spots were penetrated.
12. After each sample was tested, a portion of the compacted specimen was extracted for water content determination which required sample weighing and oven drying for 24 hours at 105°C.
13. Samples 2-5 were soaked over varying time periods; sample 2 = 24 hours, sample 3 = 168 hours, sample 4 = 336 hours, sample 5 = 504 hours and sample 6 = 1248 hours.
14. The data gathered were used to calculate the undrained vane shear strength of the compacted, soaked samples.

Chapter 4

Results

4.1 Introduction

This chapter presents the results acquired in various laboratory tests conducted over a period of 5-6 months. Atterberg Limits, X-ray diffraction method for mineralogy, and laser diffraction for grainsize distribution results are presented individually under soil characterisation. A number of attempts at compacting Hamilton Ash samples to the Optimum Moisture Content (w_{opt}) and Maximum Dry Density $(\rho_d)_{max}$ were executed until the key compaction parameters were successfully obtained, all of which are documented under Standard Compaction and Shear Strength respectively. The results for the soil characterisation tests will enable Hamilton Ash to be defined methodically from grain sizes down to the specific mineral contents. Furthermore, the key compaction parameters and corresponding shear strengths before and after a subsequent period of soaking for the compacted samples will provide some insight into the strength and deformation characteristics of Hamilton Ash.

4.2 Soil Characterisation

4.2.1 Grain Size Analysis

The size, shape and distribution of particles in a soil mass strongly influences the properties and behaviour of any type of soil, be it cohesive or cohesionless. Like all soils, Hamilton Ash is comprised of a mixture of minerals of various shapes and sizes. The analysis of the grain size distribution of Hamilton Ash samples involved determining the volume percentage within the different size ranges according to the New Zealand standards. Grain size measurements and analyses were achieved through the laser diffraction (LD) technique and the results, which are represented as percentage of the total mass of soil occupied by a given size fraction in the form of distribution curves, are presented in this section. Repeatability of the initial results was able to be carried out successfully in 4 additional tests.

Table 4.1. Tabulated numerical values of clay, silt and sand for all 5 test samples.

Sample Name	Grain size ranges (μm)					D_{10}	D_{50}	D_{90}
		Clay	Silt	Sand				
	< 0.01	< 2	< 63	< 2000	< 3500			
Hamilton Ash_1	0.00	9.69	47.94	100	100	2.09	72.5	443
Hamilton Ash_2	0.00	25.86	77.17	100	100	0.262	8.28	166
Hamilton Ash_3	0.00	19.84	69.8	100	100	0.376	15.4	236
Hamilton Ash_4	0.00	13.03	56.72	100	100	1.01	42.6	318
Hamilton Ash_5	0.00	26.89	83.93	100	100	0.261	6.89	108

Summarized in Table 4.1 are the various size ranges established by the USDS soil classification system and their corresponding cumulative percentages for the grain size measurements of the initial test and subsequent repeatability tests. The most common percentiles of D_{10}, D_{50} and D_{90} generated by the Malvern software represents the maximum particle diameter below which 10%, 50% and 90% of the sample volume exists respectively. According to Table 4.1, Hamilton Ash_1 has the highest D_{10}, D_{50} and D_{90} compared to the rest of the samples. However, when considering the cumulative percentages for individual samples, Hamilton Ash_1 has the lowest values or the widest gap between each size range in comparison to the other samples.

The distribution curves in Figure 4.1 represent the data for the first LD test and four consecutive repeatability tests conducted sequentially thereafter. A relatively similar distribution trend is observed in all 5 test samples. The initial distribution curves generated by the LD software projected graphs that calculated the amount of particles within a specific size range by measuring the intensity with a unit measurement of volume percentage and the range of sizes are measured by angle of the diffracted beams. This graph is represented in Figure 4.2. However, the initial size distribution graph was converted to what is displayed in Figure 4.1 where the quantity of the particles measured within the different size ranges are calculated by cumulative percentages.

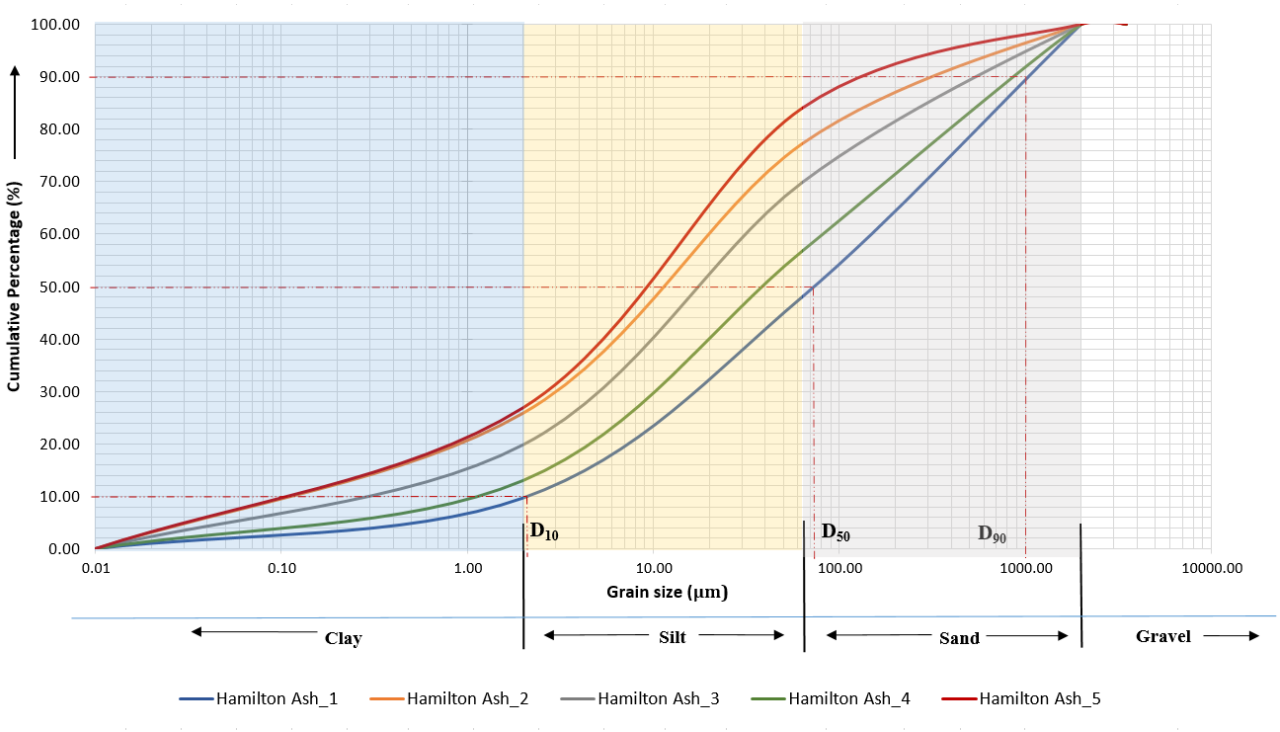

Figure 4.1. An illustration of the distribution of the different grain sizes in all 5 test samples. Marked D_{10}, D_{50} and D_{90} represent the common percentiles for Hamilton Ash_1.

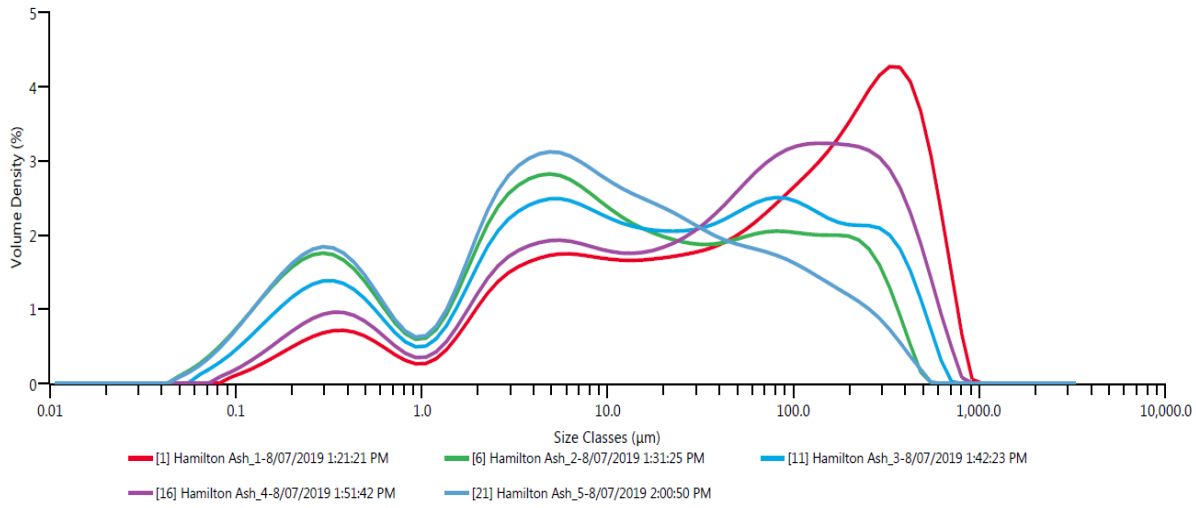

Figure 4.2 Laser sizer diffraction distribution curves showing particle size measurements in volume percentage.

The classification of Hamilton Ash can be defined based on Figure 4.1 and Table 4.2 by using the different size ranges for clay, silt and sand and subtracting them from their corresponding cumulative percentages. The results in *Table 4.2* show that the lowest percentage of clay and silt, and the highest percentage of sand particles are found in Hamilton Ash_1 whereas Hamilton Ash_5 contains the highest percentage of clay and silt and the second lowest percentage of sand particles. The samples are classified to the New Zealand Geotechnical Society's soil classification system. Even though, a similar distribution trend is created by all 5 test samples as illustrated in Figure 4.1, the results for Hamilton Ash_1 varies significantly from those belonging to the repeatability test samples. The standard deviation values in Table 4.2 show high variance between the clay, silt and sand fractions of the repeatability tests (Hamilton Ash_2-5) and the initial test (Hamilton Ash_1), especially in the sandy portion. However, the results from all 5 tests do conclude in general that the materials can be classed as silts, with significant portions of clay and sand. They should be considered as fine-grained soils.

Table 4.2. Classification of Hamilton Ash based on its particle size distribution

	Hamilton Ash_1	Hamilton Ash_2	Hamilton Ash_3	Hamilton Ash_4	Hamilton Ash_5	Average (%)	Standard Deviation
Clay (%)	9.69	25.86	19.84	13.03	26.89	19.06	6.4
Silt (%)	38.25	51.31	49.96	43.69	57.04	48.05	5.5
Sand (%)	52.06	22.83	30.2	43.28	16.07	32.888	11.7
Classification	Silty SAND with minor clay	SILT with clay and sand	Sandy SILT with some clay	Sandy SILT with traces of clay	Clayey SILT with some sand	Sandy SILT with some clay	

4.2.2 Mineralogical Analysis

Mineralogical analysis for a sample of Hamilton Ash was undertaken in a laboratory of the University of Waikato to determine and characterise its mineral fraction. The process of mineralogical characterization and estimation was accomplished through the widely used X-ray diffraction (XRD) Method. The composition and properties of the mineral fractions of a soil sample differs from one another and due to this it is imperative to clearly define the quantity and nature of each fraction. The standard XRD method compiled by Cunningham (2012, after Whitton & Churchman, 1987, and Lowe & Nelson, 1983) dictates that two sets of samples be prepared, bulk and clay. The former to test for the overall mineral fraction and the latter specifically for clay content analysis. Since the clay fraction of a soil is most reactive and generally tends to have the greatest amount of

influence on the soil, the results from the clay analysis test were considered to be of utmost interest. Both samples were prepared and tested accordingly and the results are presented separately in this section.

4.2.2.1 Bulk Sample Analysis

An untreated (dry) bulk sample was tested for the overall mineralogical content determination and the minerals quartz, kaolinite, halloysite and minor traces of cristobalite were detected. The results for the bulk sample test are displayed in the trace plot in Figure 3.5 where the samples were run from 5-80 °2θ, at 50 seconds per step.

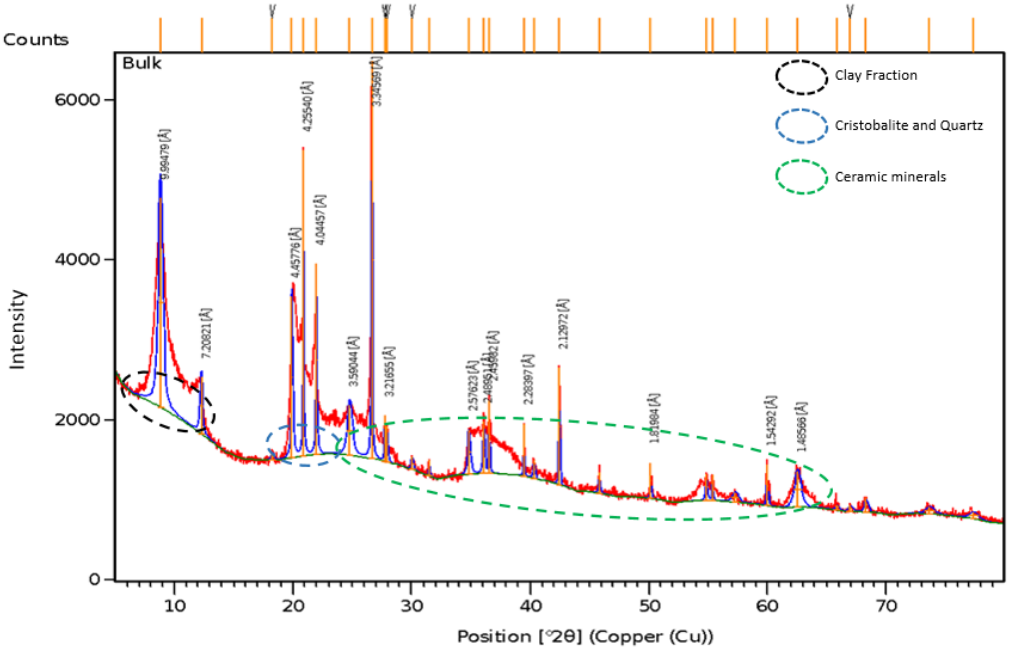

Figure 4.3 The variation in peaks in all four diffraction patterns represent the different mineral phases present in the bulk sample.

When a sample is subjected to x-ray diffraction, a wide range of peaks are generated which are later compared against reference diffraction patterns to precisely identify the types of minerals that are present in the sample. In general, clay mineral peaks are much broader with noticeable widths on both sides whereas well defined crystalline minerals typically produce sharp, narrow peaks. As observed in *Figure 4.3Figure 3.5*, the well-defined crystalline minerals like quartz and cristobalite have high intensities and high diffraction angles compared to clay minerals.

In Figure 4.3 the clay fraction of the sample, encircled by the black circle, were identified as 10Å-halloysite and 7.2Å-kaolinite. Both clays and the crystalline minerals were verified by known diffraction patterns. The presence of other well defined crystalline minerals like quartz and cristobalite are distinguishable by smaller d-spacing in the range of 4.5 – 4.0 and sharper peaks (blue circle). The rest of the peaks in the higher angles represent the minerals of the ceramic tile that was used for sample placement and are therefore not regarded as part of the sample's mineral content.

4.2.2.2 Clay Content Analysis

When identifying the clay minerals in an XRD trace plot, the d-spacing of the basal layer is regarded as a key identification marker because it represents the thickness of the silicate layer and ultimately distinguishes one clay mineral from another. As established in the bulk sample analysis, clay minerals are characterized by broad diffraction peaks of low intensity. Based on this understanding, it can be concluded from Figure 4.4 that there are two different phases of clays in the sample. Using the diffraction peak patterns for each phase, the d-spacing can be calculated.

The clay sample was tested under four different treatments; untreated (dry), glycolation, and heated to 110°C and 550°C separately. The results are represented by four diffraction patterns as depicted in Figure 4.4 where the samples were run from 2-45 °2θ at 120 seconds per step. The red and blue diffraction patterns represent the untreated clay sample and sample treated with ethylene glycol, respectively while the green and grey diffraction patterns depict the samples that were heated to 110°C and 550°C respectively. For the clay fraction of the sample, x-rays diffracted by the untreated sample peaked at 10Å (~8.8 °2θ) and was identified as halloysite. However, when treated with ethylene glycol, the d-spacing layer between clay molecules expanded to 11Å while the °2θ decreased to 8. In Run 3, the diffraction peak became more intense when heated at 110°C but no change in d-spacing was encountered. When the temperature was increased to 550°C in Run 4, the atomic structure of the clay fraction became completely destroyed.

Similar observations were made on kaolinite which shoulder peaked at 7.4Å (~12.1 °2θ) in Run 1 and 7.2 Å (~12.3 °2θ) in Runs 2 and 3. Table 4.3 summarises

the use of Bragg's Law to calculate the basal spacing for the two primary clay fractions identified in the sample.

Table 4.3 A quantitative analysis of the clay fraction XRD data – using diffraction peak patterns to calculate the unit cell dimensions (d-spacing) via Bragg's Law. The equation used to calculate the halloysite and kaolinite d-spacing is used after the British Crystollographic Association (2018).

Bragg's Law				
d = nλ/(2Sinθ)				
Order of Reflection (n) =	1			
Wavelength (λ) =	1.5406			
	Halloysite		Kaolinite	
Diffraction Patterns	*°2θ*	*Interplanar spacing (d) (Å)*	*°2θ*	*Interplanar spacing (d) (Å)*
Red (Run 1)	8.8	10.040534	12.1	7.3693
Blue (Run 2)	8	11.042703	12.3	7.1902
Green (Run 3)	8	11.042703	12.3	7.1902
Grey (Run 4)	Clay structure completely destroyed		Clay structure completely destroyed	

The rest of the peaks in the higher angles represent the minerals that comprise the quartz standard and blank ceramic tiles used in the test.

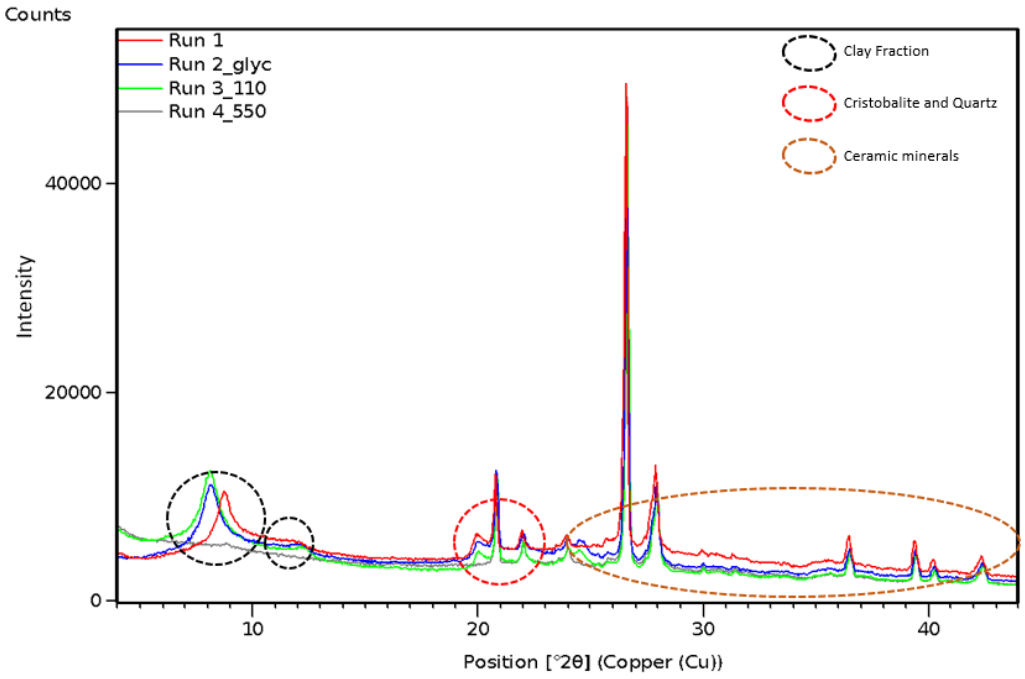

Figure 4.4 A trace plot for clay content analysis that depicts the different diffraction patterns for 4 treated and non-treated samples. The analysis revealed the presence of 10Å-halloysite and 7.4Å-kaolinite

4.2.2.3 Allophane Identity Test

The XRD tests for both the bulk and clay analyses did not detect any trace of allophane in the samples which contradicted a myriad of reports (Birrel & Fieldes, 1952; Bishop *et al.*, 2013; Lowe, 2010b; Lowe & Percival, 1993; Parfitt, 1990; Ward, 1967) that recognized allophane to be a key component of volcanic soils, Hamilton Ash included, throughout New Zealand and globally. On account of this, a simple identification test developed by Fieldes and Perrott (Brydon & Day, 1970) was implemented to test for the presence of allophane. According to the Fieldes and Perrott sodium fluoride test, the soil is allophanic if the filter paper holding the soil turns pink, which was the case in this instance, as seen in Figure 4.5. After adding 3 drops of sodium fluoride (NaF) to the soil, the filter paper that was dipped in phenolphthylein turned a moderate to strong hue of pink after roughly 5 mins. No further tests were conducted thereafter to quantify the percentage of allophane in the sample.

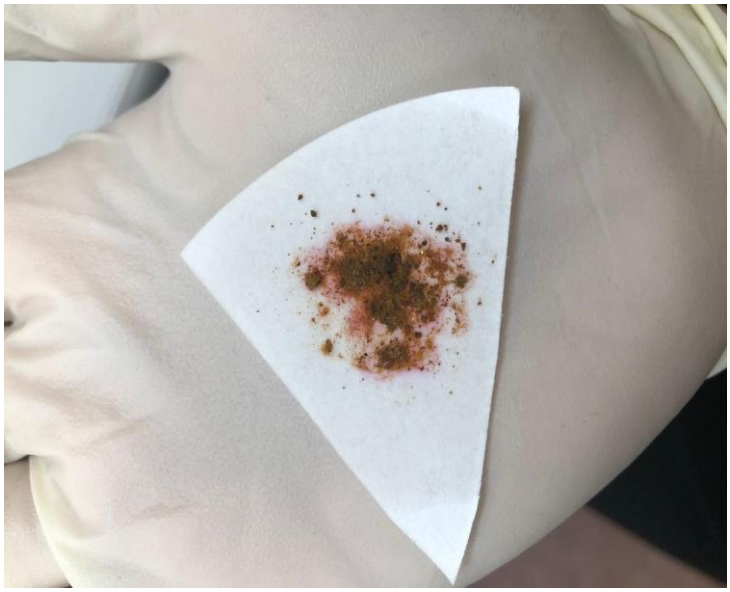

Figure 4.5 Three drops of saturated sodium fluoride (NaF) added onto the sample altered the filter paper colour to pink, an indication that the soil is allophanic.

4.2.3 Soil Consistency – Atterberg Limits

An important attribute of cohesive soils is that variations in water content can significantly influence the consistency of the sample from a state of liquidity where it is capable of flowing under its own mass, to plastic where the sample can be moulded or deformed readily and finally where the sample can traverse into a solid

state at which point brittle rupturing under small deformations is experienced. In this study, the consistency of Hamilton Ash was investigated in terms of the three primary Atterberg limits - liquid, plastic and shrinkage – using the standard drop-cone penetrometer and thread-rolling methods. These limits are important parameters in classifying soils and evaluating their behaviour in field applications. All three limits including the plasticity and liquidity indices were determined and quantified in terms of water content variation and the results are presented in this section.

Since air-drying was mandatory for this research prior to conducting compaction tests, all the samples tested under the series of laboratory tests in this research have been air-dried for a maximum of 7 days. The samples were at 26 % moisture content when Atterberg limits tests were performed. After the addition of a significant amount of water to the dry soil to form a structureless paste, the new moisture content for the paste used to determine the consistency limits and indices was 66 %.

4.2.3.1 Liquid Limit

A Standard Drop-Cone Penetrometer was used in place of the Casagrande device to determine the liquid limit of the soil under study. As seen in Table 4.4, average cone penetrations achieved from 5 rounds of tests range from 16.0 mm to 27.2 mm, a clear representation of the ease in soil penetration as the moisture content was gradually increased with each test. The natural moisture content (NMC) of the soil was determined on the day the samples were extracted and transported to the laboratory, prior to the air-drying phase. The soil was observed to be in a mildly saturated state at time of extraction and as expected, the water content determination test revealed the soil's NMC to be at 50.7%. However, after air-drying for a week, the initial moisture content (NMC_i) at time of testing was 26%.

Table 4.4 Measurements for liquid limit determination via drop-cone penetrometer test.

Test No.	1	2	3	4	5	NMC_i	w_i
Mass of container (g)	0.89	0.89	0.89	0.89	0.89	10.79	0.89
Mass of container + wet soil (g)	11.63	12.47	14.25	16.06	16.34	73.09	22.34
Mass of container + dry soil	7.20	7.59	8.57	9.49	9.49	52.13	17.92
Mass of water (g)	4.43	4.88	5.68	6.57	6.85	20.96	4.42
Mass of dried soil (g)	6.31	6.70	7.68	8.60	8.60	41.34	17.03
Water content (%)	70.21	72.84	73.96	76.40	79.65	50.7	25.95
Average cone penetrations (mm)	16.0	18.1	20.3	22.9	27.2		

The soil's liquid limit was determined from the graphical representation of the relationship between water content (%) and cone penetration depth (mm) where the water content corresponding to 20 mm of cone penetration yields the soil's liquid limit. According to Figure 4.6, the liquid limit for the test sample is 74%.

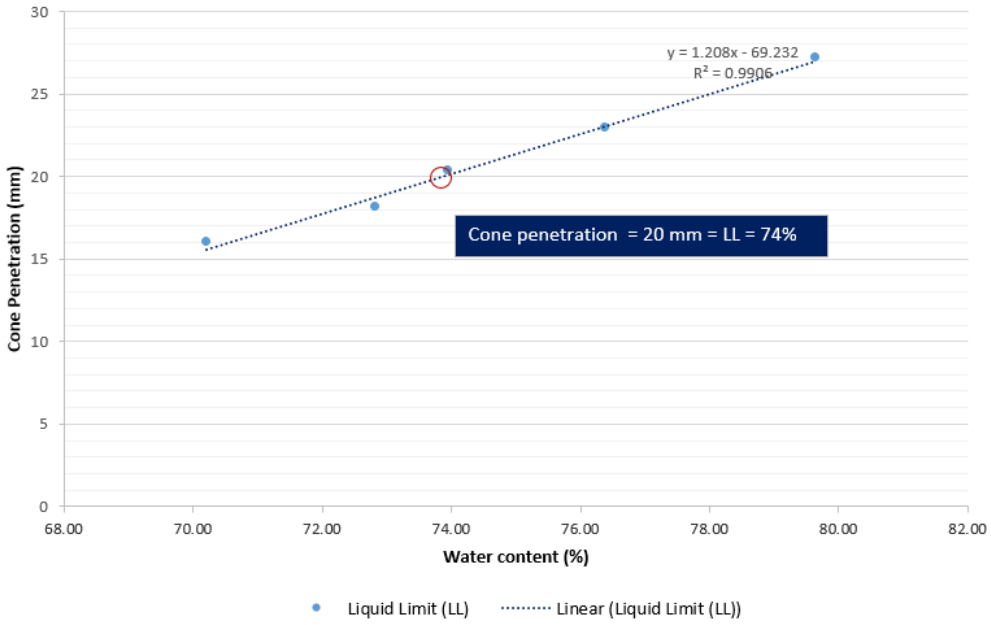

Figure 4.6 A graphical representation of the liquid limit of the sample derived from a linear relationship between the soil's water content and cone penetration.

4.2.3.2 Plastic Limit

The limit where the soil ceased to behave in a liquid manner and transitioned into a plastic behaviour through loss of moisture was determined using the thread-rolling method. The moisture content at which the soil threads crumbled under pressure is the soil's plastic limit. According to Table 4.5, moisture content after air-drying for 7 days was 26 % but after significant addition of water to create an ideal workable paste that yielded an initial cone penetration of 15 mm, the new moisture content

(w_i) was now at 66 %. However, during the process of rolling moisture was lost to the environment thus reducing the final average moisture content, also known as the plastic limit to 53 %.

Table 4.5 Measurements for plastic limit determination through thread-rolling

Water Content	1	2	NMC_i	w_i
Mass of container (g)	0.89	0.89	0.89	0.89
Mass of container + wet soil (g)	8.38	8.06	22.34	22.84
Mass of container + dry soil (2)	5.60	5.79	17.92	14.12
Mass of water (g)	2.78	2.27	4.42	8.72
Mass of dried soil (g)	4.71	4.90	17.03	13.23
Water content (%)	59.02	46.33	26	66
PL (average moisture content of threads) (%)	53			

The arithmetic difference between the liquid limit and plastic limit is the plasticity index (PI). When the PI and LL values were plotted against the A-line chart for soil classification (Figure 4.7), the soil was found to be of a rusty coloured, high plasticity and compressibility SILT in composition.

Table 4.6 A summary of Hamilton Ash's Atterberg Limits and indices.

Soil Consistency	
Liquid Limit	74%
Plastic Limit	53%
Plasticity index (PI)	21 %
Liquidity Index (LI)	-0.11
Activity Index (AI)	1.1
Consistency Index (CI)	1.1
Soil Classification	MH

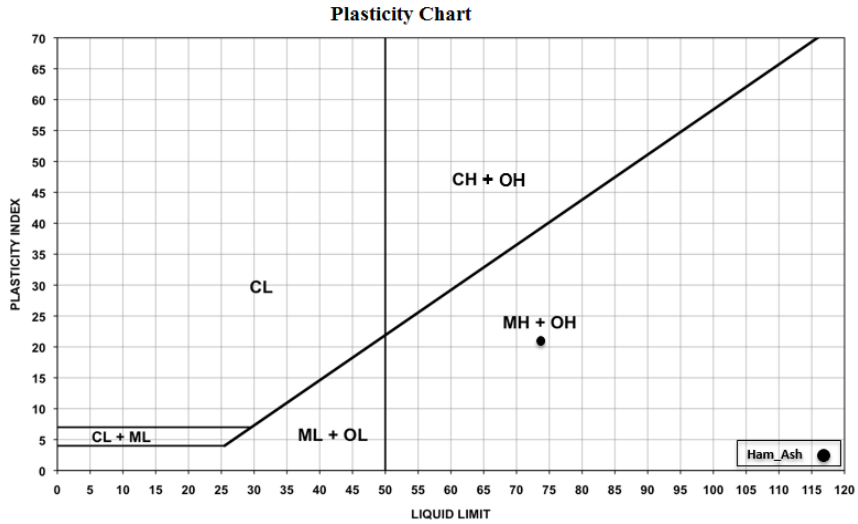

Figure 4.7 *A-line chart classifying the tested sample of Hamilton Ash as high compressibility SILT (MH).*

4.3 Standard Compaction Test

The aim of a Standard Compaction test is to increase the soil density by air void reduction under a constant compactive energy. A number of standard laboratory compaction tests were carried out on Hamilton Ash samples to determine the key compaction parameters which are the Optimum Moisture Content (w_{opt}) and Maximum Dry Density $(\rho_d)_{max}$). Governed by the general understanding that at a certain moisture content, the soil subjected to a constant compactive effort achieves its maximum dry density, 11 compaction tests were executed on air-dried Hamilton Ash samples over a period of time.

A wide variety of results were generated from the 11 tests which was most likely due to differences in sampling location and sample preparation methods. Essentially, all 11 rounds of testing were separated into two main groups based on sampling location and the results generated. In both group of samples, pre-drying at room temperature was carried out, the first group was dried for ~6 months while the second group was air-dried for ~ 7 days. The differences in the results acquired from these two categories of tests are presented and further elaborated in the following sub-sections.

4.3.1 Group 1 Samples: Questionable or Invalid

The first set of samples were obtained from a stockpile at the residential development area in the Rotokauri suburb, in the outskirts of Hamilton, New Zealand. A total of six compaction tests were carried out. Prior to compaction, the samples were air-dried at room temperature (~24°C) for approximately 6 months.

4.3.1.1 Test results

The standard compaction test procedure dictates the addition of water to the soil sample at different increments in order to determine the w_{opt} at which the $(\rho_d)_{max}$ is obtained. At time of compaction, the soil was at 8.8% (2.81 g of water) moisture content after ~6 months of air-drying but different ranges of added water contents were estimated and assigned to each test based on the results produced by the initial test (Test No.1). It is important to note that the New Zealand Standard for Soil Compaction did not specify a certain figure or a range of figures to establish the

range of added moisture content for fine-grained clayey soils. However, emphasis was placed on compacting two samples dry of w_{opt} and at least three wet of w_{opt}. For instance, in Test No.1, the working range of water content was defined by increments of three; 9 % (225 g), 12 % (300 g), 15 % (375 g), 18% (450 g) and 21 % (525 g). The added water contents were calculated as a percentage of 2500 g of air-dried soil per sample. The range of added water contents were altered for each test until the w_{opt} was determined which was essentially realized in a bell-shaped curve as those seen in Figure 4.8. The different range of added water contents for each compaction tests are highlighted in Table 4.7. Notice that 3% - 11% was used four times for Tests No. 3-4 and Repeatability Tests No.1 because the w_{opt} was obtained at 7%.

Table 4.7. Range of added water contents for all the compaction tests conducted.

	Added water content range		Total soil water content at time of compaction (grams)
Test No.	%	Grams	
1	9 - 21	225 - 525	227.81 – 527.81
2	3 - 11	75 – 375	77.81 – 277.81
3	3 - 11	75 – 275	77.81 – 277.81
4	3 - 11	75 – 275	77.81 – 277.81
Repeatability 1	3 - 11	75 – 275	77.81 – 277.81
Repeatability 2	3 - 11	75 – 275	77.81 – 277.81

In Figure 4.8, the relationship between dry density and water contents in Tests No. 2 – 4 and Repeatability Test No.1 are clearly defined and expressed by the bell-shaped curves. Essentially, the w_{opt} at which the $(\rho_d)_{max}$ were achieved were successfully determined in Tests No.2 – 4 at 7 % moisture content and 1242.82 kg/m^3 maximum dry density whereas in Repeatability Test No.1, the $(\rho_d)_{max}$ of 1205.99 kg/m^3 was achieved at 8 % w_{opt}. However, the same cannot be said for Test No.1 and Repeatability Test No.2 because the w_{opt} and $(\rho_d)_{max}$ could not be determined. The w_{opt} and $(\rho_d)_{max}$ for the 6 compactions tests are tabulated in Table 4.8. The water contents displayed in Figure 4.8 represent the added water contents and not the actual water contents of the soil. The actual water contents of the soil at different added moisture contents were determined after compaction of each sample.

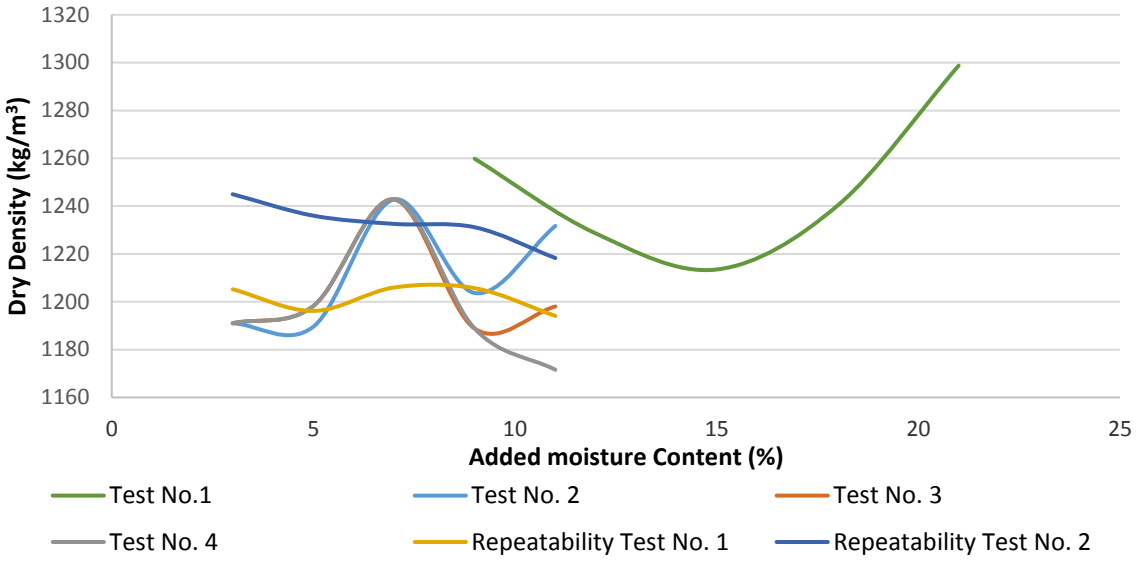

Figure 4.8 A graphical representation of all Standard Compaction tests carried out from the first group of samples with the aim to determine the key compaction parameters, w_{opt} and $(\rho_d)_{max}$ for every tests. Five samples were prepared under various initial water contents and compacted for every test.

As observed in Figure 4.8, the results for Test No. 1 varied significantly from all the other tests. In this initial test, the added moisture content range commenced at 9 % and was increased by a 2 % increments for every sample in that test, in this case 5 samples. The results for Test No.1 were inconclusive because w_{opt} and $(\rho_d)_{max}$ could not be ascertained. After reviewing the data gathered from Test No.1, the added moisture content range for Test No. 2 was reduced to commence at 3% and end at 11% while still maintaining 2 % increments for each sample. Accordingly, Tests No. 2 - 4 and Repeatability Tests No. 1 and 2 were all compacted according to the added moisture content range of 3 % – 11 % on the account that this estimated range generated a bell-shaped curved when plotted, i.e. w_{opt} and $(\rho_d)_{max}$ were able to be determined. Given that the w_{opt} and $(\rho_d)_{max}$ were determined in Test No.4 under the added water content range of 3 % – 11 %, an attempt to reproduce similar w_{opt} and $(\rho_d)_{max}$ values was undertaken through two separate repeatability tests. However, as seen in Figure 4.8, Test No.4 was not repeatable in the case of Repeatability Test No.2 whereas Repeatability Test No.1 proved to be somewhat repeatable. As summarized in Table 4.8, the added optimum moisture content and the actual optimum moisture content are not the same. The actual optimum moisture content (39.6 %) is the sum of the soil's moisture content at time of compaction (8.8 %) and the added moisture content (13%) at which the maximum dry density

was achieved. The added optimum moisture content range does not include the soil's moisture content.

Table 4.8 A summary of the data collected from compaction Tests No. 1-4 and Repeatability Tests No. 1-2. The added optimum moisture contents do not include the soil moisture content at time of compaction whereas the actual optimum moisture contents (w_{opt}) includes the soils moisture content of 8.8 % and reflects the total moisture content of the soil at the optimum level.

Test Type	Added Optimum Moisture Content (w_{opt}) (%)	Actual optimum moisture content (%)	Maximum Dry Density ($(\rho_d)_{max}$) (kg/m^3)
Test No. 1		Inconclusive	
Test No. 2	7	15.8	1242.82
Test No. 3	7	15.8	1243.82
Test No. 4	7	15.8	1243.82
Repeatability Test No. 1	8	16.8	1205.99
Repeatability Test No. 2		Inconclusive	

4.3.1.2 List of potential errors

Natural Moisture Content (NMC)

The soil's natural moisture content is an important property that requires immediate action for determination prior to air-drying but this was not actioned in this instance. The samples were air-dried without determining the natural moisture content (NMC) which may have potentially affected the components of the compaction tests in terms of added moisture content, consequently rendering the generated results questionable. However, after 6 months of air-drying, 31.86 grams of dry soil was oven-dried for 24 hours and the moisture content at time of compaction was found to be at 8.8 % or 2.81 g of water.

Extensive sample air-drying and crushing

The differences in the results for this set of samples are most likely to have stemmed from excessive sample drying and fragmenting. The samples were air-dried for roughly 6 months before being tested. Samples were laid out in shallow trays to air-dry in order to force apart the flocculated clay particles and permit effortless fragmentation by hand. However, to hasten the process of breaking down the soil to reasonable workable sizes, a wooden mullet was used to fragment the larger chunks of stiff clay which were otherwise impossible to separate by hand. The latter

process most likely had a more profound impact on the soil's fabric, if not completely destroying the intricate structure, which largely influenced the results generated from the compaction tests.

Individual Sample Compaction Tests

The general understanding is that, once the w_{opt} is determined and $(\rho_d)_{max}$ is attained, the soil's dry density beyond the optimum moisture content will decrease, resulting in a downward slope on the bell-shaped curve. The added water content range of 3% – 11% was initially experimented in Test No. 2 and w_{opt} and $(\rho_d)_{max}$ were determined. However, the data after the w_{opt} showed an increase in dry density (ρ_d) after the w_{opt} and $(\rho_d)_{max}$ were achieved. To correct this supposed error, sample 5 of Test No.2 was singled out and re-tested alone instead of running the entire test again; this in itself was a mistake that contributed towards the invalidity of these tests. Samples in each tests should not have been tested individually to generate the perfect curve. The same mistake was repeated in Tests No.3 and 4, in each instances compacting sample 5 independently with the aim of achieving a ρ_d less than what was obtained in sample 4. Eventually, the supposed perfect curve was generated in Test No. 4, however when repeatability tests were performed, the results differed considerably from Tests No. 2 – 4. This stark contrast can be distinguished in the curves produced in Figure 4.8 and Table 4.8.

4.3.2 Group 2 Samples: Valid

A second trip to the field for soil sampling was prompted when tests from Group 1 samples produced questionable results due the factors outlined in the previous sub-section. In order to avoid repeating the same mistakes made in the first group of samples, the sample batches transported back to the laboratory were air-dried for a maximum of 2 weeks during which the bulky portions of the soil were torn apart by hand only. Soils that were reduced to workable sizes (≤ approx. 2-3 cm) were immediately packed in air-tight plastic bags and stored away. The short air-drying period ensured the soil retained almost half of its natural moisture content. An assessment of the soil's natural moisture content (NMC*)* prior to air-drying placed the figure at 50.7%, however after a week of drying the NMC was reduced to 26%.

The graph in Figure 4.9 demonstrates all the tests compacted under varying initial water content ranges. Based on the added moisture content range established in Test No. 2 of the Group 1 samples, an assumption was made to apply the same 3% - 11% value range to the Group 2 samples without considering the differences between the NMC of both group of samples; NMC for Group 1 samples was undefined but the soil was at 8.8% NMC_i at time of compaction whereas Group 2 samples were at 50.7 % NMC but was reduced to 26% at time of compaction. Consequently, Tests No. 1 - 4 produced curves that appeared in general, to be approaching a peak but failed to decline, thus giving no measure of w_{opt}. However, Test No. 5 generated a perfect bell-shaped curve under a much higher added moisture content range of 9 % - 17 %. The w_{opt} and $(\rho_d)_{max}$ for the compacted soil was resolved as 13 % (325 g of water) and 1267.2 kg/m^3 respectively. Similar to Figure 4.8 in sub-section 4.3.1, the water contents displayed in Figure 4.11 do not represent actual water contents of the soil, rather the added water contents. The actual water contents of the soil at different added moisture contents were determined after compaction of each sample.

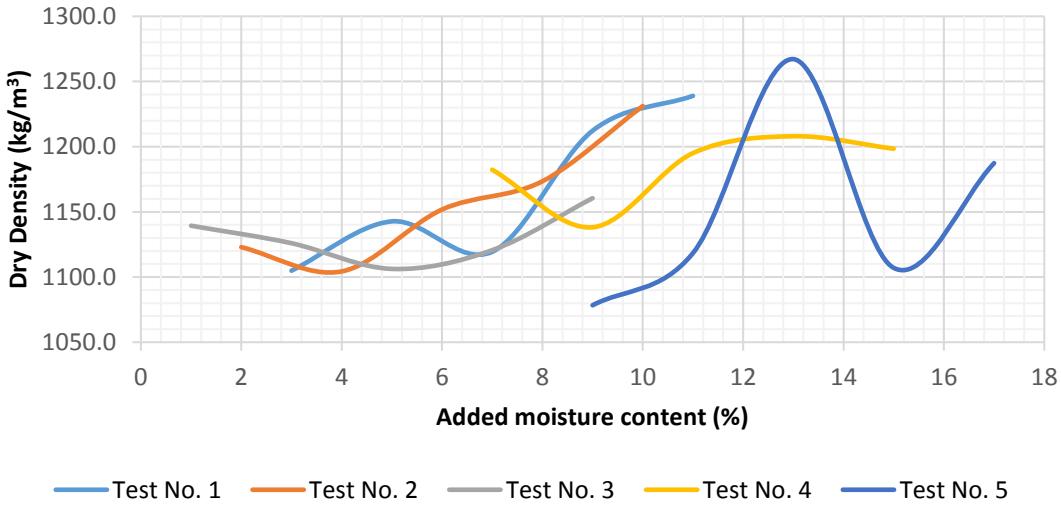

Figure 4.9 This graph displays the compaction test results for the 5 sets of tests conducted from the second batch of samples.

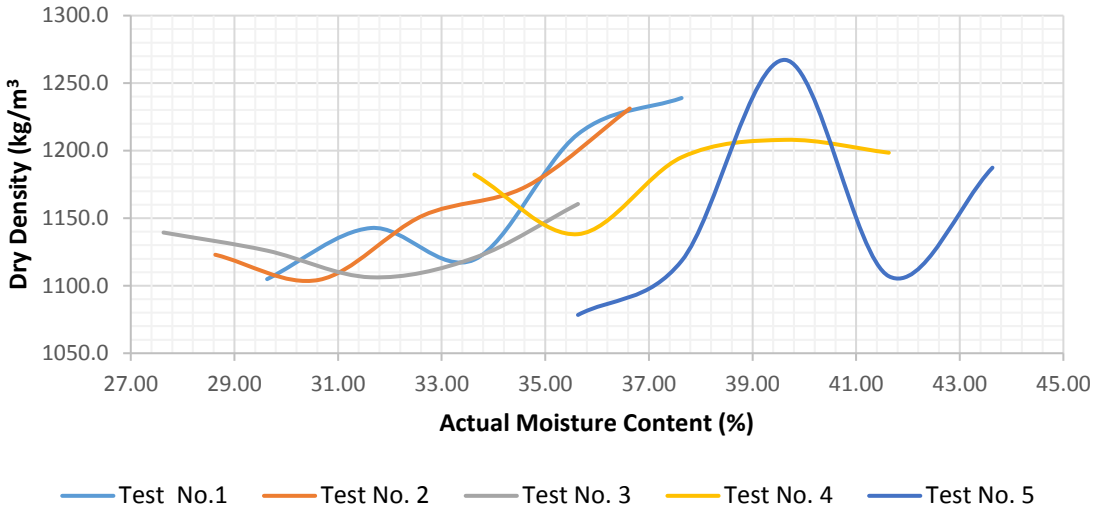

Figure 4.10 Water-density curves for Tests No.1 – 5 based on the actual moisture content of the soil. The optimum moisture content for Test No. 5 is 39.6 %.

Since Test No. 5 was able to produce the much anticipated results, repeatability tests were deemed necessary to verify the validity of the method through which the results were obtained and to determine whether or not that process was repeatable and the results were reproducible.

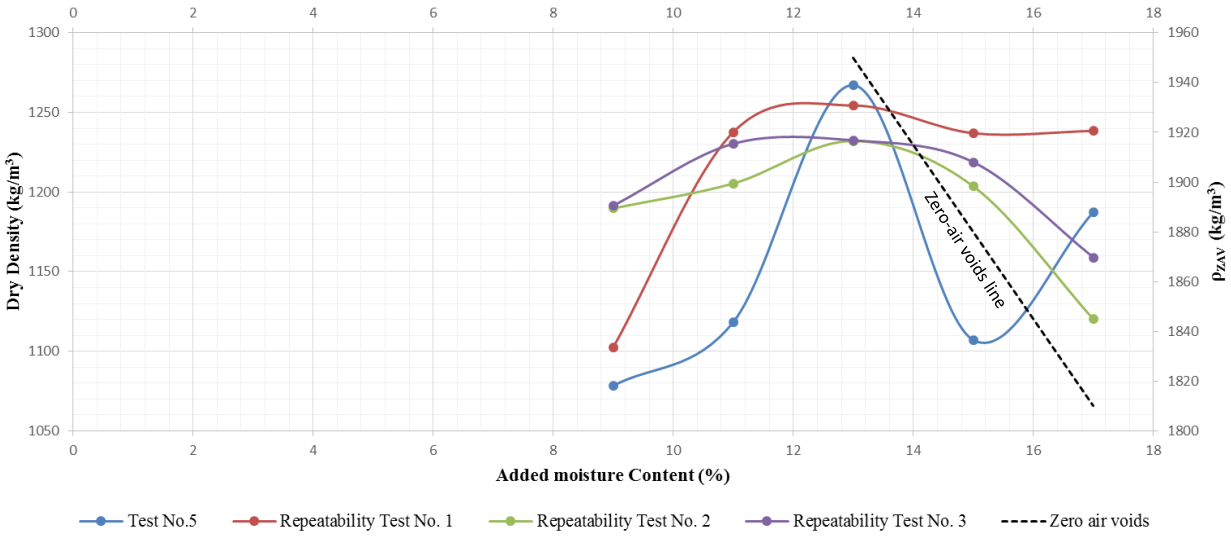

Figure 4.11 A graphical representation of the results generated from the Repeatability Tests carried out after Test No.5. The moisture contents used here represent the added moisture contents only and does not include the soil's moisture content at time of compaction (26 %).

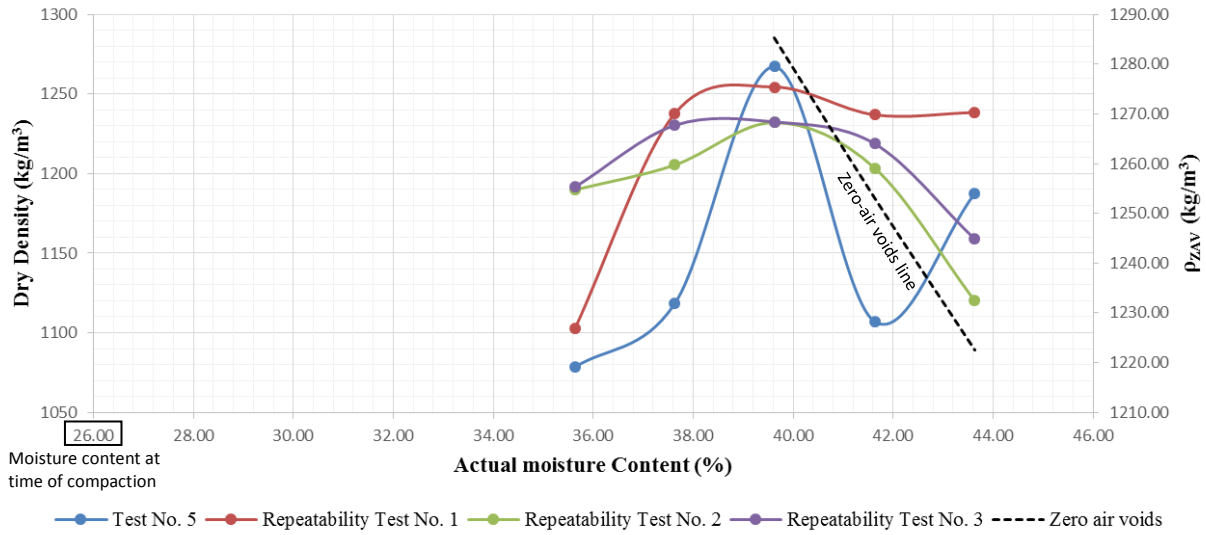

Figure 4.12 Water-density curves for Test No. 5 and Repeatability Tests No. 1-3. The moisture content (%) used here are the actual moisture contents for the soil (26 % + added moisture contents). The actual optimum moisture contents for all compaction tests here is 39.6 %.

Figure 4.11 displays compaction curves generated from 3 different repeated tests that were purposely carried out to reproduce results produced by Test No.5. All three repeatability tests (RT) were able to identify the added w_{opt} at 13 % where the $(\rho_d)_{max}$ for each compacted sample was obtained. As far as degree of similarity extends, the $(\rho_d)_{max}$ for RT No. 1, 2 and 3 slightly varied by 10 kg/m^3 and 30 kg/m^3 respectively, from the original test (No. 5). Note however, that the curves do not show a classical bell-shape, but are rather more spread around the w_{opt}. In Figure 4.12 the water-density curves represent the actual moisture contents for the compacted samples. The actual w_{opt} for Test No. 5 and RT 1- 3 is 39.6 % where by $(\rho_d)_{max}$ values ranging from 1267.2 – 1232.5 kg/m^3 were achieved. Note Table 4.9 outlines the different actual moisture contents for the soil after various compaction tests and their respective w_{opt} and $(\rho_d)_{max}$ values.

Table 4.9. A comparison of the key compaction parameters obtained in the repeatability tests carried out after Test No. 5.

Test Type	Optimum Moisture Content (w_{opt}) %	Added optimum moisture content (%)	Maximum dry density ($(\rho_d)_{max}$) kg/m^3
Test No. 5	13	39.6	1267.2
RT No.1	13	39.6	1254.4
RT No.2	13	39.6	1232.1
RT No.3	13	39.6	1232.5

4.4 Soil Shear Strength

4.4.1 Soaking Tests

A total of 6 samples were compacted to the added optimum moisture content of 13 % (39.6 % actual w_{opt}) defined by the Group 2 samples and soaked in distilled water over a range of time periods prior to vane shear testing. Several key input parameters were formulated to target the primary objectives of this research which included determining the rate of seepage of moisture from the environment into a compacted soil mass, the degree of saturation in the compacted mass, and its impact on the soil shear strength. The key input parameters considered for all the tests include; soaking period, mass of compacted soil before and after soaking, initial water content and water content after soaking, height of water in the bucket before and after soaking and the seepage rate to measure the degree of saturation in the compacted mass (Table 4.10).

Sample 3 in Figure 4.13 depicts the visual changes that occur on a compacted mass over a given soaking timeframe. In this instance, the surface appears to be moderately to highly saturated with no evidence of cracks and little to no swelling.

Figure 4.13. Sample 3 before (left) and after (right) 1 week of soaking.

In general, the data in Table 4.10 show a minor increase in soil water content after longer periods of soaking and this is indicated by the decline in water depths in the

bucket at the start and end of each soaking period in all tests. The small drop in water level typically ranges from 1-2 mm. Moderate elevation in moisture content in all the compacted samples was apparent after soaking. Due to the fact that the samples were compacted at the defined added w_{opt} of 13 %, all the samples were assumed to have an initial actual moisture content of 39.6 % before soaking. Notice in Table 4.10 that all of the samples' actual moisture contents after soaking increased slightly between 41.30 – 45.11 %. Furthermore, the declining trend observed in the rate of seepage correlates inversely to soaking period.

Table 4.10. Tabulated below are the measurements for the soaking test parameters.

Sample No.	SP	c_i	c_s	$c_s - c_i$	w_i	w_s	Δw	v_b	wd_i	wd_a	wd_s	SR
1	1 hour		1782.83	11.79	39.6				163	200	198	2
	2 hours		1790.96	19.92	39.6				161	198	197	0.5
	3 hours	1771.04	1793.36	22.32	39.6	43.06	3.46	18.8	160	197	196	0.333
2	1 day	1768.00	1784.5	16.50	39.6	42.91	3.31	11.5	162	191	190	0.042
3	7 days	1702.21	1758.32	56.11	39.6	45.11	5.51	18.8	160	199	197	0.012
4	14 days	1750.33	1772.5	22.17	39.6	41.30	1.7	18.8	160	198	196	0.0060
5	21 days	1694.51	1783.26	88.75	39.6	42.63	3.03	18.8	160	198	196	0.0040
6	52 days	1765.67	1782.19	16.52	39.6	42.68	3.08	18.8	160	200	198	0.0016
7	0	1770.49	Dry sample		41.73							

Key: SP – soaking period in days and hours, c_i – compacted mass before soaking (g), c_s – compacted mass after soaking (g), c_s - c_i = mass of moisture in soil (g) w_i – actual moisture content (%) since the samples were compacted to the w_{opt}, w_s – water content after soaking (%), Δw – change in actual moisture content (%), v_b – volume of bucket (L), wd_i – initial water depth in bucket (mm), wd_a – water depth at start of soaking (mm), wd_s – water depth in bucket after soaking (mm), SR – seepage rate (mm/hour).

It is important to note that even though a different sized bucket was used to conduct Test # 2, the results generated mainly align with those obtained from the 18.8 L bucket and therefore, does not affect the consistency of the soaking test nor does it invalidate the results produced. Soils that contain clay minerals are known to encounter some degree of swelling upon interaction with water, in some instances almost immediately and other times a delay is experienced. Observations made in the first batch of extensively air-dried samples revealed instantaneous swelling of the surface of the compacted sample when placed in water (Figure 4.14). However, these observations were disregarded due to the reasons outlined in sub-section 4.3.1.

In contrast, the tests conducted from the second batch of samples whose results are presented in this section generally exhibited little to no swelling. In Sample 1, where vane shear testing was performed in intervals of 1 hour of soaking for 3 hours, no swelling was noted in the first hour. However after the second hour of soaking, the surface of the soil expanded by 1.5-2 mm and remained constant even after the third hour of soaking. Minor swelling of ~1 mm was noted on sample 2 after 24 hours of

soaking. Further observations made on samples soaked for 1 to 3 weeks and 52 days showed little (<1 mm) to no swelling.

Figure 4.14. A comparison of compacted samples from batch 1(left) and batch 2 (right) that were soaked for 1 day. A considerable amount of swelling is evident on the sample from batch 1 compared to batch 2.

In all the test samples, no visible cracks were identified on the surface of the soil except for samples 2 and 4. The hairline cracks on sample 2 originated from the centre of the mould and radiated towards its edges whereas on sample 4, a single hairline fracture originated and extended for about 3 cm along the edge of the sample and closer observations showed the hairline fracture to be relatively shallow. It appeared that the crack was created as a result of approximately 1-1.5mm of the upper soil material detaching itself from the rest of the compacted mass during soaking. Another interesting observation recorded that proved to be common in all soaked samples was that moisture was only able to infiltrate the soil to a depth of approximately 5 cm below the surface. The compacted mass past the 5 cm mark appeared to be partially saturated with little to no evidence of moisture retention.

The degree of saturation for each sample was calculated after soaking to investigate the likelihood of moisture to infiltrate soil samples that were compacted to the optimum dry density. Table 4.11 is a summary of the calculated values of the key soil parameters which include porosity (n), void ratio (e) and the degree of saturation (%). These values were determined for each sample both before and after soaking to identify the changes that added moisture can have on compacted Hamilton Ash materials.

Table 4.11. Calculations of the degree of saturation for the compacted Hamilton Ash samples before and after soaking.

Degree of saturation for compacted samples prior to soaking							
Measurements	Sample 1	Sample 2	Sample 3	Sample 4	Sample 5	Sample 6	Sample 7
Soil mass (kg) (M_s)	1.771	1.768	1.702	1.750	1.695	1.766	1.770
Specific Gravity (G_s)	2.62	2.62	2.62	2.62	2.62	2.62	2.62
Dry Density (kg/m^3) (ρ_d)	1233.43	1231.31	1185.49	1219.00	1180.13	1233.04	1233.00
Water content (kg) (w)	0.332	0.332	0.331	0.331	0.331	0.331	0.331
Bulk density (kg/m^3) (ρ_b)	1748.14	1745.14	1680.20	1727.70	1672.60	1747.84	1747.60
Total volume of compacted soil (m^3) (V)	0.001013	0.001013	0.001013	0.001013	0.001013	0.001013	0.001013
Water density (kg/m^3) (ρ_w)	1000	1000	1000	1000	1000	1000	1000
Volume of solid (V_s) (m^3)	0.000676	0.000675	0.000650	0.000668	0.000647	0.000674	0.000676
Volume of voids (V_v) (m^3)	0.000337	0.000338	0.000363	0.000345	0.000366	0.000339	0.000337
Volume of water (V_w) (m^3)	0.000331	0.000331	0.000331	0.000331	0.000331	0.000331	0.000331
Void Ratio (*e*)	0.4987	0.5013	0.5593	0.5165	0.5664	0.5033	0.4992
Porosity (*n*)	0.3328	0.3339	0.3587	0.3406	0.3616	0.3348	0.3330
Degree of Saturation (S_r)	0.9832	0.9798	0.9121	0.9606	0.9048	0.9772	0.9825
Degree of Saturation (S_r) (%)	98.3	98.0	91.2	96.1	90.5	97.7	98.3

Degree of saturation for compacted samples after soaking						
	Sample 1	Sample 2	Sample 3	Sample 4	Sample 5	Sample 6
Soil mass (kg) (M_s)	1.789	1.7845	1.758	1.773	1.783	1.782
Specific Gravity (G_s)	2.62	2.62	2.62	2.62	2.62	2.62
Dry Density (kg/m^3) (ρ_d)	1234.41	1232.57	1196.06	1238.24	1290.56	1232.91
Water content (kg) (w)	0.3327	0.3312	0.3324	0.3315	0.3318	0.3309
Bulk density (kg/m^3) (ρ_b)	1765.916	1761.425	1735.584	1749.580	1760.201	1759.145
Total volume of compacted soil (m^3) (V)	0.0010131	0.0010131	0.0010131	0.0010131	0.0010131	0.0010131
Water density (kg/m^3) (ρ_w)	1000	1000	1000	1000	1000	1000
Volume of solid (V_s) (m^3)	0.000683	0.000681	0.000671	0.000677	0.000681	0.000680
Volume of voids (V_v) (m^3)	0.000330	0.000332	0.000342	0.000337	0.000332	0.000333
Volume of water (V_w) (m^3)	0.0003327	0.0003312	0.0003324	0.0003315	0.0003318	0.0003309
Void Ratio (*e*)	0.4836	0.4874	0.5096	0.4975	0.4885	0.4894
Porosity (*n*)	0.3260	0.3277	0.3376	0.3322	0.3282	0.3286
Degree of Saturation (S_r)	1.0073	0.9977	0.9719	0.9849	0.9958	0.9940
Degree of Saturation (S_r) (%)	100.7	99.8	97.2	98.5	99.6	99.4
Difference in degree of saturation between samples before and after soaking (%)	2.4	1.8	6.0	2.4	9.1	1.7

The results in Table 4.11 are plotted in Figure 4.15 . Figure 4.15 expresses the relationship between degree of compaction in terms of maximum dry density and void ratio before and after soaking. A general declining trend is observed in all of the samples' dry densities whereas no distinctive pattern is apparent for void ratio

before soaking. However, after continuous increase in sample 1, void ratio values for the rest of the samples experienced a brief decline before maintaining a steady pattern to the end. A relationship also exits between the rate of seepage and the degree of saturation. Notice in Table 4.11 that the rate at which moisture seeped through the compacted mass decreased with longer soaking periods while the degrees of saturation declined shortly after peaking in sample 1 but began climbing after sample 3, whose soaking time was 168 hours (7 days).

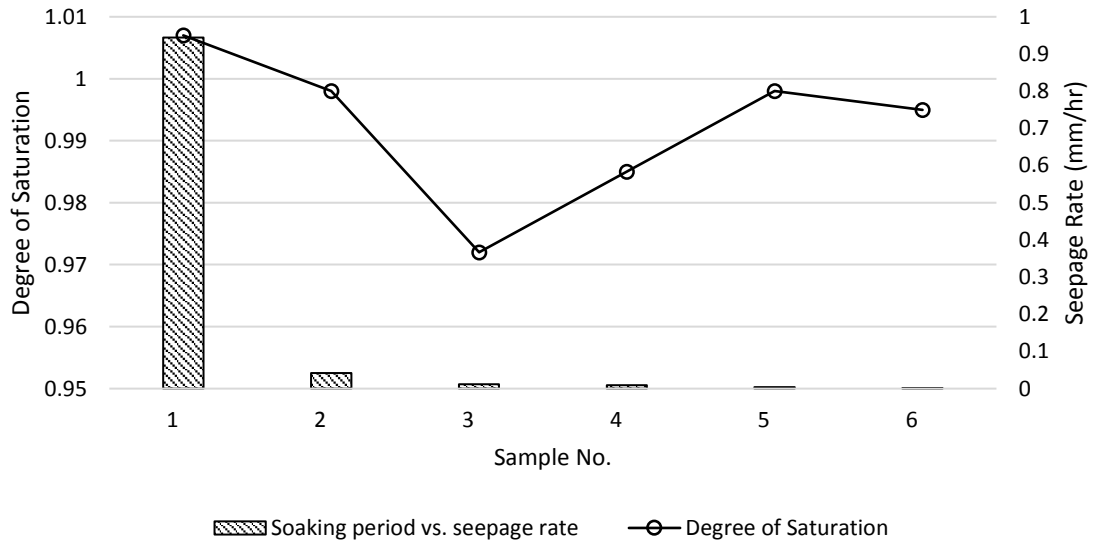

Figure 4.15. Graph showing the relationship between soaking periods (represented by sample no.) and degree of saturation and seepage rate (mm/hr).

A water content of 0.328 kg was used in calculating the dry densities for all compacted, unsoaked samples and it was derived from the added w_{opt} of 13% and moisture content at time of compaction which was 20 %. Note that soils compacted for soaking and vane shear testing were packed away in tightly sealed plastic bags but still experienced moisture loss, mostly likely through condensation. The soil moisture content at time of compaction had reduce slightly from 26 % (air-dried soil w) to 20 %. On the other hand, different water contents were used for the soaked sample calculations because these were determined individually through 24 hours oven-drying after subsequent soaking periods. The total volume of the soil is constant for both soaked and unsoaked samples and it is derived from the volume of the standard proctor mould which is 1.01×10^{-3} m^3.

4.4.2 Vane Shear Tests

A series of laboratory vane shear tests were performed on compacted soaked and non-soaked samples to determine the undrained shear strength of the soil mass. A total of 7 compacted samples were subjected to vane shear testing, 6 of which were soaked in distilled water over a range of time periods prior to vane shearing and one was tested as a dry, compacted sample to make known the initial shear strength of compacted Hamilton Ash.

It was hypothesized that a compacted soil mass subjected to prolonged saturation overtime will result in a reduction of the soil's shear strength. In order to explore this hypothesis and draw a concrete conclusion, several parameters considered to be of utter importance to the success of the test were identified and addressed individually in sub-section 4.4.1. Data collected from this and vane shear tests will aid in forming a clear deduction of whether compacted soils are more susceptible to instability issues when exposed to saturation over a certain period of time.

All the samples were subjected to vane shear testing at the end of allotted soaking timeframe except the one compacted, dry sample that was tested to determine the initial shear strength. The raw data for each sample can be found in Appendix 1 and Table 4.12 only summarises the shear strength of each soaked sample. The data in Table 4.12 show a sudden decrease in shear strength for short soaking periods, but a steep increase for longer periods of soaking. This deduction can be viewed in a graphical form in Figure 4.16.

The procedures of laboratory vane shear testing dictates that the top of the vane must be at least 10-20 mm below the surface of the soil. In all 7 tests, the tip of the vane was approximately 10 mm below the surface. It is important to note that the vane was only able to penetrate the saturated layer of the soil that was established in sub-section 4.4.1, thus implying that the shear strength value is not representative of the entire soaked, compacted mass but only for the top 5 cm of saturated layer.

Table 4.12. A summary of the soil undrained and remoulded shear strength for each sample after various soaking periods. Note that 0.001 hours represents the dry, unsoaked sample.

Sample No.	Soaking Periods (hours)	Undisturbed shear Strength (kPa)	Remoulded vane shear strength (kPa)
0	0.001	50.6	8.8
1	1	30.2	2.4
	2	23.8	3.7
	3	16.9	2.6
2	24	34.3	5.4
3	168	32.5	10.7
4	336	41.1	8.3
5	504	48.7	23.1
6	1248	74.5	41.2

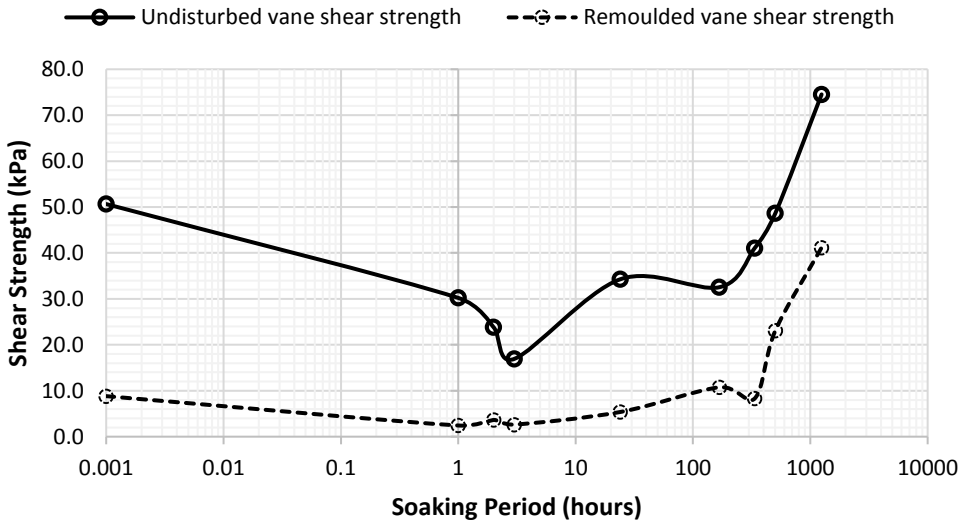

Figure 4.16. Logarithmic scale of the change in shear strength after various wetting periods. A sudden decline in shear strength is observed initially followed by an increasing trend that fluctuated initially but stabilized eventually.

The calculated rate at which moisture was seeping through the compacted soil is understood to be dependable on the degree of compaction. It is also understood that the degree of compaction is closely associated to the dry density of the soil which has a close correlation to its shear strength. In Figure 4.17 this relationship is realized. According to data plotted below, soil strength suddenly drops after the first, second and third hour of soaking but escalates after 24 hours of soaking and continually rises as soaking period increases. The rate of seepage however, declines with prolonged soaking periods and increasing soil strength.

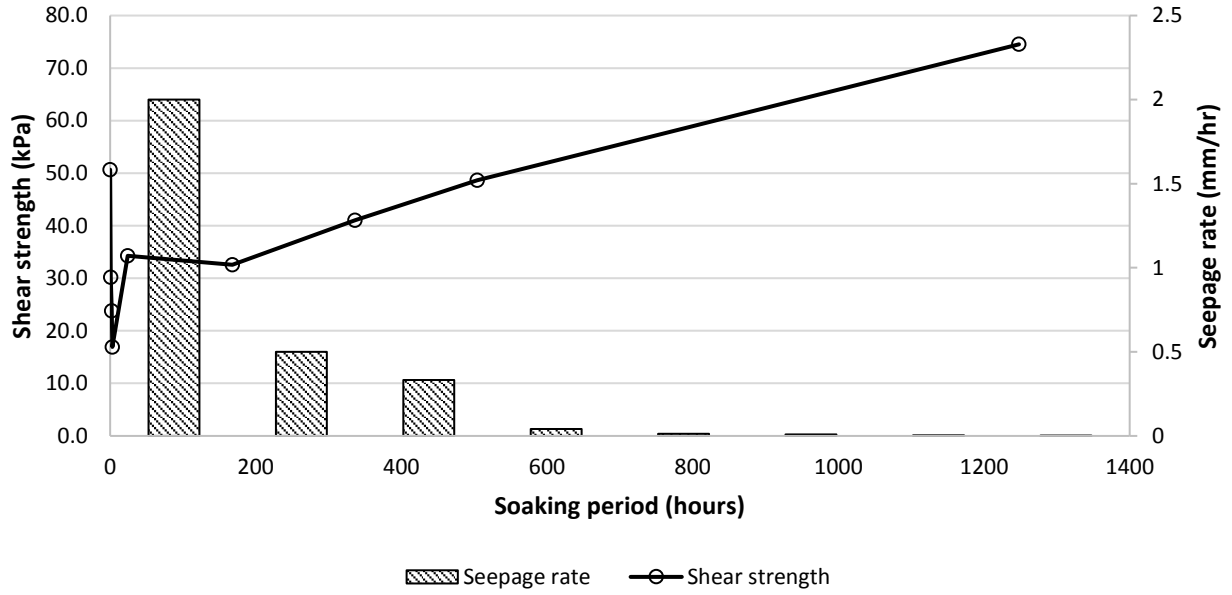

Figure 4.17. A linear graphical representation of the relationship between changes in the soil shear strength and seepage rate over time.

Chapter 5

Interpretation and Discussion

5.1 Introduction

This chapter interprets and discusses the results acquired by means of geotechnical laboratory tests conducted on Hamilton Ash samples throughout the course of this research. Discussions on the characterisation of Hamilton Ash samples through grain size analysis, mineralogical analysis and Atterberg Limits will be presented in section 5.2. In section 5.3, investigations into the successful determination of optimum moisture content and maximum dry density of Hamilton Ash through standard compaction test will be discussed in detail. The failed attempts at obtaining the optimum moisture content and maximum dry density of the soil will not be addressed in this chapter as it was explained in Chapter 4. Furthermore, the statistical analysis for all repeatability tests will be examined and presented in this section also. The strength and deformation characteristics of compacted, soak and non-soaked Hamilton Ash samples investigated through vane shear testing will be interpreted and conveyed in section 5.4 of this chapter.

5.2 Soil Characterisation

For every type of soil used in the construction of any of the four basic geotechnical structures; foundations, slope stability, retaining walls and earth-fill dams (Atkinson, 2007), possessing a basic knowledge of the soil index properties and mineralogical composition is crucial in assessing the soil's qualitative behaviour when subjected to various types of external or internal stresses. Understanding the soil's physical index properties can ensure the designing of safe and stable geotechnical structures (Ishibashi & Hazarika, 2010).

Geotechnical failures surrounding any of these structures can often be attributed to a lack of knowledge regarding the geotechnical properties of founding subsoils or fill material and substandard ground investigations. Orense *et al.*, (2006) described a failure of a dike constructed from volcanic soils wherein a direct link between the collapse and a lack of knowledge of the physical properties of fill material was

identified. Mohr (2004) highlighted 3 different cases studies in a conference paper regarding geotechnical failures as a result of poor site investigations.

Hamilton Ash is used extensively throughout the Waikato region, especially in earthworks as a fill material for construction of earth structures and foundation designs. Observations noted throughout the years (Holland, 2018: personal communication) showed that compacted, fill materials that have Hamilton Ash as the primary soil formation, have the tendency to shrink or swell depending on length of exposure to rainfall overtime. This behaviour can potentially lead to ground settlement on foundations and instability issues on earth structures like embankments. For this reason, a comprehensive study into the physical properties and mineralogical composition of Hamilton Ash was undertaken to determine the relationship between these key properties and how they affect the overall behaviour of the soil after compaction, after being subjected to additional loads and collectively, how these properties permit or restrict the soil to react under various saturated conditions.

5.2.1 Grain size Analysis

Understanding how different particles in soil are spread out over a range of sizes is important as the size of the particles determines the mobility of water throughout the soil, ultimately affecting the overall behaviour of the soil. The Hamilton Ash samples tested had a rusty, yellowish-brown colour in the field but after several days of air-drying, the colour changed to both pale brown and dark brown. As mentioned previously, the samples were sourced from an existing stockpile, meaning the soil is in a disturbed state. Closer visual examination of the soil revealed traces of organic materials (roots) and granular particles estimated to be greater than 2 mm which were believed to be remnants of construction aggregates. These coarse and inorganic contents of the soil were sieved out prior to laser diffraction (LD) testing.

Five different samples of Hamilton Ash were tested through LD and the results presented in Chapter 4 revealed a moderately ranged distribution of clay, silt and sand particles only. As observed in Figure 4.1, grading curves that represent the

distribution of the particles are gently sloping across the three dominant size ranges which is distinctly indicative of a medium to well graded soil profile (Atkinson, 2007). When the results from all 5 tests were averaged (Table 4.1), it became apparent that there is an appreciably greater percentage of coarse materials (~ 48 % silt and 35 % sand) than of fines (~19 % clay). Additionally, the average D_{50} for all samples was 29.1 μm meaning 50 percent of particles in the samples tested were larger than 29.1 μm and the other 50 percent were smaller than 29.1 μm. This led to the classification of Hamilton Ash as medium to well-graded clayey SILT. Evidently, this conclusion strongly correlates to the findings in Atterberg Limits which will be discussed later in this chapter.

The distribution and grading of the different sized particles in a soil mass has a strong influence on its packing capacity. Orense *et al.,* (2006) reported that due to the wide variety of grain sizes in well-graded soils, they are more likely to be compactible because the particles can be easily rearranged during compaction to produce a denser bulk. However, careful interpretation must be exercised when evaluating the results for this test. Based on Wesley's (2009) argument on soil identification and classification, the fragile particles of residual soils that are broken down easily during testing need to be taken into consideration. The breakdown of particles may have actuated during the air-drying and light crushing process prior to particle sizing tests, which may have potentially affected the results. Studies have shown that soil drying can cause irreversible changes in the soil structure and the extent of crushing can reduce the original size of the surviving particles (Herrera *et al.*, 2007).

It is possible that weaker particles were broken down into fines during crushing and were mistakenly classed as fines, thus increasing the fines content in the process. The fragility of these particles is intensified when pre-sample drying is undertaken as a test requirement increase. From these considerations, it is recommended that extensive drying or crushing be limited to a minimal range in order to preserve the quantity of the coarser fractions.

5.2.2 Mineralogical Analysis

As previously outlined in chapter 1, Hamilton Ash formation is a tephra-derived residual soil of volcanic origin. Typically, soils developed from volcanic materials have distinguishable features that are directly attributable to their parent material. A distinctive characteristic of tephra-derived soils is the dominant presence of non-crystalline or amorphous clay minerals and lesser occurrence of clay-size mineral assemblages (Shoji *et al.,* 1993a).

Analyses carried out on the bulk and clay samples of Hamilton Ash using the X-ray diffraction (XRD) method generated diffraction patterns that confirmed the presence of quartz, cristobalite, minerals belonging to the kaolinite group; kaolinite and dehydrated halloysite and minerals that were unquantifiable by XRD. Each clay mineral peaked at 10 angstrom (10Å) and 7 angstrom (7Å) respectively in both the bulk and clay samples. It is to be noted that quartz and cristobalite occurrence were more dominant in the bulk analysis than in the clay analysis. The clay minerals were characterized by broad diffraction patterns (Shoji *et al.,* 1993a; Whitton & Churchman, 1987) whereas the more crystalline-structured minerals like quartz and cristobalite were defined by narrow, high intensity peaks (Whitton & Churchman, 1987).

Minerals that were unquantifiable by XRD were believed to be allophane. Numerous studies considered allophane to be a common clay mineral in volcanic soils (Birrel & Fieldes, 1952; Lowe, 2010b; Shoji *et al.*, 1993a; Wesley, 2009), including Hamilton Ash (Ward, 1967) but due to its non-crystalline (Moon, 2016) structure it could not be identified and quantified in the series of diffraction patterns generated by the bulk and clay samples. However, performing the Fieldes and Perrott's sodium fluoride (NaF) test (Brydon & Day, 1970; Gautheyrou *et al.*, 2001) on a small portion of Hamilton Ash confirmed the occurrence of this amorphous mineral. Although, it is noteworthy that the reaction time between the hydroxy-aluminium in the soil and NaF solution was approximately 5 minutes which was 4 times longer than the 60 seconds timeframe described in the procedure by Gautheyrou *et al*., (2001). The longer reaction time may be due to the irreversible drying of the clay minerals in the soil (Birrel & Fieldes, 1952). The gradual change in colour of the indicator paper treated with phenolphthalein to a strong, bright pink

as seen in Figure 4.5 is evident of an appreciable amount of allophane in the soil (Clough & Payn, 1988; Herrera *et al.*, 2007).

Overall, the x-ray diffraction data and allophane identity test results generally agreed with previous studies done broadly on volcanic soils and particularly on Hamilton Ash mineralogy that showed the concurring occurrence of kaolinite, halloysite and allophane (Birrel & Fieldes, 1952; Pullar, 1967; Shoji *et al.*, 1993a; Ward, 1967; Wesley, 1973; Wesley, 2009). The behaviour of these clay minerals upon interaction with water during compaction and subsequent soaking show that there is no potential for swelling but shrinkage is likely to occur due to the presence of halloysite. These will discussed more in-depth later in this chapter.

More emphasis is placed on the clay components of the Hamilton Ash because cohesive materials in soils have been known to have a considerable influence on a soil's behaviour from an engineering standpoint. Clay minerals tend to undergo significant volume change by shrinking or swelling as a result of change in loading and water content (Atkinson, 2007; Yunusa *et al.*, 2013). For instance, Birrell and Fieldes (1952) examined volcanic soils at a proposed building site in New Plymouth and found the soils to have "high water capacity, high shrinkage and irreversible drying". Further investigation into the soil's mineralogy revealed an excessive occurrence and widespread distribution of allophane. It was concluded that the presence of allophane in the soil was the likely cause of the strikingly unfavourable conditions of the volcanic soils. Moon (2016) asserted that in a concurrent occurrence of allophane and halloysite in residual volcanic soils, halloysite was highly problematic for soils around the Bay of Plenty and Waikato region. Even though Wesley (2009) stated that soils containing halloysite generally have good engineering properties because of its low-activity status, some studies have exposed halloysite to be the main cause of weakness and sensitivity in natural and cut slopes (Moon *et al.*, 2017).

5.2.3 Soil Consistency – Atterberg Limits

Atterberg limits vary from soil to soil as these limits are affected by factors such as the natural water content, particle size distribution, clay minerals, organic matter

contents, and exchangeable cations (Shoji *et al.*, 1993a). Other key factors that alter the Atterberg limits in terms of the soil properties and behaviour pertain to the methods incorporated in any Atterberg Limit standard procedure; these are drying and remoulding (Townsend, 1985). In their natural, undisturbed state, most tephra-derived volcanic soils typify a low water content, silty sand mixture with little to no plasticity but after remoulding, the water content increases and a highly plastic behaviour is displayed (Herrera *et al.*, 2007). For clarification purposes, the term allophanic soils or andosols used in this discussion alludes to residual volcanic soils dominated by allophane and halloysite while lateritc/latosols/kandoids refer to soils with kaolinite and halloysite as the predominant clay minerals. These classifications are based on the definition provided by Townsend (1985).

The consistency limits and index properties determined for air-dried Hamilton Ash samples showed reasonable liquid and plastic limits of 74% and 53 %, respectively and a plasticity index of 21 % which subsequently placed the soil below the A-line implying a silt-like nature. According to the plasticity chart (Figure 4.6), Hamilton Ash is a high compressibility SILT (MH) (Figure 5.1). This result correlates well with the classification obtained from the grain size analysis test which classed Hamilton Ash as clayey SILT. The distinctions between the present study and historical studies are stemmed primarily from soil treatment in the methods and less from soil type. For instance, Shoji *et al*., (1993a) demonstrated that allophanic soils have very high liquid limit compared to other types of soils. Townsend's (1985) observations on the effects air-drying of allophanic volcanic soils showed that higher liquid limits and plasticity indexes are characteristic to soils that were not subjected to drying prior to testing whereas air-dried samples generally yield lower liquid limits and plasticity indexes. Furthermore, Wesley's (1973) findings on the liquid limit and plasticity index of andosol reported higher liquid limits of 80 to 250 % whereas latosols LL only varied from 60 to 120 %. Much less variation was seen in the plasticity index (min. 18, max <80) for both soils, the PI of andosol ranges from 18 to 80 % while latosols varied from 25 to 80 %. These limits and index properties were derived from soils tested in the natural state (Figure 5.1). Given that air-drying was executed prior to testing in this research, Townsend (1985) and Wesley's (1973) conclusions differ marginally from the results obtained in this

study in terms of liquid limit (74%) but the plasticity index of 21% determined for Hamilton Ash in this study is consistent with both author's observations.

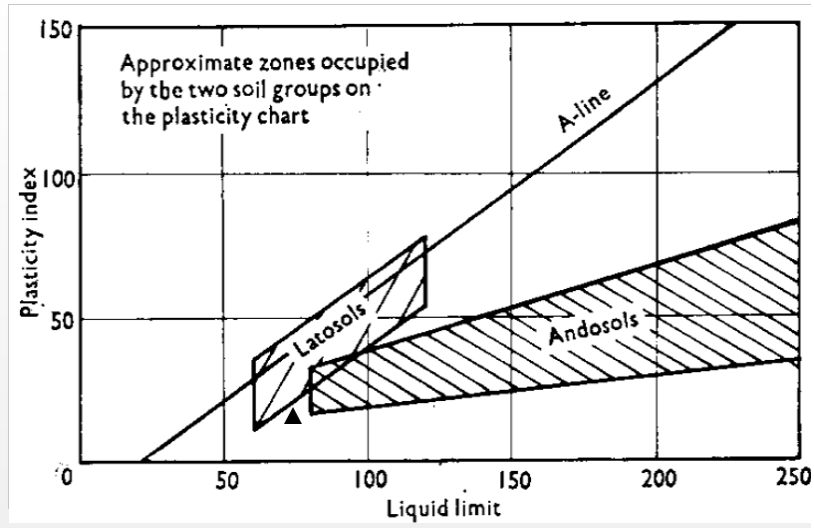

Figure 5.1. A comparison between liquid limit and plasticity index values from Wesley (1973) (left) and present study (Black triangle). According to Wesley's (1973) graph, andosols which consists predominantly of allophane and some halloysite fall below the A-line and are therefore more silt-like in nature. Latosols which comprises of kaolinite and halloysite will generally display a clayey behaviour because they mostly fall above and along the A-line. In the present study, the 74% LL and 21% PI placed the soil below the A-line indicating a similar behaviour to andosols.

The determined natural moisture content of the reworked soil excavated at a depth of ~0.5 – 0.6 m was 51 %. This moisture content is reasonably high given that the samples were obtained in March, one of the driest months of the year for Hamilton wherein a mean monthly precipitation of 44.6 mm was recorded (Weather Station, 2019). This suggests that the soil naturally has a high tendency to store moisture (Wesley, 1973) because 5 days before the sampling date, Hamilton experienced 2 consecutive days of rainfall (1.6 - 34.2 mm). This was followed by 3 consecutive dry days prior to the sampling date. This deduction can be supported by Wesley's (1973) observation of soils comprising halloysite and allophane where he concluded that soils of such nature were generally unaffected by evaporation to atmosphere or drainage and were capable of maintaining the same water content all year round.

Consolidation tests were not performed in this study to quantify the compressibility of the soil but the plasticity chart in Figure 5.2 indicates that Hamilton Ash is highly

compressible. A study by Gradwell and Birrel (1954) claimed that volcanic soils with allophane and halloysite as dominant constituents, such as Hamilton Ash do have high compressibility. According to Vargas, Foss and Prusza (as cited in Townsend, 1985), allophanic along with lateritic soils typically undergo a soil structural collapse upon saturation. From an engineering perspective, soil behaviour such as this is considered unfavourable as internal structural collapse in the soil mass can potentially cause major settlement issues (Townsend, 1985). The high compressibility nature of Hamilton Ash thus explains the settlement issues that are often encountered in compacted fills after some period of time.

5.3 Standard Compaction Test

5.3.1 Achieving Optimum Moisture Content and Maximum Dry Density

Soil characterisation tests classified Hamilton Ash as a moderately-well graded clayey SILT with a measured specific gravity of 2.62 which is typical for clayey soils (Yunusa *et al.*, 2013). Mineralogical analyses confirmed the occurrence of clay minerals like kaolinite, halloysite and allophane in the finer fractions and quartz and cristobalite plus other non-quantifiable minerals in the coarser silt and sand fractions. The soil's classification indices largely determines the soil's key compaction characteristics, namely the optimum moisture content and maximum dry density (Townsend, 1985).

When performed correctly, compaction improves the physical and mechanical properties of soils. The process of compaction is defined by Craig (1997) as the use of constant mechanical effort on a soil mass to increase densification by pore space reduction with no significant change to the volume of water in the soil. It is understood that soil strength is related to its water content and because of this, there is an optimum moisture content where maximum strength for the soil is yielded (Atkinson, 2007). The underlining principle is that high degree of compaction results in higher shear strength and lower soil compressibility. On that basis, standard compaction tests performed on Hamilton Ash samples were aimed at obtaining an optimum moisture content (w_{opt}) that yields a maximum dry density

$(\rho_d)_{max}$. It is noteworthy to mention that samples were air-dried and compacted at an initial moisture content of 26 % (NMC was 50.7 %).

Compaction test results for Hamilton Ash showed that the highest average $(\rho_d)_{max}$ of 1247 kg/m^3 was achieved at 13 % added w_{opt} which was 39.6% actual w_{opt} . However, repeatability tests proved that satisfactory dry densities are achievable over the range of 11% - 15% added moisture contents. The zero air voids line which represents the maximum possible value of dry density, a scenario that is practically unattainable but describes the complete expulsion of air from the soil rendering it fully saturated, was established at 1954.4 kg/m^3 and was plotted alongside the water - density curves in Figure 4.11 and 12. The range of maximum dry density values obtained in this research align with typical $(\rho_d)_{max}$ values for clayey volcanic soils but differ markedly in the w_{opt} values (Matsumura & Tatsuoka, 2018; Townsend, 1985; Wesley, 1973).

When comparing the determined compaction parameters of Hamilton Ash with previous work on soils with similar composition to Hamilton Ash, the w_{opt} determined for Hamilton Ash is significantly lower than those in earlier studies. For instance, Wesley (1973) investigated the compaction parameters of natural, air and oven-dried Javanese volcanic soils and generated compaction curves illustrated in Figure 5.2. Results from his investigation showed that air-dried latosols yielded $(\rho_d)_{max}$ values ranging from 1200 – 1340 kg/m^3 at w_{opt} varying between 35.5 – 48% which appear to be lower than andosols but relatively similar to Hamilton Ash whose actual w_{opt} was 39.6%. Comparatively, air-dried andosols generated lower degree of compactions with $(\rho_d)_{max}$ values ranging from 692 – 1084 kg/m^3 at even higher w_{opt} range of 53 - 95%. In another study, Townsend (1985) presented similar observations to Wesley (1973). He verified that latosols commonly exhibited higher $(\rho_d)_{max}$ and lower w_{opt} while andosols displayed lower $(\rho_d)_{max}$ at higher w_{opt}. Evidently, Hamilton Ash compaction results agree more with the compaction parameters of latosols than they do andosols. However, I am more inclined to propose a notion that Hamilton Ash can display compaction characteristics of both latosols and andosols because of its halloysitic, kaolinitic and allophanic mineralogical contents. Matsumara and Tatsuoka (2018) compacted fine sand/silt

materials of pyroclastic flow origin and derived $(\rho_d)_{max}$ values varying from 1030 to 1125 kg/m^3 at a w_{opt} range of 32.5 to 37.5%.

Soil pre-treatment such as drying can have significant impact on the soil properties and consequently on the compactness of clayey volcanic soils as established by Wesley (1973) and Townsend (1985). The distinctions made by Wesley (1973) between the compaction of natural, air- and oven-dried soils indicated that volcanic soils compacted in their natural state generally have very low degree of compactions with higher w_{opt} which reflect lower shear strengths compared to pre-dried samples. In agreement, Herrera *et al*. (2007) recommended drying out of volcanic soils before compaction in field-based applications due to the fact that the natural moisture content (NMC) of the soil in the field is typically wetter than the w_{opt}. As mentioned earlier, samples of Hamilton Ash were pre-dried (air) and compacted. No compaction test was conducted on soils in their natural moisture content. Studies supporting pre-sample drying indicate the possibility that the $(\rho_d)_{max}$ and w_{opt} values obtained for Hamilton Ash could be higher than what would be generated if the samples were compacted at their NMC. Drying back to a reasonable moisture content that is less than the w_{opt} and subsequently adding moisture to each sample to reach the w_{opt} allows for a wider range of satisfactory to high dry densities to be obtained under relatively lower moisture contents.

As added moisture content value was increased for each sample and compacted, it became apparent that samples compacted dry of w_{opt} were stiff and somewhat difficult to compact whereas those compacted wet of w_{opt} were too soft and became easily remoulded by the compaction rammer. This observed behaviour is a result of effect of water on the structure and orientation of the clay particles (Craig, 1997; Rahmat & Ismail, 2018). According to Craig (1997) and Rahmat and Ismail (2018), a dry soil will not compact easily and will display a rather stiff behaviour because of the intergranular friction. When water is added to the soil, it acts as a lubricant allowing particles to rearrange easily into a compact state under a constant compactive energy thus resulting in increased density. However, when moisture content exceeds the w_{opt}, the dry density decreases because the air voids between the grains become occupied with water. This is expressed by the weak state of the soil for samples compacted wet of w_{opt}. The soil that was once able to fail and

deform plastically under a constant mechanical energy begins to display liquid-like behaviour (Atkinson, 2007). As the results from this research and previous studies have demonstrated, at water contents below and above the w_{opt} the degree of compaction which is measured through stiffness and strength diminishes. Therefore, if the goal is to achieve maximum stability and strength in any earth structures, soils must be compacted at or as close to the optimum moisture content as possible (Atkinson, 2007).

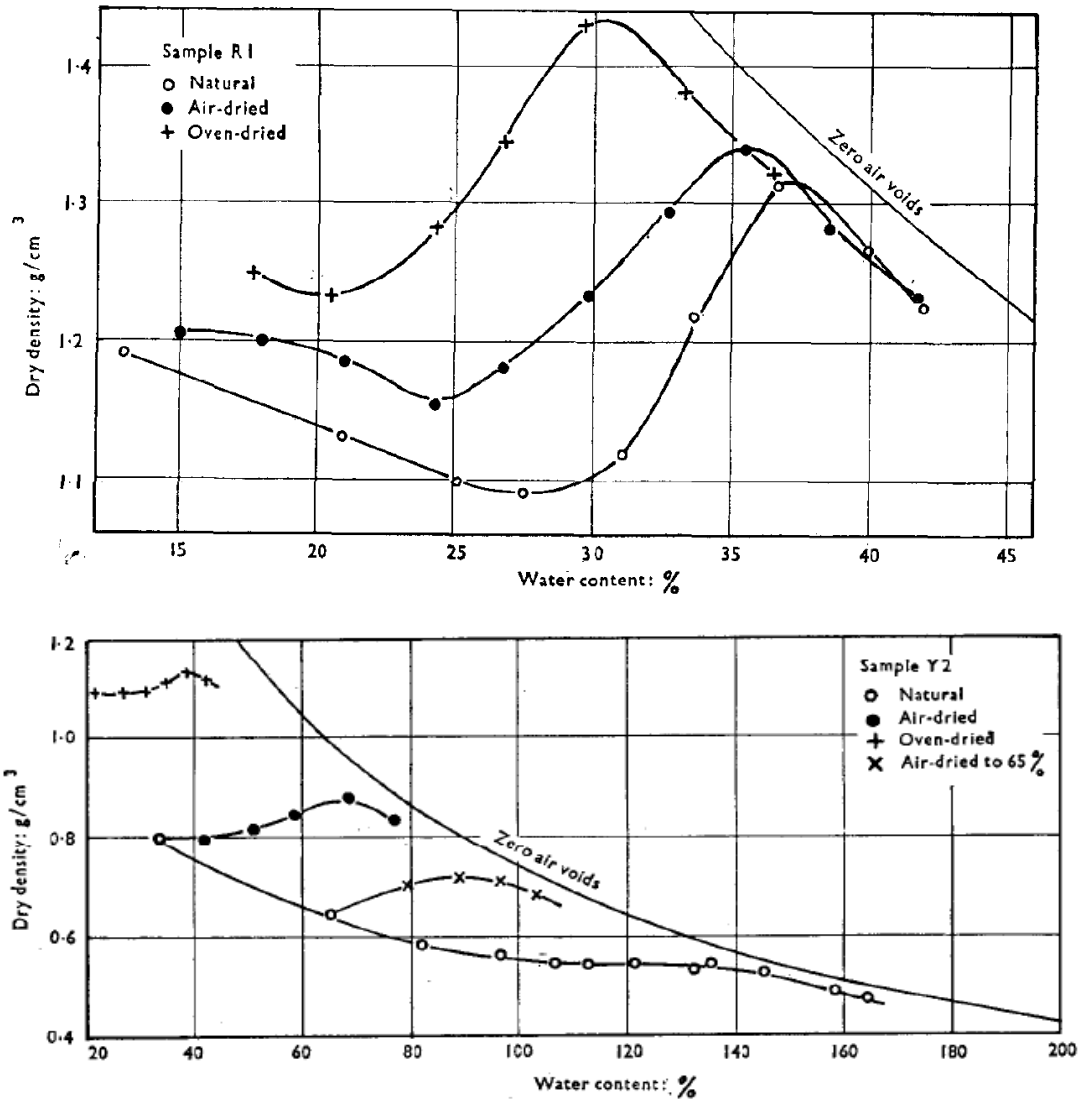

Figure 5.2. A comparison of compaction key parameters obtained by Wesley (1973) for a sample of latosols (top) and andosols (bottom).

For field-based applications, great emphasis must be placed on adding the right amount of moisture to the soil to achieve maximum compaction because the moisture content of the soil strongly influences the compactness and stability of the

soil (Rahmat & Ismail, 2018). Other key factors to be taken into consideration include soil drying (oven or air). As established in this section, many researches strongly encourage soil drying before compaction because moisture reduction in soil prior to compaction enhances the compaction characteristics of the soil, i.e. higher maximum dry density values are obtained at lower optimum moisture contents. Increased mechanical effort can also be beneficial to achieving favourable compaction parameters and has proven to be economically viable too as it requires less amount of time and work (Atkinson, 2007).

5.3.2 Repeatability Statistical Analysis

Repeatability (*r*) is defined as the statistical measurement of variation in repeated experiments on an object under the same conditions (Bartlett & Frost, 2008). Harper (1994) identified two types of repeatability; proportion and measurement. Proportional repeatability measures on a scale of 0 to 1. A repeatability of 1 denotes a perfectly consistent measurement with zero measurement error or changes to conditions of the object under investigation, on the other hand, a repeatability of 0 indicates variability in measurements owing to measurement error (Bartlett & Frost, 2008; Harper, 1994). Furthermore, according to Harper (1994) measurement repeatability dictates that there is a 95% chance that the measurement of repeatability (*r*) will be greater than the likely discrepancy between two measurements of the same object under study.

All compaction tests were conducted by the same researcher (author) and each set of tests was completed over a period of 2 weeks. The air-dried samples used for repeatability testing were tested at ~19 % natural moisture content. Since Test No.5 generated the anticipated results, i.e. $(\rho_d)_{max}$ of 1267 kg/m^3 was determined at 39.6 % actual w_{opt}, the experiment was repeated 3 more times within a short period of time to measure the ability of the experiment to reproduce similar results. Repeatability is understood to be related to standard deviation therefore the reliability of any measurements is determined by the standard deviation of the set of results. Standard deviation simply refers to the variability of measurements in a given sample (Altman & Bland, 2005), it is in fact a measure of the repeatability of the tests, in this case standard compaction, that produced the results.

The statistical quantities of the maximum dry densities were calculated and tabulated in Table 5.1. Only the $(\rho_d)_{max}$ were considered because all three $(\rho_d)_{max}$ were obtained at 13% added moisture content.

Table 5.1. Standard deviation calculations for the three repeatability tests.

Test Name	Score ($(\rho_d)_{max}$) g/mL
RT 1	1.254
RT 2	1.232
RT 3	1.233
Test No.5	1.267

Count	4
Mean (g/mL)	1.2466
Standard dev.	0.017

A very low standard deviation of 0.017 was determined for the repeatability tests. This is indicative of low measurement variability and close proximity to the average repeatability test $(\rho_d)_{max}$ values. This is not surprising since the compaction method and soil condition for the repeatability tests were similar to Test No.5. For this reason, a low variance was anticipated for all repeatability experiments. However, the sample group from which the standard deviation was derived is small and therefore places limitations on the reliability of the results. Ideally, 6-8 repeatability tests would provide a better representation of the variability of the experiments. But in the present study, only three repeatability tests were conducted due to shortage of Hamilton Ash samples and approaching research deadline.

Overall, statistical analysis of the results showed that standard compaction test of Hamilton Ash is repeatable, the results are reliable and there is negligible variance between the repeatability tests $(\rho_d)_{max}$ values and mean $(\rho_d)_{max}$ of 1240 kg/m^3 and Test No.5 $(\rho_d)_{max}$ of 1267 kg/m^3. However, it is important to note that even though an acceptable repeatability measurement was obtained for Test No.5 and Repeatability Tests No. 1 – 3, one thing that cannot be ascertained is the reproducibility of results. Reproducibility as defined by Bartlett and Frost (2008) refers to measurement variability from the same objected due to changing conditions. The observations made by the current researcher, the measurements of certain parameters and execution of the standard methodology of compaction test will almost certainly differ from any other observers undertaking the same experiment on Hamilton Ash samples in the future. The extent of variability

between the results from this study and future study will depend on the conditions in which the soils are tested and the observer's discretion.

5.4 Soil Shear Strength

In this section, the results for the soaking and vane shear tests are analysed and discussed accordingly. One of the key objectives of this research is to determine how saturation from the environment influences the compacted shear strength of the Hamilton Ash.

5.4.1 Soaking Test

A distinct relationship between soil compactness, void ratio, permeability and degree of saturation was realized in the results detailed in Chapter 4 of this paper, specifically in Table 4.11. The distinction between the non-soaked and soaked tests are defined by the aforementioned parameters of each sample. As stated earlier, compaction greatly impacts the physical properties of the soil and aims at improving the soil's shear strength, reducing the potential for future settlement problems and decreasing its permeability (Liu & Evett, 2008). Evidently, the compactness of Hamilton Ash dictates the magnitude and behaviour of its physical properties in relation to its void ratio, permeability and degree of saturation. In this section, the relationships between soil compactness vs. void ratio, soil compactness vs. permeability, and soil compactness vs. degree of saturation of Hamilton Ash will be evaluated sequentially.

5.4.1.1 Porosity and Void Ratio

Porosity and void ratio (e) are closely related when discussing the air and water components of soil. However, void ratio is commonly used by researchers and engineers when dealing with soil compaction. For the purpose of differentiation, porosity is a measure of void spaces in any volume of soil and is expressed in percentages whereas void ratio, denoted by e, is a comparison of the soil's volume of voids to the volume of solids. The e of Hamilton Ash samples were calculated individually for all six samples before and after each soaking period. The results

showed that the degree of compaction exerted a more dominant influence on the *e* values than soaking period did. Unsoaked samples with lower $(\rho_d)_{max}$ values generated slightly higher *e* values than the soaked samples as evidenced by Samples 3 and 5 with 0.559 and 0.566, respectively. Subsequent wetting for 7 and 21 days of Samples 3 and 5 detected no major impact of prolonged saturation on the compacted samples. Instead, an overall increase in both porosity and void ratio was apparent in all samples as depicted in Figure 4.13. Conversely, soils with higher compactness produced lower *e* values in both soaked and non-soaked scenarios. Essentially, these results attest to the claim that the higher the degree of compaction, the denser the packing is and the smaller the distribution of pore spaces within the soil.

Published literature reported volcanic ash soils, especially those of allophane and kaolinite-halloysite composition in their natural, undisturbed state, to have reasonably high porosities and void ratios because of their high silt/sand fractions (Gradwell & Birrel, 1954; Rouse *et al.*, 1986; Shoji *et al.*, 1993b; Wesley, 2009). Allophane-rich and kaolinite-halloysite rich soils recorded porosities of 0.72 and 0.66 respectively by Rouse *et al.* (1986) while Wesley (2009) reported larger void ratios ranging from 1.5 to 8 depending on NMC for the same type of soils. Comparatively, the *e* and porosity values derived for Hamilton Ash were relatively low which is not surprising given that the samples were extensively reworked, stockpiled and later compacted according to NZ standard methodology. As some studies have proven, remoulding through compaction can significantly reduce the soil's porosity and permeability (Townsend, 1985). A conclusion can be drawn that at a w_{opt} of 13 % and $(\rho_d)_{max}$ ranging from 1.233 - 1267 kg/m^3, void ratio within the soil was effectively reduced via three possible scenarios; a physical reduction of pore sizes, a smaller distribution of pore spaces or a combination of both (Gregory *et al.*, 2006).

5.4.1.2 Swelling Potential

Due to their high water retention capacity, allophane-rich volcanic soils *in situ* are seldom affected by climatic changes as claimed by Wesley (1973). The soil moisture is contained within the granular pores and is neither lost through

evaporation nor through drainage. Thus, there is little avenue for swelling when there is a change in soil moisture content.

Visual assessments and subsequent measurements showed little to no swelling and very low seepage rate (see Figure 4.14). Basically, swelling potential in Hamilton Ash is rather non-existent under prolonged saturation. This observation can be attributed to the high water retention capacity of the clay constituents of Hamilton Ash. It can also be speculated that due to the low porosity and permeability of the compacted samples, the soil was unable to retain substantial amount of water during soaking which may account for the small reduction (1-2 mm) in water height in all the buckets.

The lack of swelling can also be explained through the Activity Index, a single parameter that is used to predict swelling potential of clayey soils (Özdemir & Gülser, 2017). A clayey soil's AI is determined based on Skempton's (1953 as cited in Özdemir & Gülser, 2017) classes of clays; (1) inactive (AI <0.75), (ii) normal (AI >0.75 and ≤1.25) and (iii) active (AI >1.25). According to this classification, the clay fractions (allophane, kaolinite and halloysite) of Hamilton Ash samples examined are considered normal with a measured AI of 1.10. A normal activity index implies that there zero to low potential for compacted Hamilton Ash to swell in relation to prolonged exposure to saturation. However, there is potential for shrinkage due to the characteristic behaviour of halloysite to dehydrate irreversibly and kaolinite's inability to uptake water. Any moisture addition moisture intake would only be contained within the pore spaces.

5.4.1.3 Permeability

A soil's permeability largely depends on the interconnectivity of the voids between the particles. A parallel relationship exists between void ratio and permeability in any type of soil. Soils with sizable pore spaces typically have large void ratios with higher permeability than soils with smaller voids. One of the primary effects of compaction on soil is reduction of permeability (Liu & Evett, 2008). In this research, no laboratory test was performed on the compacted, soaked samples to determine the hydraulic conductivity (permeability) of Hamilton Ash. Nonetheless,

it can be assumed that permeability was effectively reduced during compaction. Based on published literature of permeability values pertaining to compacted volcanic soils, a rough estimation of permeability can be derived for Hamilton Ash. Typically, undisturbed soils of volcanic origin are highly permeable (Wesley, 2009). Herrera *et al*. (2007) stated that volcanic soils are generally more permeable for soils with high specific surface. In another study, Wesley (1977) noted that despite the higher clay contents, volcanic ash-derived soils tend to be more permeable than sedimentary-derived soils and evidently reported permeability (*k*) coefficient values ranging from 1-13 x 10^{-8} m/s and 0.8-27 x10^{-8} m/s for halloysite-rich and allophane-rich soils, respectively.

Permeability is drastically reduced when soils are remoulded during compaction as described by Wesley (1977) whereby the soil structure is irreversibly destroyed. In a later study, Wesley (2009) further elaborated that when highly permeable volcanic ash soils, especially allophanic soils, are remoulded the spherical allophane aggregates that are enclosed in a thread of imogolite are destroyed upon impact causing a drastic reduction of permeability within the soil mass (Figure 5.3).

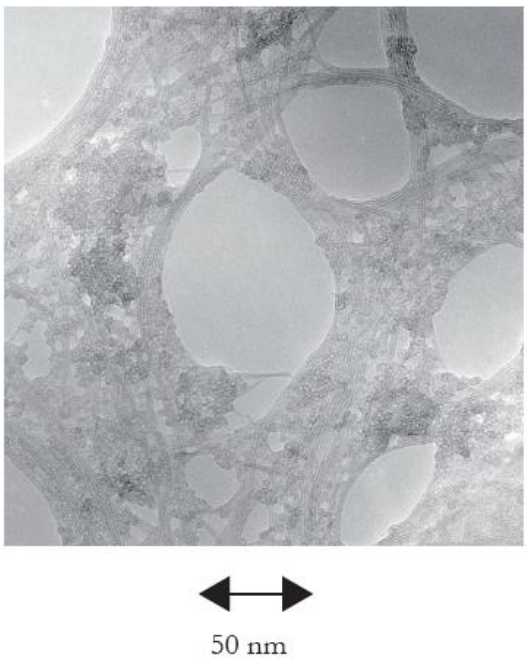

Figure 5.3. An electron microscopy image of allophane and imogolite (after Wada, 1989 as cited in Wesley, 2009).

When a soil's porosity and permeability are lowered through compaction, infiltration rate of surface water into the soil is also reduced (Gregory *et al.*, 2006). Infiltration rate is impeded when the governing hydraulic properties of the soil are affected as a result of compaction. These primary hydraulic properties include water retention capacity, diffusivity and hydraulic conductivity (Gregory *et al.*, 2006). This is believed to have occurred to the samples compacted and subjected to various wetting periods. A progressively declining trend in seepage or infiltration rate is apparent across Samples 1-6 as portrayed in Figure 4.14. The rate of seepage/infiltration was determined through change in water level in each bucket after subsequent soaking episodes. The declining trend observed in the rate of seepage correlates inversely to an increase in soaking period, that is, the longer the soaking period, the slower water infiltrated into the compacted soil.

The graph shows a rather significant drop in seepage rate from Sample 1 to 2 and Samples 2 to 6 generated a slow and steady pattern, thus indicating a gradual drop in seepage rate. Sample 1 had the highest seepage rate due to repeated wetting and soil disturbance via vane penetration. The compacted mass was soaked for an hour, then was subjected to vane shear penetration and then re-soaked for another hour. This cycle was repeated for 3 hours in total. The premise is that penetration on the surface of the compacted soil lessened the soil's compactness and permitted a larger amount of water to infiltrate the soil when the sample was subjected repeatedly to the hourly wetting cycles for 3 hours, hence a high seepage rate. The results do conclude that when Hamilton Ash is compacted to the optimum moisture content and maximum achievable dry density, surface water is less likely to percolate into the soil, even under prolonged exposure to saturation from the environment. Minimal seepage can be expected but only in the first few centimetres beneath the surface. However, if the soil is disturbed after maximum compaction and is simultaneously exposed to excessive moisture, there is potential for increased infiltration throughout the soil which may, in turn, impact the shear strength of the soil (to be discussed in the next section).

5.4.1.4 Degree of Saturation

A general decline in the degree of saturation is also noted for compacted soils before and after the soaking period as illustrated in Table 4.11 of the results section. The calculated degree of saturation for compacted soils before soaking varied between 90% and 98 %, however after soaking, a wide range of values was exhibited (97 – 100.7 %), exposing an overall increasing trend in all six samples as a result of soaking. The results also revealed a strong relationship between the soil compactness and degree of saturation. Higher degree of compaction results in lower saturation because pore space distribution and permeability are reduced which impede flow of water throughout the soil. Samples (3 and 5) with lower maximum dry densities (1185.5 and 1180.1 kg/m^3 respectively) exhibited the highest increase in the degree of saturation. To an extent, these results stress the importance of achieving maximum compaction in order to sufficiently reduce the level of saturation present within the soil.

5.4.2 Vane Shear Strength Test

The method of compaction is used extensively in the construction of earth structures. In order to prevent future geotechnical issues involving bearing capacity, slope stability and lateral earth pressures, determining and understanding the shear strengths of these compacted earth structures is considered as very important (Çokça & Tilgen, 2010).

A soil's strength, whether *in situ* or disturbed is defined by its ability to support any type of load without giving into failure. Displacement is a direct result of failure. Geotechnical failures of any earth structure occur when the amount of stress applied to the soil mass is equal to (Craig, 1997) or exceed the shear strength of the soil (Bergaya & Lagaly, 2013). In general, higher shear strength means greater resistance to failure. When dealing with soil shear strength, two key parameters are considered; cohesion intercept and angle of shearing resistance (friction angle). A soil's resistance to failure is derived from these two Mohr-Coulomb shear strength parameters. The shear strength parameters of any soils can be determined by means of laboratory tests.

It was hypothesized that shear strength of compacted Hamilton Ash in the construction earth structures such as embankments or foundations will degrade over time after prolonged exposure to increased saturation, particularly through rainfall or groundwater. To test this theory, vane shear tests were performed on seven compacted Hamilton Ash samples, six of which were subjected to different wetting periods between 1 to 1248 hours (52 days). All seven samples were compacted under the determined optimum moisture content of 13 % added water (39.6% actual w_{opt} but minor variations were observed in the corresponding numerical maximum dry density values. The highest $(\rho d)_{max}$ of 1233.43 kg/m^3 was achieved by sample 1 and was followed in close range by the non-soaked sample (sample 0) with 1233.04 kg/m^3 while the lowest $(\rho d)_{max}$ was yielded by sample 5 at 1180.13 kg/m^3. Dry density or dry unit weight is an important factor in soil compaction as it is an expression of the degree of compaction of the soil which ultimately reflects the soil shear strength. The general understanding is that larger maximum dry densities reflect higher soil strength (Craig, 1997). On this account, it can be assumed that compacted Hamilton Ash samples were more or less at their highest strength before soaking.

Marinho *et al*., (2013) cited two studies conducted separately by Toll and Ong (2003) and Rahardjo *et* al., (2004a) that described the interrelationship between moisture content and shear strength. Both studies showed that residual soil shear strength is sensitive to wetting and drying cycles after compaction. In order to effectively examine the change in shear strength before and after prolonged wetting, a dry (non-soaked) sample that was compacted to the optimum moisture content (~13 %) was subjected to vane shearing and a shear strength of 50.6 kPa was measured. This initial shear strength was used as a reference point to investigate the shear strength behaviour of the six remaining soaked samples in relation to water content after each soaking period.

The resulting graph in Figure 4.16 portray a linear relationship between soaking time and shear strength. The data presented in these graphs suggest that lengthened exposure to saturation after compaction does not necessarily promote shear strength degradation, but instead additional moisture in the soil tends to increase its undrained vane shear strength (τ_v). These results contradict the baseline concept that

shear strength declines with elevated moisture content in soil (Bergaya & Lagaly, 2013). The highest τ_v recorded in this study was 74.5 kPa and this was achieved after almost 2 months (1248 hours) of soaking. Bearing in mind that the initial shear strength of compacted Hamilton Ash is 50.6 kPa, the sample that was soaked for almost 2 months generated an incredibly high shear strength value that far exceeded the dry-compacted sample. According to Prinz and Strauß's (2006, as cited in Bergaua & Lagaly, 2013) classification of undrained shear strength, the shear strength of Hamilton Ash both before and after soaking will be considered as medium strength. From an engineering standpoint, soils with medium to high strength is highly favourably because this inherently means that stability is guaranteed. On the other hand, lower numerical values for remoulded strength was generated (2.6 – 41.2 kPa) which consequently classed them as low strength. This is not surprising because lower strength values are generally expected in remoulded samples. In investigating the behaviour of halloysite-rich soils, Moon (2016) characterized halloysite-rich soils as having lower remoulded shear strength with typical values for cohesion obtained at less than 5 kPa and friction angles valued between 15-35°. Other authors (Wesley, 1977; Campbell & Parry, 2002; Parry *et al*., 2004) cited by Moon (2016) also indicated lower shear strength parameters in the remoulded samples except Reading (1991) and Wang *et al*., (2014) who reported higher friction angle values for halloysitic soils.

The following speculations are proposed in an attempt to understand the unexpected shear strength behaviour of compacted Hamilton Ash and its relationship to prolong wetting periods. Firstly, the initial drop in shear strength in sample 1 within the first hour of soaking was hardly surprising as this phenomenon is attributable to clay hydration, minor expansion and lubrication upon interaction with water (Craig, 1997; Hensen & Smit, 2002). Given that Hamilton Ash is a cohesive soil with only 19% clay and larger percentage of silt and sand fractions, the shear strength of the soil will be determined by both the apparent cohesion and frictional angle of the soil. However, Bergaya and Lagaly (2013) stated that shear strength depends mainly on the quantity of the granular portion in the soil. In any case, this does not disregard the fact that presence of clays in any amount within a soil mass can also have a dominating influence on the behaviour of the soil.

One of the characteristics of allophane-rich and halloysite-rich soils is their high sensitivity to the effects of drying and remoulding before and during testing as described by Townsend (1985). During remoulding, the allophane structures are destroyed resulting in further loss of shear strength but as proven otherwise in the present study, remoulding through compaction increases soil shear strength. Townsend (1985) also observed that remoulding of lateritic soils have the tendency to generate finer fractions when the cementing bonds between the clay clusters are broken down. The introduction of additional moisture (soaking) into the soil after compaction (remoulding) most likely formed interactions between these finer fractions and water, hydrating them and causing further lubrications of the particles. It is important to note that the clays are not rehydrated by this process, rather water is filling up the remaining pore spaces within the soil mass.

As mentioned earlier, clay hydration in Hamilton Ash was considered as a contributing factor to the sudden drop in shear strength. According to previous research, halloysite cannot be rehydrated once dehydrated (Moon, 2016; Townsend, 1985). In the present study, Hamilton Ash samples were air-dried prior to testing which suggests that halloysite was largely affected by this soil treatment and allophane to a lesser extent but kaolinite remain somewhat unchanged dehydration (Rouse *et al.*, 1986).

Finally, clay expansion was also deemed responsible for the sudden decline in shear strength in sample 1. Some studies have shown that LL can be used to estimate the degree of expansion in cohesive, volcanic soils (Janardhana & Abdul-Aleam Ahmed, 2016). Based on the results presented by Janardhana and Abdul-Aleam Ahmed (2016), Hamilton Ash has a very high degree of expansion and will expand significantly upon interaction with water due to its very high LL of 74 %. Expansive soils are well known for causing engineering problems because of their receptive response to alterations in moisture content causing volumetric changes within the soil mass which may ultimately affect the stability of the structures built on them (Al-Rawas *et al.*, 2005). These soils tend to shrink or swell when moisture content is reduced or increased respectively. Low shrink or swell capacity is generally viewed positively in engineering. Soils with severe swelling potential are closely associated with the presence of montmorillonite and smectite in the soils (Al-Rawas

et al., 2005; Janardhana & Abdul-Aleam Ahmed, 2016). Conversely, volcanic soils such as kandoids (kaolin/halloysitic-rich; "latosols" as defined earlier), and allophanic soils reflect low swelling potential (Moon, 2016; Rouse *et al.*, 1986). In the case of Hamilton Ash, x-ray diffraction confirmed no occurrence of the montmorillonite or smectite clay minerals, meaning no swelling potential exist for compacted Hamilton Ash. This was evident in all the soaked samples. Visual observations and measurement recorded little to no swelling on the compact surfaces. However, shrinkage potential is rather apparent in Hamilton Ash due to the presence of halloysite. Moon (2016) expressed concern for halloysite-rich soils having high shrinkage potential when dehydrated.

Furthermore, it can be reliably assumed that the continual decline for the next 2 hours was due to elevated water infiltration as a result of soil penetration via vane shearing. In other words, subjecting the compacted soil to multiple shearing caused significant disturbances in the compacted structure of the soil, which may have permitted an excessive flow of water into the soil over a short span of soaking time. The now elevated moisture content is guaranteed to reduce the shear strength because increased soil saturation have the tendency to decrease effective cohesion and increase the soil's pore pressure (Hidalgo *et al.*, 2017).

The continual decline in soil strength was halted after the third hour of soaking. After the third hour of soaking, shear strength increases linearly with soaking period. It is rather apparent that with longer soaking period, the compacted soil became increasingly stronger. The increase in shear strength can be correlated to clay interaction with added moisture. Typical clay behaviours regarding shear strength development is centred on restructuring or orientation and enhanced cohesion. Wesley (1977) remarks that higher shear strength in volcanic soils stem from high moisture contents. While this is true for allophanic soils whose key characteristic involves high water retention capacity, the same cannot be said about halloysite. Halloysite-rich soils derive their high frictional resistance from the tubular morphology and aggregation of the clay minerals (Moon, 2016). From these considerations, the predominant occurrence of both of these clay minerals in Hamilton Ash and their reaction to prolonged soaking thus explain the growing shear strength observed in the results of the present study.

Townsend (1985) compiled a list of strength parameter data from previous studies on residual soils by various researchers (Horn, 1982a; Townsend, 1970; Pursza, 1983; Vargas, 1953; Wesley, 1974; Horn, 1882b) who implemented a wide variety of testing methods to produce these data. The shear parameters outlined in these studies are representative of tropical residual soils only which means a certain degree of variance is expected between these published data and data from this present study. According to these published data, typical andosol (allophane-rich) strength parameters ranged between 36° and 24 kPa respectively for effective friction angles (ϕ') and *ć*. Lateritic soils (kaolin/halloysite-rich) generally have higher shear strength parameters with ϕ' typically varying between 20° to 30° for lateritic clays and between 30° and 40° for lateritic gravels while *ć* values ranged from 0 – 100 kPa and 0 – 40 kPa respectively for clayey and gravelly latosols. Wesley (1977) also reported slightly lower shear parameters for compacted andosols in the order of 38-40° for ϕ' and apparent *ć* varying from 14.7 to 17.7 kPa but higher *ć* value of 23 kPa and lower ϕ' measurement of 31° in latosols. Moon (2016) noted in a study of the geomechanical properties and behaviour of halloysite-rich soils that peak cohesion values of 0-70 kPa are characteristic to these type of soils while other authors reported values ranging from 12-18 kPa which agreed with value of 14 kPa for andosols that was reported initially by Wesley (1977). The cohesion values of halloysite reported by Moon (2016b) are consistent with Wesley's (1977) latosols which ranged between 0-100 kPa.

In the case of soil shear strength, none of the studies reviewed above made direct mention of the shear strength of the soils under study. Instead, brief statements were made on the high shear strength of these soils but primary focus revolved greatly around defining the shear strength parameters of the Mohr-Coulomb criterion; cohesion and frictional angle. However, in the present study the shear parameters could not be determined due to the testing method implemented (vane shear). Rather, soil shear strengths for each sample were computed directly from application of torque to the soil that induced shearing. Since shear parameters typically reflect soil shear strength, a deduction can be drawn from the early studies for compacted volcanic soils rich in halloysite and or allophane. Therefore, it can be concluded that to a degree, the Hamilton Ash shear strength values which

evidently range from 16.9 to 74.5 kPa for wet samples and 50.6 kPa for the single dry sample are consistent with high shear strength values reported by Moon (2016b), Townsend (1985) and Wesley (1977).

Ultimately, the results from the present study clearly demonstrated that shear strength of Hamilton Ash after compaction was improved significantly when moisture contents within the compacted mass was elevated. However, it is important to note that elevated shear strengths are achievable only if the maximum degree of compaction is targeted for the dry density values ranging 1233 to 1267 kg/m^3 at the determined actual w_{opt} of 39.6 %. By ensuring that a higher degree of compaction is attained, other engineering properties of the soil that influence shear strength such as porosity and permeability will be subsequently lowered as well. In effect, this will control the movement of water into the soil during prolong wetting periods. As the results have shown, a very low moisture infiltration rate is preferable if higher shear strength is to be yielded.

5.5 Limitations and Future Research Recommendations

The overall outcome of this study was unexpected as mentioned in section 5.4. Contrary to the proposed hypothesis, shear strength of compacted soils react positively to prolonged exposure to moisture under very low infiltration rates. However, there are a few limitations to the present study that must be addressed accordingly. Ideally, more than one soil strength test is required for effective data comparison but in the case of this study, only laboratory vane shear test was performed on the compacted samples. The initial plan for this research included California Bearing Ratio (CBR) and triaxial testing but due to equipment unavailability, these tests could not be conducted. The strength values derived from the single use of vane shear are reasonably consistent with the shear strength values generated through triaxial tests by other researchers. Nevertheless, further strength tests are recommended for the present study to obtain highly reliable results.

This study on the strength and deformation characteristics of Hamilton Ash materials can be used as a starting point for additional research. Further investigation surrounding this topic is recommended, especially the following:

- Proper testing using known standard methodologies for hydraulic conductivity (permeability) determination is recommended. The permeability of the compacted samples in the present study was assumed and correlated based on published literature.
- The rate of seepage or infiltration from added moisture during soaking was calculated based on the soaking time in hours and change in water depth in in the soaking tank (mm). In future studies, double or single ring infiltrometers can be used instead of measuring infiltration rates based on changes in water level and soaking period.
- Vane shear test was the only strength test implemented in this study to determine the shear strength of the compacted samples. This is not advisable for more comprehensive and extensive studies. It is more ideal to employ more than one strength test in future studies, such as the triaxial, direct shear or CBR tests.
- The compressibility of Hamilton Ash materials were determined based on Atterberg Limits only. It is recommended that consolidation tests be performed on the compacted samples to determine the soil's compressibility values numerically.
- Further investigation into the positive effects of water on compacted soil strength is recommended. Scanning Electron Microscope (SEM) work can be engaged after each soaking stage to see if structural changes can be observed in the soils.

Chapter 6

Conclusion and Future Research

6.1 Conclusion

The extensive use of Hamilton Ash materials in earthworks renders it important to investigate its engineering properties. A hypothesis was formulated with the basis being that compacted fill materials comprising of Hamilton Ash units will deteriorate in shear strength progressively over time after much exposure to intense and prolonged rainfall periods. For this reason, a comprehensive study into determining the optimum moisture content and maximum dry density wherein the highest shear strength is accomplished, was undertaken for Hamilton Ash materials. It is understood that a soil compacted to the optimum dry density is an indication of the soil being in its highest shear strength.

A review of studies surrounding the engineering properties, especially the compaction characteristics of Hamilton Ash revealed that little attention has been given to this volcanic soil. However, a myriad studies (Birrel & Fieldes, 1952; Bishop *et al.*, 2013; Lowe, 2010b; Lowe & Percival, 1993; Parfitt, 1990; Ward, 1967) involving its dominant clay fractions namely, allophane and halloysite and kaolinite and their respective index properties have been conducted extensively. These known information were used to compare the results obtained from the characterisation tests performed in the present study. The results generally align with published literature. Grainsize and mineralogical analyses were performed using laser and x-ray diffraction techniques, respectively while the Atterberg Limits were determined using the drop cone penetrometer and thread-rolling methods. Atterberg Limits and Grainsize analysis characterized Hamilton Ash materials as a high compressibility, moderately to well graded, sandy SILT with some clay. The plotting of Hamilton Ash below the A-line is consistent with previously published data.

Mineralogical analysis confirmed the presence of quart and cristobalite as the dominant coarse fractions while 10Å-hayllosite, 7.2Å-kaolinite and allophane constituted the clay fractions of Hamilton Ash. Due to the amorphous structure of

allophane, this clay mineral could not be detected and quantified by x-ray diffraction, instead the field identity test developed by Fieldes and Perrott (Brydon & Day, 1970) was used to confirm its occurrence in Hamilton Ash. Overall, the results from the soil characterisations tests revealed that Hamilton Ash contains a higher percentage of silt and sand fractions (48.1 % and 35.5%) than clay (19.1%), which is considered favourable for field-based applications.

Soil compaction is commonly used to increase soil strength and ensure stability. For this purpose, samples of Hamilton Ash were compacted under various added moisture contents to determine the optimum moisture content (w_{opt}) wherein the maximum dry density ($(\rho_d)_{max}$) was obtained. The actual w_{opt} for Hamilton Ash was determined at 39.6% moisture content where the highest $(\rho_d)_{max}$ of 1267 kg/m^3 was achieved. However, the results showed that satisfactory dry densities can also be obtained between the 1233 to 1267 kg/m^3 at 39.6 % w_{opt}. Further soaking tests performed on compacted samples revealed that at 39.6% w_{opt} and $(\rho_d)_{max}$ range of 1233 to 1267 kg/m^3, porosity and void ratio was significantly lowered and so was permeability. The degree of saturation depended on the soil compactness, that is, soils with higher dry densities typically have lower degree of saturation because of the reduced void ratio and permeability within the compacted soil mass. Visual observations also confirmed that moisture did not infiltrate the entire compacted sample, instead only ~5 cm below the surface of the compacted soil was saturated. In general, the results showed that prolonged exposure to rainfall after compaction increase the moisture content of the soil but at a very slow rate of seepage/infiltration. In addition, due to reduced porosity and permeability of the soil, moisture does not fully infiltrate the soil to greater depths.

As numerous studies have shown, water typically has a negative effect on soil strength. The presence of moisture in soil has the tendency to reduce the effective shear strength between the soil particles which can force apart the particles as moisture content increase continually, eventually resulting in a complete loss of shear strength which can lead to failure or instability problems. In order to understand the impact of prolonged moisture exposure on the compacted soil, six samples were soaked for various time periods and vane shear test was performed after each soaking period. The final vane shear strength of the compacted soil after

52 days of soaking was 74.5 kPa. This value exceeded the initial shear strength of the compacted soil (unsoaked sample) by 20 kPa; the non-soaked sample had a vane shear strength of 50.6 kPa. The results suggested a strong linear correlation between shear strength and soaking period. Contrary to the hypothesis of the present study, the results indicated that prolonged exposure to moisture does not reduce the soil shear strength but increases it progressively overtime. Even though the reasons for this effect are speculated in this study, the reasons still remain unclear. Hence, further research is required to investigate this effect.

6.2 Research Benefits

The outcome of this research is beneficial to the engineering community in the greater Waikato region, especially in civil or geotechnical engineering works that requires the use of Hamilton Ash materials. This research has provided critical information regarding the engineering properties of Hamilton Ash that can be carefully factored when designing earth structures comprising of said material or calculating loads to be supported by said material. The results from this research, particularly the compaction parameters, were obtained from a laboratory setting which means they can only be used as a guide when considering field applications.

References

Al-Rawas, A. A., Hago, W. A., & Al-Sarmi, H. (2005). Effect of lime, cement and Sarooj (artificial pozzolan) on the swelling potential of an expansive soil from Oman. *Building and Environment, 40*, 681-687.

Altman, G. D., & Bland, M. J. (2005). Standard deviation and standard errors. *BMJ, 331*, 903.

Atkinson, J. (2007). *The Mechanics of Soils and Foundations*. Chapter 3: Essentials of Material Behaviour (2nd ed.). New York: NY: Taylor and Francis.

Bartlett, W. J., & Frost, C. (2008). Reliability, repeatability and reproducibility: analysis of measurement errors in continuos variables. *Ultrasound Obstet Gynecol, 31*, 466-475.

Beca Limited. (2018). *Cambridge C1 C2 & C3 Plan Change Liquefaction Hazard Assessment.* Geotechnical Parameters. Beca Limited. 17-60p. https://www.waipadc.govt.nz/our-council/Waipa2050/wdc-part-operative/Variations/Documents/Plan%20Change%207/Cambridge%20C1%20C2%20%20C3%20Plan%20Change_Liquefaction%20Assessment%20Report%20FINAL_16%20April%202018.PDF.

Bergaya, F., & Lagaly, G. (2013). Mechanical Properties of Clays and Clay Minerals. In *Handbook of Clay Science* (2 ed., Chapter 9, pp. 354-359). Amsterdam: The Netherlands: Elsevier.

Birrel, S. K., & Fieldes, M. (1952). Allophane in Volcanic Ash Soils. *Journal of Soil Science, 3*(2), 156-166.

Bishop, L. J., Rampe, B. E., Bish, L. D., Abidin, Z., Baker, L. L., Matsue, N., & Henmi, T. (2013). Spectral and Hydration Properties of Allophane and Imogolite. *Clays and Clay Minerals, 61*(1), 57-74.

Blotz, R. L., Benson, H. C., & Boutwell, P. G. (1998). Estimating Optimum Water Content and Maximum Dry Unit Weight for Compacted Clays. *Journal of Geotechnical and Geoenvironmental Engineering, 124*(9), 907-912.

British Standard BS 1377-7:1990, *Methods of test for soils for civil engineering purposes. Shear strength tests (total stress).*

Brydon, E. J., & Day, H. J. (1970). Use of the Fieldes and Perrot Sodium Fluoride Test to distinguish the B horizons of Podzols in the field. *Canadian Journal of Soil Science, 50*, 35-41.

Clough, E. M., & Payn, W. T. (1988). The Fieldes and Perrott field test as an aid to identification ofor podzol B horizons. *South African Journal of Plant and Soil, 5*(1), 43-45.

Çokça, E., & Tilgen, P. H. (2010). Shear strength-suction relationship of compacted Ankara clay. *Applied Clay Science, 49*, 400-404.

Craig, R. F. (1997). *Soil Mechanics*. Soil Compaction (6th ed.). New York, NY: E & FN Spon.

Fener, M., & Nazli, Y. (2013). Vertical pore structure profile of a compacted clayey soil. *Engineering Geology, 166*, 204-215.

Gautheyrou, J., Loyer, Y. J., & Pansu, M. (2001). *Soil Analysis*. (1st ed.). Taylor & Francis.

Gradwell, M., & Birrel, S. K. (1954). Physical properties of certain volcanic clays. *New Zealand Journal of Science and Technology, 36*(2), 108-122.

Gregory, H. J., Dukes, D. M., Jones, H. P., & Miller, L. G. (2006). Effect of urban soil compaction on infiltration rate. *Journal of Soil and Water Conservation, 61*(3), 117-124.

Gue, S. S., & Liew, S. S. (2001). *Fill Compaction and its consequences of non-compliance*. Presented at the Conference Technology CONTEC, retrieved from http://www.gnpgeo.com.my/download/publication/kl_01.pdf.

Harper, G. C. D. (1994). Some comments on the repeatability of measurements. *Ringing and Migration, 15*(2), 84-90.

Hensen, J. M. E., & Smit, B. (2002). Why Clays Swell. *Journal of Physical Chemistry B, 106*, 12664-12667.

Herrera, M. C., Lizcano, A., & Santamarina, J. (2007). Colombian volcanic ash soils. *Characterisation and Engineering Properties of Natural Soils, 3*, 2385-2409.

Hidalgo, A. C., Vega, A. J., & Obando, P. M. (Compiler) (2017). *Effects of the Rainfall Infiltration Processes on the Landslide Hazard Assessment of Unsaturated Soils in Tropical Mountainous Regions*. Engineering and Mathematical Topics in Rainfall: IntechOpenhttps://www.intechopen.com/books/engineering-and-mathematical-topics-in-rainfall/effect-of-the-rainfall-infiltration-processes-on-the-landslide-hazard-assessment-of-unsaturated-soil.

Horn, R., Domzal, H., Slowinska-Jurkiewicz, A., & Ouwerkerk van, C. (1995). Soil compaction processes and their effects on the structure of arable soils and the environment. *Soil & Tillage Research, 35*, 23-36.

International Standards Organization ISO/TS 17892-12:2004, *Geotechnical Investigation and testing - Laboratory testing of soil - Part 12: Determination of Atterberg limits.*

Ishibashi, I., & Hazarika, H. (2010). *Soil Mechanics Fundamentals*. Florida; NY: CRC Press.

Janardhana, M. R., & Abdul-Aleam Ahmed, A. D. (2016). Geotechnical Characteristics of Volcanic Soils in an around Taiz City, Yemen. *International Journal of Earth Sciences and Engineering, 9*(3), 420-425.

Jesmani, M., Manesh, A. N., & Hoseini, M. R. S. (2008). Optimum Water Content and Maximum Dry Unit Weight of Clayey Gravels at Different Compactive Efforts. *Electronic Journal of Geotechnical Engineering, 13*, 1-14.

Liu, C., & Evett, B. J. (2008). Permeability, Capillarity, and Frost Heave. In A. Vernon (Ed.), *Soils and Foundations* (7th ed., Chapter 2-7, pp. 39-40). Upper Saddle River: Ohio: Pearson, Prentice Hall.

Lowe, J. D., & Percival, J. H. (1993). *Clay mineralogy of tephras and associated paleosols and soils, and hydrothermal deposits, North Island [New Zealand]*. Guide book for New Zealand Pre-onference Field Trip F.1. Adelaide, Australia: Tenth International Clay Conference, AIPEA.

Lowe, J. D. (2010a) Introduction to the landscapes and soils of the Hamilton Basin. In J. D. Lowe, E. V. Neall, M. Hedley, B. Clothier & A. Mackay (Eds.), *19th World Congress of Soil Science: Solutions for a changing world* (Vol. 3). Brisbane, Australia: New Zealand Society of Soil Science.

Lowe, J. D. (2010b) Quaternary volcanism, tephras, and tephra-derived soils in New Zealand: an introductory review. In J. D. Lowe, E. V. Neall, M. Hedley, B. Clothier & A. Mackay (Eds.), *19th World Congress of Soil Science: Soil solutions for a changing world* (Vol. 3, pp. 7-29). Brisbane, Australia: New Zealand Society of Soil Science

Marinho, A. M. F., Oliveira, M. O., & Vanapalli, S. (2013). Shear strength behaviour of compacted unsaturated residual soil. *International Journal of Geotechnical Engineering, 7*(1), 1-9.

Massarsch, R. K., & Fellenius, H., Bengt. (2002). Vibratory compaction of coarse-grained soils. *Canada Geotechnical Journal, 39*, 695-709.

Matsumura, S., & Tatsuoka, F. (2018). Effect of compaction conditions and fines content on cyclic undrained strength of saturated soils. *Soil Dynamics and Earthquake Engineering, 112*, 152-161.

Moh, Z.-C. (2004). *Site Investigation and Geotechnical Failures*. Presented at the International Conference on Structural and Foundation Failures, retrieved from http://ftp.maa.com.tw/common/publications/2000/2000-082.pdf.

Moon, G. V., Mills, R. P., Kluger, M. O., Lowe, J. D., Churchman, J. G., de Lange, P. W., Hepp, A. D., Kreiter, S., & Morz, T. (2017) Sensitive pyroclastic soils in the Bay of Plenty, New Zealand: microstructure to failure mechanisms. In J. G. Alexander & Y. C. Chin (Eds.), *20th NZGS Geotechnical Symposium*. Napier, New Zealand. https://researchcommons.waikato.ac.nz/handle/10289/11555.

Moon, V. (2016). Halloysite behaving badly: geomechanics and slope behaviour of halloysite-rich soils. *Clay Minerals, 51*(3), 517-528.

Orense, P. R., Zapanta Jr, A., Hata, A., & Towhata, I. (2006). Geotechnical characteristics of volcanic soils taken from recent eruptions. *Geotechnical and Geological Engineering, 24*, 129-161.

Otalvaro, F. I., Neto, P. C. M., Delage, P., & Caicedo, B. (2016). Relationship between soil structure and water retention properties in a residual compacted soil. *Engineering Geology, 205*, 73-80.

Özdemir, N., & Gülser, C. (2017). Clay activity index as an indicator of soil erodibility. *Eurasian Journal of Soil Science, 6*(4), 307-311.

Parfitt, L. R. (1990). Allophane in New Zealand - A Review. *Australian Journal of Soil Research, 28*, 343-360.

Pullar, A. W. (1967). Volcanic Ash Beds in the Waikato District. *Earth Science Journal, 1*(1), 17-30.

Rahmat, N. M., & Ismail, N. (2018). Effect of optimum compaction moisture content formulations on the strength and durability of sustainable stabilised materials. *Applied Clay Science, 157*, 257-266.

Ridley, A. M. (2015). *Soil Suction - what it is and how to successfully measure it*. Presented at the Field Measurements in Geomechanics, retrieved from https://papers.acg.uwa.edu.au/p/1508_0.2_Ridley/.

Rollins, M. K., Jorgensen, J. S., & Ross, E. T. (1998). Optimum Moisture Content for Dynamic Compaction of Collapsible Soils. *Journal of Geotechnical and Geoenvironmental Engineering, 124*(8), 669-708.

Rouse, C. W., Reading, J. A., & Walsh, P. D. R. (1986). Volcanic Soils Properties in Dominica, West Indies. *Engineering Geology, 23*, 1-28.

Samim, S. A., & Sugiyama, M. (2016) A consideration on the shear strength characteristics of unsaturated volcanic soils. In M. B. Lehane, E. H. Acosta-Martínez & R. Kelly (Eds.), *5th Internation Conference on Geotechnical and Geophysical Site Characterisation* (Vol. 1, pp. 1143-1148). Gold Coast, Queensland, Australia: Australian Geomechanics Society. https://www.issmge.org/files/ISC5.pdf.

Selby, J. M., & Lowe, J. D. (1992). The middle Waikato Basin and hills. In M. J. Soons & J. M. Selby (Eds.), *Landforms of New Zealand* (Second ed., Chapter 10, pp. 233-255). Auckland, New Zealand: Longman Paul.

Shoji, S., Nanzyo, M., & Dahlgren, R. (1993a). Mineralogical Characteristics of Volcanic Ash Soils. In *Volcanic Ash Soils: Genesis, Properties and Utilization* (Chapter 5 pp. 101-135). Amsterdam: The Netherlands: Elservier Science Publishers B.V.

Shoji, S., Nanzyo, M., & Dahlgren, R. (1993b). Physical Characteristics of Volcanic Ash Soils. In *Volcanic Ash Soils: Genesis, properties and utilization* (Chapter 7, pp. 189-205). Amsterdam: The Netherlands: Elservier Science Publishers B.V.

Sivrikaya, O., & Soycan, Y. T. (2010). Estimation of compaction parameters of fine-grained soils in terms of compaction energy using artificial neural networks. *Internation Journal for Numerical and Analytical Methods in Geomechanics, 35*, 1830-1841.

Standards Association of New Zealand (Compiler) (1986). *New Zealand Standard - Methods of Testing Soils for Civil Engineering Purposes*. Determination of Dry Density/Water Content Relationship - New Zealand Standard Compaction Test. Wellington, New Zealand: Standards Association of New Zealand.

Townsend, C. F. (1985). Geotechnical Characteristics of Residual Soils. *Journal of Geotechnical Engineering, 111*(1), 77-94.

Ward, T. W. (1967). Volcanic ash beds of the lower Waikato basin, North Island, New Zealand. *New Zealand Journal of Geology and Geophysics, 10*(4), 1109-1135.

Weather Station. (2019). *Hamilton City Weather* Retrieved August 15, 2019, from http://hamiltoncityweather.co.nz/index.php.

Wesley, D. L. (1973). Some basic engineering properties of halloysite and allophane clays in Java, Indonesia *Geotechnique, 23*(4), 471-494.

Wesley, D. L. (1977). Shear strength properties of halloysite and allophane clays in Java, Indonesia. *Geotechnic, 27*(2), 125-136.

Wesley, L. (2009). Behaviour and geotechnical properties of residual soils and allophane clays. *Obras y Proyectos, 6*, 5-10.

Whitton, S. J., & Churchman, J. G. (Compiler) (1987). *Standard Methods for Mineral Analysis of Soil Survey Samples for Characterisation and Classification in NZ Soil Bureau*. Instrumental and Chemical Techniques used. Lower Hutt, New Zealand: Department of Scientific and Industrial Research.

Yokohama, S., Muira, S., & Matsumura, S. (2014). Change in the hydromechanical characteristics of embankment material due to compaction state conditions. *Soils and Foundations, 54*(4), 731-747.

Yunusa, H. G., Hamza, U., Abdulfatah, Y. A., & Suleiman, A. (2013). Geotechnical Investigation into the Causes of Cracks in Building: A Case Study. *Electronic Journal of Geotechnical Engineering, 18*, 2823-2833.

Appendices

Appendix 1 - Vane Shear Test raw data

Sample 1 = 1hr of Soaking

Original Sample	Trial 1	Trial 2	Trial 3	Average
Initial Reading, IR (°)	0	0	0	
Final Reading, FR (°)	0	39	0	
Angle of deflection (FR-IR)	0	39	0	
Angel of rotation	13	79	57	
Torque, *M* (N *mm*)	33.93	206.19	148.77	
Shear strength, *τvr* (kPa)	7.91	48.06	34.68	30.22

Remoulded Sample

	Trial 1	Trial 2	Trial 3	Average
Initial Reading, IR (°)	0	0	0	
Final Reading, FR (°)	0	0	0	
Angle of deflection (FR-IR)	0	0	0	
Angel of rotation	2	4	6	
Torque, *M* (N *mm*)	5.22	10.44	15.66	
Shear strength, *τvr* (kPa)	1.22	2.43	3.65	2.43

Sample 1 = 2hrs of Soaking

Original Sample	Trial 1	Trial 2	Trial 3	Average
Initial Reading, IR (°)	0	0	0	
Final Reading, FR (°)	65	57	0	
Angle of deflection (FR-IR)	65	57	0	
Angel of rotation	31.5	37	49	
Torque, *M* (N *mm*)	82.215	96.57	127.89	
Shear strength, *τvr* (kPa)	19.16	22.51	29.81	23.83

Remoulded Sample

	Trial 1	Trial 2	Trial 3	Average
Initial Reading, IR (°)	0	0	0	
Final Reading, FR (°)	0	0	0	
Angle of deflection (FR-IR)	0	0	0	
Angel of rotation	11	1	6	
Torque, *M* (N *mm*)	28.71	2.61	15.66	
Shear strength, *τvr* (kPa)	6.69	0.61	3.65	3.65

Sample 1 = 3hrs of Soaking

Original Sample	Trial 1	Trial 2	Trial 3	Average
Initial Reading, IR (°)	0	0	0	
Final Reading, FR (°)	80	0	73	
Angle of deflection (FR-IR)	80	0	73	
Angel of rotation	29	23.5	31	
Torque, *M* (N *mm*)	75.69	61.335	80.91	
Shear strength, *τvr* (kPa)	17.64	14.30	18.86	16.93

Remoulded Sample

	Trial 1	Trial 2	Trial 3	Average
Initial Reading, IR (°)	0	0	0	
Final Reading, FR (°)	0	0	0	
Angle of deflection (FR-IR)	0	0	0	

Angel of rotation	5	3	5	
Torque, *M* (N *mm*)	13.05	7.83	13.05	
Shear strength, *τvr* (kPa)	3.04	1.83	3.04	2.64

Sample 2 = 1 Day of Soaking

Original Sample

	Trial 1	Trial 2	Trial 3	Average
Initial Reading, IR (°)	0	0	0	
Final Reading, FR (°)	38	0	0	
Angle of deflection (FR-IR)	38	0	37	
Angel of rotation	65	77	27	
Torque, *M* (N *mm*)	169.65	200.97	70.47	
Shear strength, *τvr* (kPa)	39.54	46.84	16.43	34.27

Remoulded Sample

	Trial 1	Trial 2	Trial 3	Average
Initial Reading, IR (°)	0	0	0	
Final Reading, FR (°)	0	0	0	
Angle of deflection (FR-IR)	0	0	0	
Angel of rotation	14	9	3.5	
Torque, *M* (N *mm*)	36.54	23.49	9.135	
Shear strength, *τvr* (kPa)	8.52	5.48	2.13	5.37

Sample 3 = 7 days of soaking

Original Sample

	Trial 1	Trial 2	Trial 3	Trial 4	Average
Initial Reading, IR (°)	0	0	0	0	
Final Reading, FR (°)	16	0	50	37	
Angle of deflection (FR-IR)	16	0	50	37	
Angel of rotation	41	32	64	77	
Torque, *M* (N *mm*)	107.01	83.52	167.04	200.97	
Shear strength, *τvr* (kPa)	24.94	19.47	38.94	46.84	32.55

Remoulded Sample

	Trial 1	Trial 2	Trial 3	Trial 4	Average
Initial Reading, IR (°)	0	0	0	16	
Final Reading, FR (°)	0	0	0	89	
Angle of deflection (FR-IR)	0	0	0	73	
Angel of rotation	14	9	30	14	
Torque, *M* (N *mm*)	36.54	23.49	78.3	36.54	
Shear strength, *τvr* (kPa)	8.52	5.48	18.25	8.52	10.75

Sample 4 = 14 days of soaking

Original Sample

	Trial 1	Trial 2	Trial 3	Trial 4	Average
Initial Reading, IR (°)	1	0	0	2	
Final Reading, FR (°)	23	15	50	12.5	
Angle of deflection (FR-IR)	22	15	50	11	
Angel of rotation	87	64	75	44	
Torque, *M* (N *mm*)	227.07	167.04	195.75	114.84	
Shear strength, *τvr* (kPa)	52.93	38.94	45.63	26.77	41.07

Remoulded Sample

	Trial 1	Trial 2	Trial 3	Trial 4	Average
Initial Reading, IR (°)	7.5	0	0	5	
Final Reading, FR (°)	40.5	0	0	48	
Angle of deflection (FR-IR)	33	0	0	43	
Angel of rotation	5	28	11	2	
Torque, *M* (N *mm*)	13.05	73.08	28.71	5.22	
Shear strength, *τvr* (kPa)	3.04	17.03	6.69	1.22	8.31

Sample 5 = 21 days of soaking

Original Sample

	Trial 1	Trial 2	Trial 3	Trial 4	Average
Initial Reading, IR (°)	2	2	0	2	
Final Reading, FR (°)	70	52	46	0	
Angle of deflection (FR-IR)	68	50	46	0	
Angel of rotation	63	102	75	80	
Torque, *M* (N *mm*)	164.43	266.22	195.75	208.8	
Shear strength, *τvr* (kPa)	38.33	62.05	45.63	48.67	48.67

Remoulded Sample

	Trial 1	Trial 2	Trial 3	Trial 4	Average
Initial Reading, IR (°)	0	11	0	5	
Final Reading, FR (°)	0	82	0	35	
Angle of deflection (FR-IR)	0	71	0	30	
Angel of rotation	7.5	5	104	5	
Torque, *M* (N *mm*)	19.575	13.05	271.44	13.05	
Shear strength, *τvr* (kPa)	4.56	3.04	63.27	3.04	23.12

Sample 6 = 2 months of soaking

Original Sample

	Trial 1	Trial 2	Trial 3	Trial 4	Average
Initial Reading, IR (°)	0	0	0	0	
Final Reading, FR (°)	52	61	70	20	
Angle of deflection (FR-IR)	52	61	70	20	
Angel of rotation	108	115	129	138	
Torque, *M* (N *mm*)	281.88	300.15	336.69	360.18	
Shear strength, *τvr* (kPa)	65.70	69.96	78.48	83.96	74.53

Remoulded Sample

	Trial 1	Trial 2	Trial 3	Trial 4	Average
Initial Reading, IR (°)	0	0	0	24	
Final Reading, FR (°)	71	0	0	87	
Angle of deflection (FR-IR)	71	0	0	63	
Angel of rotation	11	110	82	11	

Torque, *M* (N *mm*)	28.71	287.1	214.02	28.71	
Shear strength, *τvr* (kPa)	6.69	66.92	49.89	6.69	41.17

Sample 7 = No soaking - Initial shear strength determination of compacted soil

Original Sample	Trial 1	Trial 2	Trial 3	Trial 4	Average
Initial Reading, IR (°)	0	0	0	0	
Final Reading, FR (°)	0	0	0	0	
Angle of deflection (FR-IR)	0	60	70	1	
Angel of rotation	47	49	106	131	
Torque, *M* (N *mm*)	122.67	127.89	276.66	341.91	
Shear strength, *τvr* (kPa)	28.59	29.81	64.49	79.70	50.65

Remoulded Sample

	Trial 1	Trial 2	Trial 3	Trial 4	Average
Initial Reading, IR (°)	0	10	0		
Final Reading, FR (°)	0	88	0		
Angle of deflection (FR-IR)	0	78	0		
Angel of rotation	0	5	24		
Torque, *M* (N *mm*)	0	13.05	62.64	Vane	
Shear strength, *τvr* (kPa)	0.00	3.04	14.60	broke!	8.82